JAS
Journal of Anatomical Sciences

Volume 34 Issue 1 January–June 2026

JAYPEE
www.jaypeebrothers.com
www.jaypeejournals.com

Journal of Anatomical Sciences

1. Aims and Scope

Journal of Anatomical Sciences is the official publication of the UP Chapter of the Anatomical Society of India. The Journal publishes two issues in English per year, i.e., January–June and July–December. It is a peer-reviewed, open-access, print and online Journal that aims to enhance and advance scientific knowledge in the field of anatomy through research findings, new techniques, and expert opinions. The Journal serves as a platform for academicians and researchers across the globe to communicate and exchange knowledge.

The Journal accepts recent original research and advances in anatomical sciences in the form of full-length original articles, brief communications including case reports, review articles, book reviews, and letters to the editor.

Scientific proceedings of the UP Chapter of the Anatomical Society of India are published in it.

Authors are encouraged to submit manuscripts directly related to the following domains of anatomical sciences: gross anatomy, comparative anatomy, histology, histochemistry, embryology, neuroanatomy, cytogenetics, radiological anatomy, clinical anatomy, and medical education.

The manuscripts submitted to the Journal of Anatomical Sciences are reviewed for publication, with the explicit understanding that they are being submitted with one Journal at a time and have not been published or accepted for publication elsewhere, completely or in part.

Target Readership: The *Journal of Anatomical Sciences* primarily aims to serve as a comprehensive resource for individuals involved in various aspects of anatomy, from basic research to clinical and educational applications, including (but not limited to) anatomists and researchers, medical students and educators, radiologists, clinicians and surgeons, cytogeneticists, educational institutions, biomedical researchers, students and academics in allied health professions, and the pharmaceutical and biotechnology industries.

2. Ethical Considerations

Investigation and surgery on human subjects should conform to the guidelines noted in the World Health Organization Chronicle 1976;30:360–362.

Manuscripts submitted for publication must comply with the following ethical considerations:

Informed Consent

Informed consent of the patients must be taken before they are considered for participation in the study. Patient-identifying information, such as names, initials, hospital numbers, or photographs should not be included in the written descriptions. Patient consent should be obtained in written and archived with the authors.

Protection of Human Subjects and Animals in Research

When conducting experiments on human subjects, appropriate approval must have been obtained by the relevant ethics committees. All the procedures must be performed in accordance with the ethical standards of the responsible ethics committee (institutional and national) on human experimentation and the Helsinki Declaration of 1964 (as revised in 2008). When reporting experiments on animals, authors must follow the institutional and national guidelines for the care and use of laboratory animals.

3. Copyright

Following guidelines must be followed before submission of the manuscript:

The articles must have declaration in relation to original research or any other material that "article has not have been published before and is not under consideration of publication elsewhere." This, however, does not include previous publication in form of an abstract or as part of published literature (review or thesis). It is the duty of the author to obtain the necessary permissions for extensive quotations, tables, illustrations or any other material they are using in the paper before a paper can be considered for publication. The authors retain the Copyright of the article. At the time of article submission, the author would be asked to sign the 'Open Access License Agreement Form' before their article is considered for publication. Once the author/authors have signed the Open Access License Agreement Form, no authorship change, or the authors' order listed on the article will be accepted by Jaypee Brothers Medical Publishers Pvt Ltd. However, if there is a genuine reason for authorship and authorship sequence changes, the authors should complete the "Authorship change request form" with a signed statement of agreement for the requested change from all listed authors and the author to be removed or added and send it to the Journal Editor-in-Chief (EIC) along with a letter explaining the reasons for the proposed changes; EIC will consider these requests on a case-to-case basis although not mandatory. Also by signing the above-mentioned form, the author reassigns the rights of copublishing or translation if considered necessary in future to the editor or Publisher. In the advent of occurrence of any dispute, the matter would be resolved within the jurisdiction of New Delhi court.

While all care will be taken to provide accurate and correct information in accordance with the date of publication, neither the authors/editors nor the Publisher takes any legal responsibility for any unintentional omission or error. The editors or Publisher makes no expressed or implied warranty with respect to the information contained herein. The published material cannot be photocopied for the following purposes: General distribution, promotion, new works or resale. If this is required, specific written permission must be obtained from the editor or Publisher. Exclusive rights to reproduce and distribute the articles in the Journal have been protected by copyright. This also covers the rights to reproduce or distribute the article as well as the translation rights. No material published in the Journal can be reproduced in digital format or stored in the forms of electronic databases, video disks, etc.

Both the conflict of interests and financial disclosure need to be handled well while conducting the research study. Disclosure of such relationships is also important in connection with all articles submitted for publication. Both of these have also been included in the Commercial Rights Transfer Form. Authors should give due acknowledgment to the individuals who provide writing or other assistance while conducting the research study and also disclose the funding source for the research study.

4. Subscription Information

ISSN 0970-1842

• Subscription rates

For information on subscription rates and the other journal-related enquiries, please contact:
subscriptions@jaypeebrothers.com

• Orders

Journals Department
Jaypee Brothers Medical Publishers (P) Ltd.
4838/24, Ansari Road, Daryaganj
New Delhi 110 002, India
Phone: +91-11-4357 4357
Fax: +91-11-4357 4314
e-mail: subscriptions@jaypeebrothers.com

5. Electronic Media

An electronic edition of this journal is available at **www.jaypeejournals.com**

Manuscripts can be submitted online at **www.asiupjas.com**

6. Advertisement

For advertisement queries, please contact:
Journals Department
Jaypee Brothers Medical Publishers (P) Ltd.
e-mail: sanjeev.kumar@jaypeebrothers.com

For any queries regarding online submission, please e-mail us at:
ayushi.goyal@jaypeebrothers.com

For editorial queries, please contact:
editor@jaypeebrothers.com

The Journal is printed on acid-free paper.

Editorial Board

Editorial and Production Office
Journals Department
Jaypee Brothers Medical Publishers (P) Ltd.
4838/24, Ansari Road, Daryaganj
New Delhi-110 002, India
Phone: +91-11-43574357
Fax: +91-11-43574314
e-mail: editor@jaypeebrothers.com

Advertisements/ Subscriptions/ Reprints
Sanjeev Kumar
Phone: +91-9868850291
e-mail: subscriptions@jaypeebrothers.com
sanjeev.kumar@jaypeebrothers.com

For Website Queries
Phone: +91-11-43574357
e-mail: journals.editor@jaypeebrothers.com

JAS
Journal of Anatomical Sciences
Volume 34 Issue 1 January–June 2026

Contents

Editorial

From Teacher to Moderator: Reframing the Teaching of Anatomy 1
Satyam Khare

Original Research

Prevalence of Rib Anomalies in Pediatric Cancer Patients—A Radiological Study 3
Supratik Pal

Assessment of Cervical Sagittal Parameters (C2 Slope, T1 Slope, and Cervical Lordosis) in Neck Pain by 1.5 Tesla Magnetic Resonance Imaging 11
Shrikant Bharti, Jolly Agarwal, Abhishek K Yadav, Abhinav Kumar

Decoding Vascular Patterns of Vasa Recta and Arterial Arcades of Small Intestine: A Morphometric Study with Novel Clinical Applications for Safer Surgeries and Improved Bowel Viability 18
Garima Sehgal, Shweta Nayak, Khushboo Yadav

To Study Heterogeneity in the Distribution of Microglia and Astrocytes at Different Sites of Brain: Immunohistochemical Analysis by Using CD68 and Glial Fibrillary Acidic Protein, Respectively 22
Shivangi Thakur, Swati Saxena, Mamta Gupta, Rajesh K Maurya, Jolly Agarwal, Mahendra K Pant

Use of Cadaveric Tissue as an Alternative to Normal Tissue/Surgical Specimen—A Histological Endeavor 28
Anurag, Shilpa Gupta, Shubha Srivastava

Case Report

Additional Muscular Extension of Coracobrachialis Muscle: A Case Report 35
Fatima Begum, Vinay Sharma

Brief Research Communication

Situs Inversus Totalis: A Pictorial Review 37
CS Ramesh Babu, Vinay Sharma, Bindu Agrawal, Arjun Kumar, OP Gupta

EDITORIAL

From Teacher to Moderator: Reframing the Teaching of Anatomy

Satyam Khare

Keywords: Anatomy, Competency-based medical education, Moderator, National Medical Commission, Psychological dimension.
Journal of Anatomical Sciences (2026): 10.5005/jas-11049-0017

Department of Anatomy, Subharti Medical College, Swami Vivekanand Subharti University, Meerut, Uttar Pradesh, India

Corresponding Author: Satyam Khare, Department of Anatomy, Subharti Medical College, Swami Vivekanand Subharti University, Meerut, Uttar Pradesh, India, Phone: +91 9837083748, e-mail: satyamkhare@subharti.co

How to cite this article: Khare S. From Teacher to Moderator: Reframing the Teaching of Anatomy. J Anat Sciences 2026;34(1):1–2.

Source of support: Nil

Conflict of interest: None

There is something almost nostalgic about the image many of us carry of the anatomy teacher—chalk in hand, standing beside a blackboard, mapping out the human body while a silent lecture hall listens. For decades, that image has defined authority in medical education. And yet, if we are honest, it now feels slightly out of place. The classroom has changed. The students certainly have. And, perhaps more quietly, the expectations of a teacher have shifted as well.

Anatomy, as a foundational subject with more than 600 hours of undergraduate teaching, has traditionally leaned heavily on teacher-centered approaches—lectures, demonstrations, and dissection hall sessions. These methods are not without merit. Many of us were trained through them and continue to rely on them when time is short or when the cohort is large. There is a certain efficiency to structured delivery, and, admittedly, a certain comfort for the instructor in being in command of the room.

But one might ask—does coverage of content necessarily translate into understanding?

The answer, though often assumed, is not entirely straightforward. Increasingly, it appears that the pace set by the teacher does not always align with the pace at which the learner processes, reflects, and internalizes anatomical knowledge.[1,2] This mismatch may not be obvious and during examinations, but it tends to surface later—during clinical application, during reasoning, during those moments when anatomy must move beyond recall and into interpretation.

It is here that the idea of the teacher as a moderator begins to take shape.

A moderator, unlike the traditional instructor, does not relinquish authority but redistributes it. The role becomes less about delivering information and more about shaping the conditions under which learning occurs. Seminars, small group discussions, peer teaching, and even student-led demonstrations begin to occupy a more central place. The learner, in such settings, speaks more, questions more, and occasionally struggles more—which may, in fact, be the point.

The learning pyramid proposed by the National Training Laboratories, often cited though sometimes debated in its exact percentages, suggests that passive methods like lectures and demonstrations may result in lower retention compared to active engagement such as practice or teaching others.[3] While one should be cautious about accepting these figures uncritically, the broader implication remains persuasive: Engagement seems to matter.[1,2]

Still, it would be too simplistic to dismiss traditional methods entirely. Lectures, when delivered thoughtfully, can provide clarity, structure, and narrative coherence—qualities that are not easily replicated in fragmented learning environments. Dissection, likewise, offers a tactile and spatial understanding that no digital model has fully replaced. The challenge, then, is not to abandon these approaches but to reposition them within a broader, more flexible pedagogical framework.

The National Medical Commission, with the introduction of competency-based medical education (CBME) in 2019, appears to have recognized this need for recalibration.[4] The emphasis has gradually moved toward learner-centered strategies, early clinical exposure, and integration across disciplines. Anatomy, in this context, is no longer an isolated subject but part of a continuum that connects structure with function and clinical reasoning.[5]

And yet, implementation on the ground is uneven.

Faculty members, often trained in earlier systems, may find the transition demanding. There is an implicit expectation to not only adapt to new methods but also to do so without compromising curricular timelines. Large class sizes, limited infrastructure, and assessment pressures add further complexity. Under such circumstances, the idea of becoming a "moderator" may seem aspirational rather than practical.

But perhaps moderation does not require a complete overhaul. It may begin with smaller shifts.

Allowing a student to explain a concept to peers rather than repeating it oneself. Pausing during a lecture to invite interpretation rather than continuing uninterrupted. Designing a session where the outcome is not predetermined but explored collectively. These are modest interventions, but they carry a different educational intent.

There is also an interesting psychological dimension to this transition. When the teacher steps back slightly, the learner steps forward—sometimes hesitantly, sometimes with surprising confidence. The classroom becomes less predictable, which can be uncomfortable. Discussions may drift. Questions may arise that do not have immediate answers. Yet, in these moments, learning

appears to take on a different texture—less polished, perhaps, but more authentic.

Anatomy, after all, is not merely a subject of memorization. It is a language of relationships—between structures, between systems, and between form and function. To grasp this fully, the learner must engage actively, not just receive passively.

There is also the matter of information overload. Today's medical student has access to an overwhelming volume of resources—videos, apps, atlases, and 3D models. The teacher is no longer the primary source of knowledge. Instead, the teacher becomes something else: A curator, a guide, and occasionally a filter.[6] Helping students decide what not to focus on may be as important as teaching them what to learn.

In that sense, the moderator's role extends beyond the classroom. It includes mentoring, advising, and sometimes even unlearning.

Of course, one must acknowledge that not all learners respond similarly to this approach. Some prefer structure and clear guidance. Others seem to do better when given space to explore and make sense of concepts on their own.[6] A balanced strategy, then, seems reasonable—one that retains the strengths of traditional teaching while gradually incorporating learner-driven elements.

If one were to reflect personally, many of us might recall a teacher who, perhaps unintentionally, acted as a moderator long before the term became fashionable. Someone who asked questions rather than answered them. Someone who encouraged discussion, even if it meant deviating from the planned content. Those sessions, though less orderly, often remain more memorable.

As we look ahead, the role of the anatomy teacher is unlikely to revert to its earlier form. Nor should it. The demands of modern medical education—critical thinking, clinical integration, and adaptability—require a different kind of engagement.

The teacher, in this evolving landscape, stands not at the center but slightly to the side. Observing, guiding, and intervening when necessary. Moderating, rather than dictating.

It is not a loss of authority. It is, perhaps, a refinement of it.

References

1. Prince M. Does active learning work? J Eng Educ 2004;93(3):223–231.
2. Michael J. Where's the evidence that active learning works? Adv Physiol Educ 2006;30(4):159–167. DOI: 10.1152/advan.00053.2006.
3. National Training Laboratories. Learning Pyramid. Bethel, Maine, USA.
4. National Medical Commission. Competency-based Undergraduate Curriculum for the Indian Medical Graduate. New Delhi; 2019.
5. Harden RM. Outcome-based education: An introduction. Med Teach 1999;21(1):7–14.
6. Knowles MS. The Adult Learner: A Neglected Species, 4th ed. Houston: Gulf Publishing; 1990.

ORIGINAL RESEARCH

Prevalence of Rib Anomalies in Pediatric Cancer Patients—A Radiological Study

Supratik Pal

Received on: 11 February 2026; *Accepted on*: 23 March 2026; *Published on*: 12 June 2026

Abstract

Purpose: To determine the prevalence of rib anomalies in pediatric cancer patients compared to age and sex-matched controls without cancer using retrospective evaluation of chest radiographs.

Materials and methods: Chest radiographs of 149 cases and 149 controls were reviewed and independently scored by four blinded observers using strict definitions. The prevalence of six major rib anomaly categories in controls was compared to their prevalence in the total group of childhood cancer patients.

Observation and results: The value of cases among children with cancer was significantly higher (37.6%) compared to the controls (16.8%, $p < 0.001$). Cervical ribs were more prevalent in controls (4 in number, 16%), than in cases (3 in number, 5.4%). Bifid ribs were more common in cases (5 in number, 8.9%), than in controls (1 in number, 4%). Rib aplasia was more common in cases (24 in number, 42.9%) than in controls (9 in number, 36%).

Conclusion: The study included an equal number of pediatric cancer patients and non-malignant pediatric controls. The most common cancer types among cases was B-ALL and T-ALL, followed by Hodgkin's lymphoma and Wilms tumor.

Keywords: Clinical anatomy, Gross anatomy, T1 slope angle.

Journal of Anatomical Sciences (2026): 10.5005/jas-11049-0020

Introduction

Pediatric oncology is an emerging branch solely dedicated to the diagnosis and treatment of cancer in children and adolescents. Although pediatric malignancy is less prevalent than adult malignancy, it remains one of the top causes of disease-related mortality in the pediatric population. According to the World Health Organization (WHO), approximately 3,00,000 children aged 0–19 years are diagnosed with cancer each year.[1] In India, the incidence of pediatric cancer cases (ages 0–19) is about 76,800 per year.[2] The National Cancer Registry Programme (NCRP) reports that childhood cancers (ages 0–14) account for about 4.0% of all cancer cases in India.[3] Age-adjusted incidence rates (AAR) vary across different regions of India. In recent years, India has witnessed a substantial increase in pediatric cancer cases, making it a significant public health concern. A secondary analysis of population-based cancer registries in India from 2006 through 2014 showed that the age-adjusted incidence rate per million for childhood cancers increased, and substantially in boys (from 156.6 to 235.3 per million).[4] The common malignancies in the pediatric age-group include acute lymphocytic leukemia (ALL), lymphomas, retinoblastoma, Wilms tumor (WT), central nervous system (CNS) tumors and bone tumors. Acute lymphocytic leukemia is common in infants and toddlers (0–4 years), and in children (5–9 years), whereas lymphoma and bone tumors are more common in the adolescent age-group (10–19 years).[5–8]

Various risk factors have been associated with the development of these malignancies, which include genetic, environmental, and perinatal factors. Unlike in adults, which is mainly due to lifestyle habits (smoking, chewing tobacco) and environmental carcinogens. Among all the identifiable risk factors, genetic syndromes, also known as tumor predisposition syndromes (TPS) have the strongest association with pediatric malignancies. Several TPS have been identified in association with specific genetic mutations. For instance, gliomas are frequently observed in individuals with neurofibromatosis (NF1) and Li-Fraumeni syndrome (LFS), both of which are linked to mutations in the NF1 gene (Fig. 1).[8–14]

Department of Anatomy, King George's Medical University, Lucknow, Uttar Pradesh, India

Corresponding Author: Supratik Pal, Department of Anatomy, King George's Medical University, Lucknow, Uttar Pradesh, India, Phone: +91 8918967210, e-mail: supratikpal97@gmail.com

How to cite this article: Pal S. Prevalence of Rib Anomalies in Pediatric Cancer Patients—A Radiological Study. J Anat Sciences 2026;34(1): 3–10.

Source of support: Nil

Conflict of interest: None

Materials and Methods

Study Design

This retrospective case -control study was approved by the Institutional Ethics Committee (IEC), King George's Medical University, Lucknow, Uttar Pradesh, India (Reference No. ECR/262/Inst/UP/2013/RR-19; approval dated 20 June 2024). The study was conducted in accordance with the ethical principles of the Declaration of Helsinki. As this was a retrospective study using anonymized radiological records, the requirement for informed consent was waived by the Institutional Ethics Committee.

Study Setting and Duration

The study was conducted over a period of one year from July 2024 to June 2025 in the Department of Anatomy in collaboration with the Departments of Pediatrics and Radiodiagnosis, King George's Medical University, Lucknow.

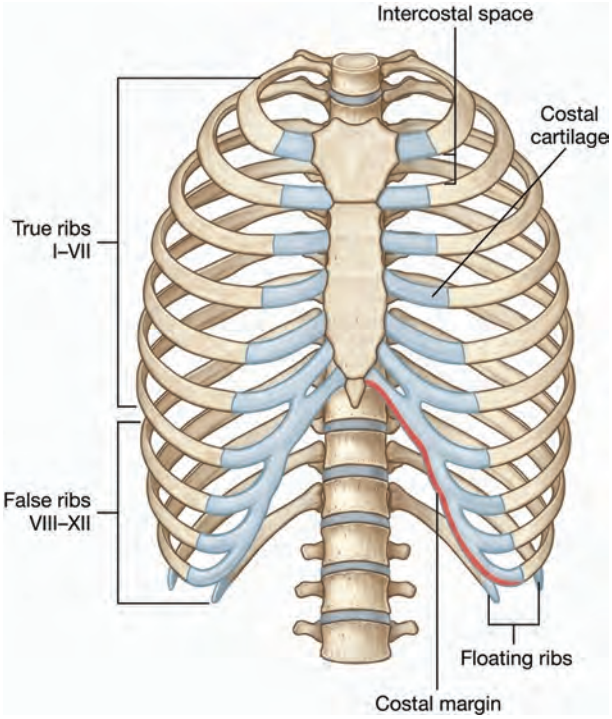

Fig. 1: Thoracic cage with 12 pairs of rib (18)

Study Population

Case Group (pediatric cancer patients). The case group consisted of pediatric patients aged 0–18 years who were diagnosed with malignant neoplasms and had undergone chest imaging (X-ray and/or CT scan) as part of their diagnosis.

Sample Size

The sample size for proposed study was calculated using prevalence ($p = 10\%$), type 1 error rate ($q = 5\%$) and margin of error ($d = 5\%$) by means of the following formula: $n = (z^2pq)/d^2$. Thus, the sample size is 149.

Inclusion Criteria for Cases

The confirmed histopathological diagnosis of malignancy (solid tumors, hematologic malignancy, CNS tumor).

Exclusion Criteria for Cases

Inadequate imaging quality.

Radiological Definitions

Cervical rib—a rib arising from the 7th cervical vertebra.
Bifid rib—a rib showing a cleft or forked appearance at its anterior end.
Fused rib—two adjacent ribs are partially or completely fused along their length.
Aplastic rib—underdeveloped or absent ribs noted on imaging.

Data Analysis

The prevalence of each rib anomaly was calculated separately for the case and control groups.

Statistical analysis was performed using statistical software, e.g., SPSS version or R software.

Table 1: Groupwise distribution of study population

Sl. No.	*Group*	*No. of patients*	*Percentage*
1.	Cases (pediatric cancer patients)	149	50.0
2.	Controls (pediatric controls)	149	50.0
		298	100.0

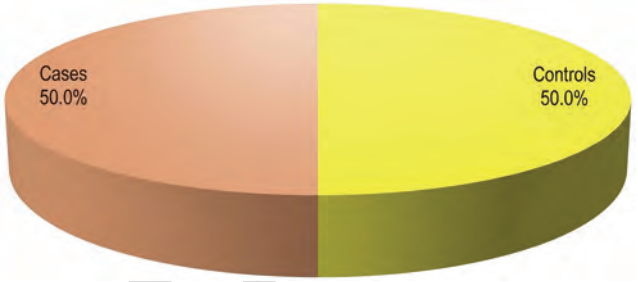

Fig. 2: Groupwise distribution of study population

Table 2: Type of cancer diagnosed in cases ($N = 149$)

Sl. No.	*Type of cancer*	*No. of patients*	*Percentage*
1.	ALL	13	8.7
2.	B-ALL	45	30.2
3.	Burkitt's lymphoma	10	6.7
4.	Ewing's sarcoma	1	0.7
5.	Hodgkin's lymphoma	17	11.4
6.	Leukemia	3	2.0
7.	Lymphoma	5	3.4
8.	T-ALL	43	28.9
9.	Wilms tumor	12	8.1

Observation and Results

The present study were conducted in the Department of Anatomy, King George's Medical University, Lucknow, to estimate the prevalence of rib anomalies in pediatric cancer patients and in non-malignant disease conditions and to determine the type of rib anomalies in pediatric cancer patients. To achieve the objectives of the present study, 149 pediatric cancer patients and 149 non-malignant pediatrics subjects were enrolled in the study as follows:

A total of 149 pediatric cancer patients and 149 non-malignant pediatric subjects were enrolled in the study. The total study population comprised 298 pediatric subjects; 149 (50.0%) subjects with cancer were categorized as cases, and 149 (50.0%) non-malignant pediatric subjects were categorized as controls (Table 1; Fig. 2).

The most common diagnosis of cases was B-ALL (30.2%), followed by T-ALL (28.9%) and Hodgkin's lymphoma (11.4%). The rest of the cases were diagnosed as ALL (8.7%), Wilms tumor (8.1%), Burkitt's lymphoma (6.7%), lymphoma (3.4%) , leukemia (2.0%), and Ewing's sarcoma (0.7%) (Table 2; Fig. 3).

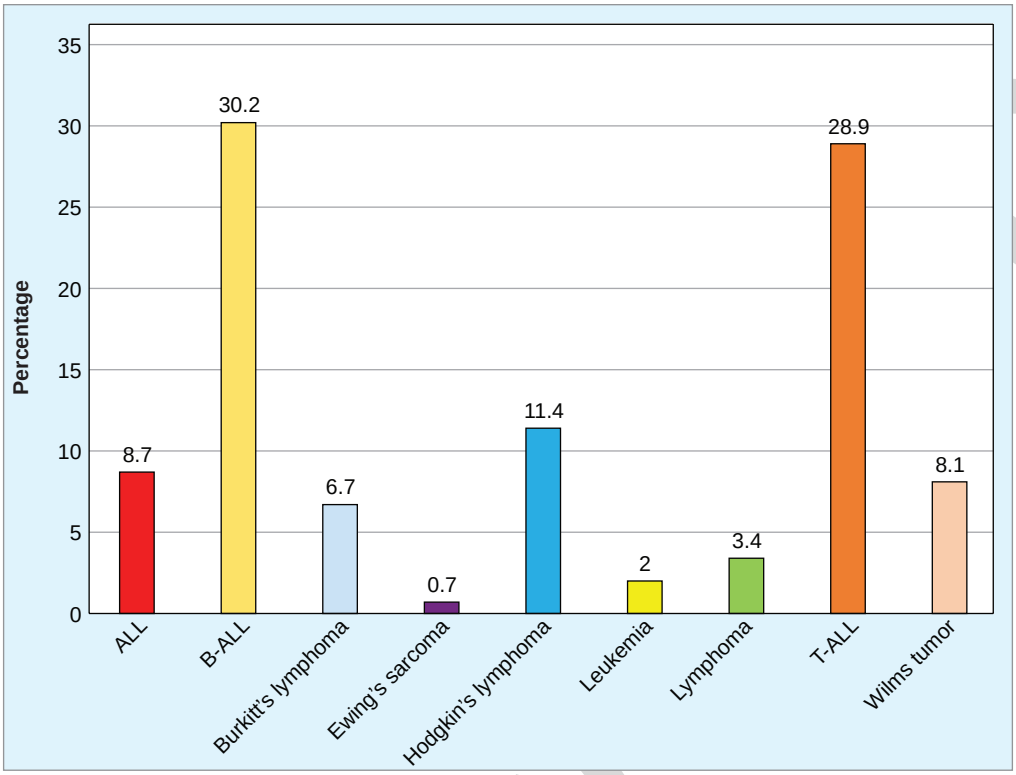

Fig. 3: Type of cancer diagnosed in cases

Table 3: Comparison of age of cases and controls

			Cases (N = 149)		*Controls (N = 149)*	
Sl. No.	*Age-group*	*Total*	*No.*	*%*	*No.*	*%*
1.	<1 year	22	22	14.8	0	0.0
2.	1–5 years	116	59	46.3	47	31.5
3.	6–12 years	160	58	38.9	102	68.5
			$\chi^2 = 38.272$; $p < 0.001$			
Mean age ± SD		6.14 ± 3.54 (1 month–12 years)	4.86 ± 3.63 (1 month–12 years)		7.42 ± 2.88 (2–12 years)	
			$t = 6.669$; $p < 0.001$			

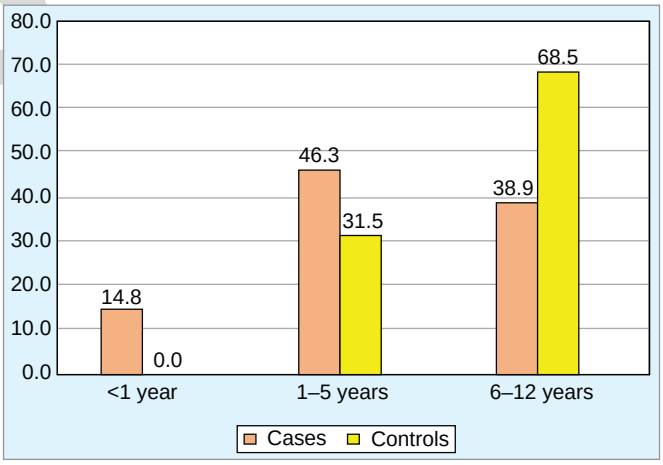

Fig. 4: Comparison of age of cases and controls

Age of children enrolled in the study ranged between 1 month and 12 years. The mean age of all children was 6.14 ± 3.54 years. A difference in the mean age of cases (4.86 ± 3.63 years) and controls (7.42 ± 2.88 years) was found to be statistically significant ($p < 0.001$).

The most common age-group of cases was 1–5 years (46.3%) followed by 6–12 years (38.9%); the rest (14.8%) were <1 year of age. The majority of controls were aged 6–12 years (68.5%); none were aged <1 year, and the rest 31.5% were aged 1–5 years. This difference was found to be statistically significant (Table 3; Fig. 4).

The majority of overall ($n = 196$; 65.8%), as well as cases (55.0%) and controls (76.5%), were males; the rest were females. The proportion of females among cases (45.0%) was significantly higher than that among controls (23.5%) (Table 4; Fig. 5).

Out of 298 children enrolled in the study, rib anomalies have been reported in 81 (27.2%). Rib anomalies were significantly higher among cases (37.6%) as compared to controls (16.8%) (Table 5; Fig. 6).

The most common rib anomaly was rib aplasia (40.7%), followed by elongated TP (18.5%). In 13.6% of cases, no conclusion could be drawn as there was poor visibility of the lower ribs due to excessive gas shadows.The rest of the children with rib anomalies had bifid rib (7.4%) and cervical rib (8.6%), 11.1% children had other rib anomalies than the above (Table 6; Fig. 7).

Table 4: Comparison of gender of cases and controls

			Cases (N = 149)		*Controls (N = 149)*	
Sl. No.	*Gender*	*Total*	*No.*	*%*	*No.*	*%*
1.	Male	196	82	55.0	114	76.5
2.	Female	102	67	45.0	35	23.5
			$\chi^2 = 15.264; p < 0.001$			

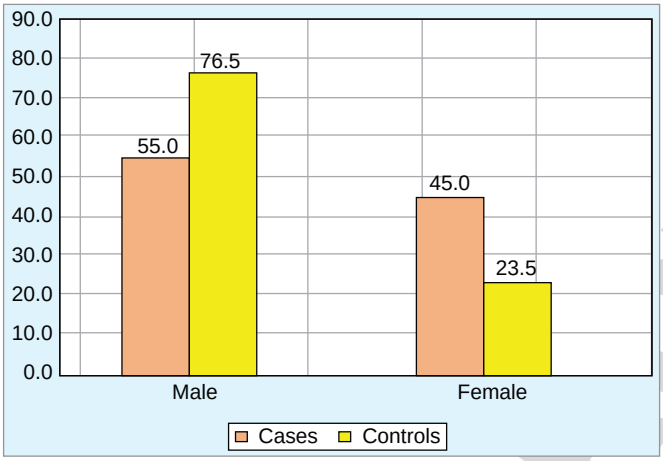

Fig. 5: Comparison of gender of cases and controls

Table 5: Comparison of prevalence of rib anomalies in cases and controls

			Cases (N = 149)		*Controls (N = 149)*	
Sl. No.	*Rib anomaly*	*Total*	*No.*	*%*	*No.*	*%*
1.	No-rib anomaly	217	119	62.4	124	83.2
2.	Rib anomaly	81	56	37.6	25	16.8
			$\chi^2 = 16.293; p < 0.001$			

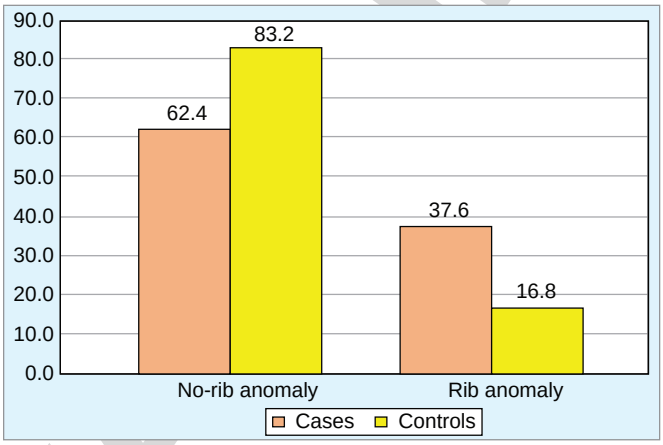

Fig. 6: Comparison of prevalence of rib anomalies in cases and controls

Table 6: Types of rib anomalies in study population (*N* = 81)

Sl. No.	*Type of rib anomaly*	*No. of patients*	*Percentage*
1.	Bifid rib	6	7.4
2.	Cervical rib	7	8.6
3.	Rib aplasia/Rib aplasia of 12 rib	33	40.7
4.	Poor visibility/Non-visible	11	13.6
5.	Elongated TP	15	18.5
6.	Other than above	9	11.1

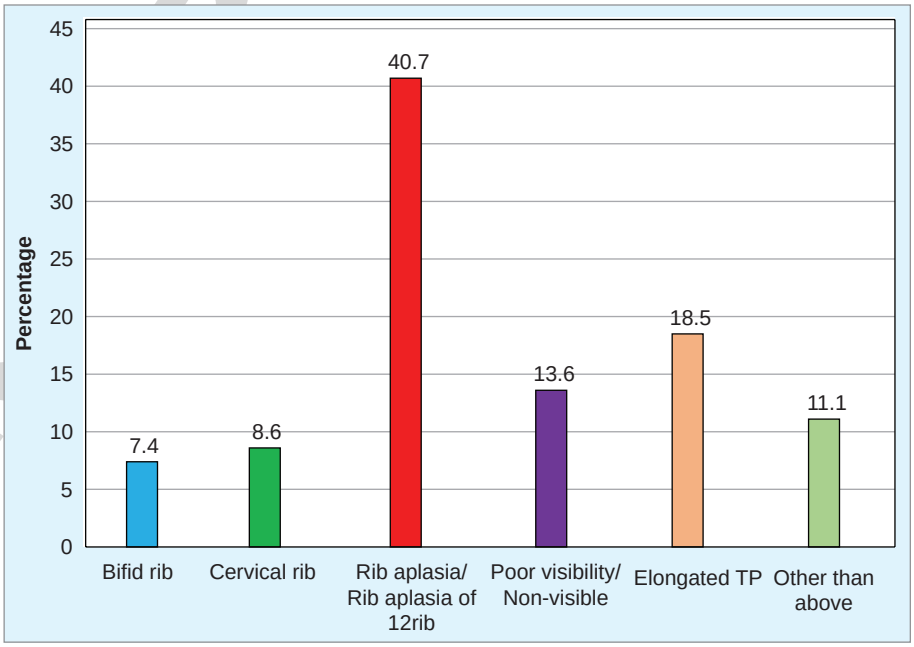

Fig. 7: Types of rib anomalies in the study population

Difference in type of rib anomalies among cases and controls was not found to be statistically significant (Table 7; Fig. 8).

Rib anomalies were more common among children diagnosed with ALL (61.5%), leukemia (100.0%), Wilms tumor (41.7%), T-ALL (39.5%) and B-ALL (35.6%) as compared to those diagnosed with Burkitt's lymphoma (10.0%).

Ewing's sarcoma (10.0%), Ewing's sarcoma (0.0%), Hodgkin's lymphoma (29.4%), lymphoma (20.0%). This difference was found to be significant when compared statistically (Table 8; Fig. 9).

Rib anomalies were more common in age-group 1–5 years (29.3%) and 6–12 years (26.3%) as compared to age-group <1 year (22.7%); this difference was not found to be statistically significant (Tables 9 and 10; Figs 10 to 15).

Rib anomalies were significantly higher among females (34.3%) as compared to males (23.5%).

Our study investigated the prevalence and patterns of rib anomalies in pediatric cancer patients compared to non-cancer

Table 7: Comparison of the types of rib anomalies in cases and controls

Sl. No.	*Type of rib anomaly*	*Total*	*Cases (N = 56)*		*Controls (N = 25)*	
			No.	*%*	*No.*	*%*
1.	Bifid rib	6	5	8.9	1	4.0
2.	Cervical rib	7	3	5.4	4	16.0
3.	Rib aplasia/Rib aplasia of 12 rib	33	24	42.9	9	36.0
4.	Poor visibility/ Non-visible	11	8	14.3	3	12.0
5.	Elongated TP	15	11	19.6	4	16.0
6.	Other than above	9	5	8.9	4	16.0

$\chi^2 = 4.000$; $p = 0.549$

Table 8: Association of rib anomalies with type of cancer

Sl. No.	*Type of cancer*	*Total*	*No-rib anomaly (N = 93)*		*Rib anomaly (N = 56)*	
			No.	*%*	*No.*	*%*
1.	ALL	13	5	38.5	8	61.5
2.	B-ALL	45	29	64.4	16	35.6
3.	Burkitt's lymphoma	10	9	90.0	1	10.0
4.	Ewing's sarcoma	1	1	100.0	0	0.0
5.	Hodgkin's lymphoma	17	12	70.6	5	29.4
6.	Leukemia	3	0	0.0	3	100.0
7.	Lymphoma	5	4	80.0	1	20.0
8.	T-ALL	43	26	60.5	17	39.5
9.	Wilms tumor	12	7	58.3	5	41.7

$\chi^2 = 13.385$; $p = 0.099$

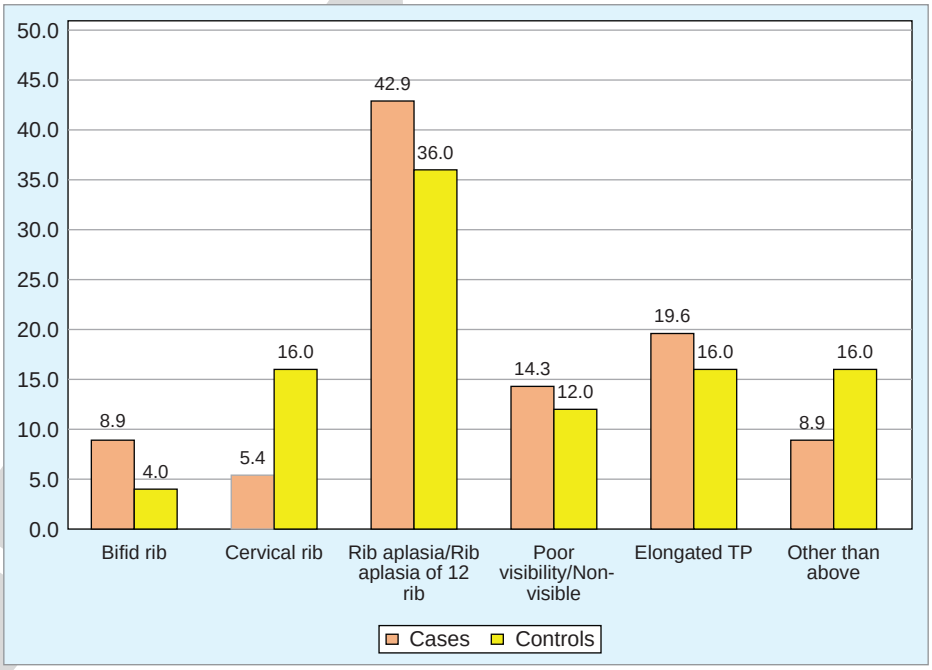

Fig. 8: Comparison of types of rib anomalies in cases and controls

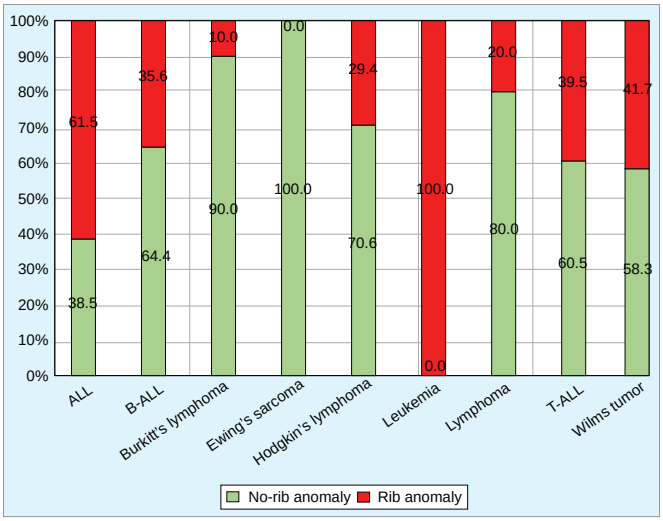

Fig. 9: Association of rib anomalies with type of cancer

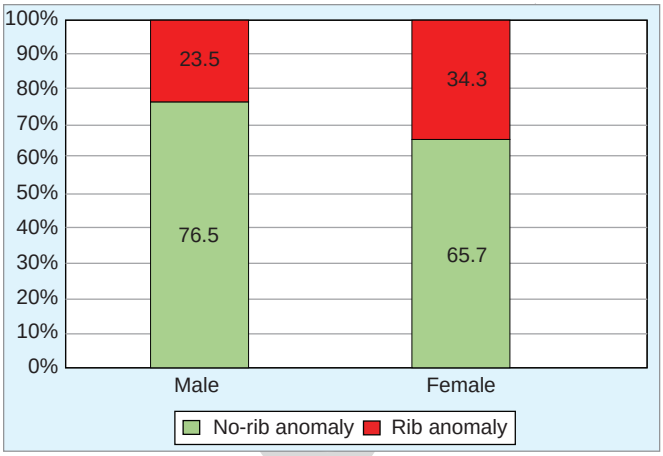

Fig. 11: Association of rib anomalies with gender of children

Table 9: Association of rib anomalies with age of children ($N = 298$)

			No-rib anomaly (N = 217)		*Rib anomaly (N = 81)*	
Sl. No.	*Age*	*Total*	*No.*	*%*	*No.*	*%*
1.	<1 year	22	17	77.3	5	22.7
2.	1–5 years	116	82	70.7	34	29.3
3.	6–12 years	160	118	73.8	42	26.3
			$\chi^2 = 0.556; p = 0.757$			

Table 10: Association of rib anomalies with the gender of children ($N = 298$)

			No-rib anomaly (N = 217)		*Rib anomaly (N = 81)*	
Sl. No.	*Gender*	*Total*	*No.*	*%*	*No.*	*%*
1.	Male	196	150	76.5	57	23.5
2.	Female	102	67	65.7	44	34.3
			$\chi^2 = 3.986; p = 0.046$			

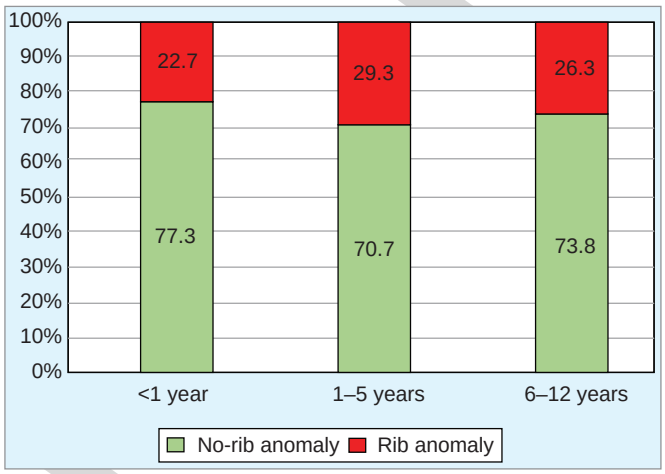

Fig. 10: Association of rib anomalies with the age of children

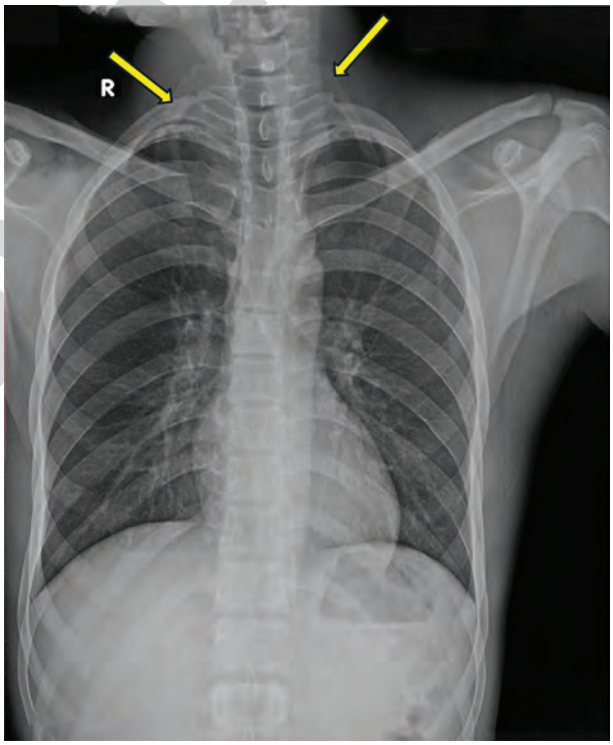

Fig. 12: Radiograph of case of leukemia showing bilateral cervical rib (yellow arrow)

controls. The findings add to the growing body of evidence supporting a link between congenital anomalies, particularly rib malformations, and childhood malignancies. The study was based on the premise that disruptions in embryonic development affecting the ribs may also be associated with pathways involved in tumorigenesis. Thus, identifying specific patterns of rib anomalies could provide insights into shared developmental mechanisms underlying both congenital malformations and childhood cancers.

We found a significantly higher prevalence of rib anomalies among children with cancer (37.6%) compared to controls (16.8%,

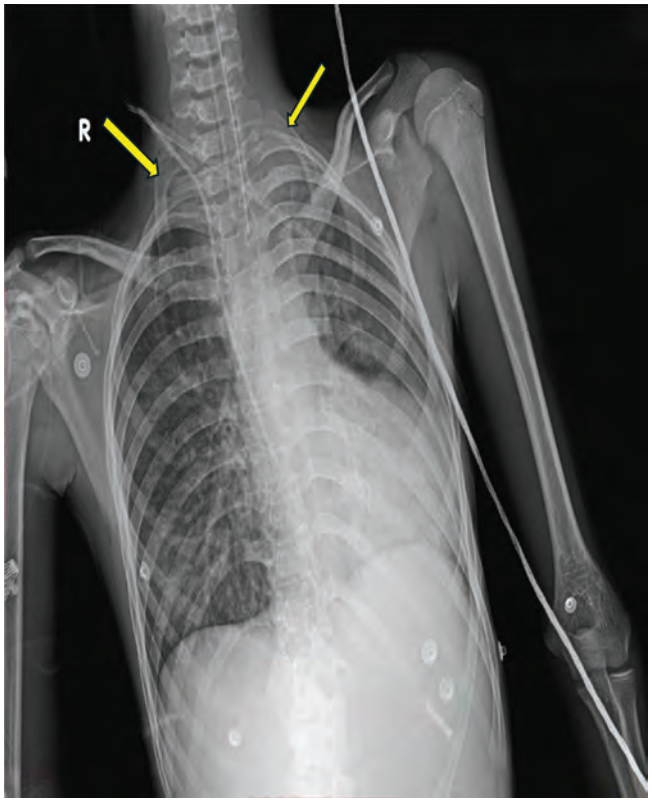

Fig. 13: Radiograph of control showing bilateral cervical rib (yellow arrow)

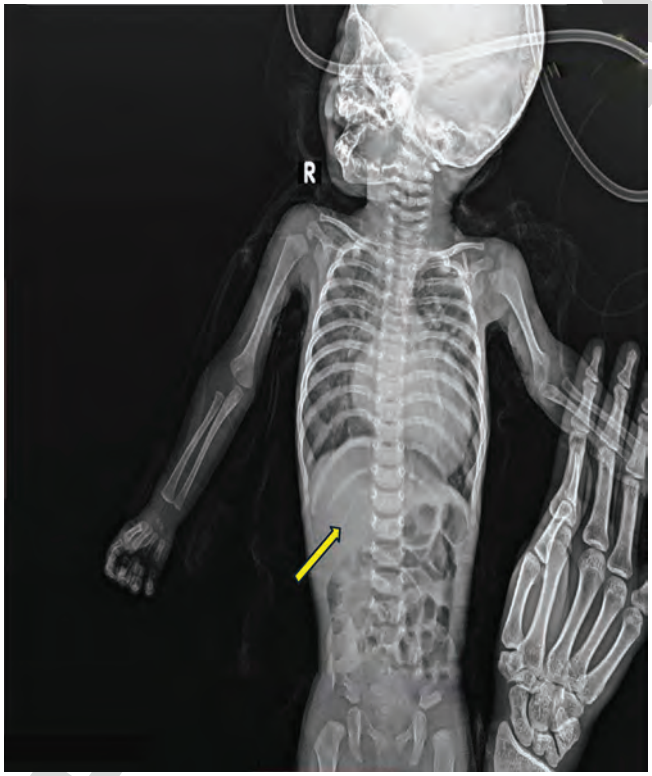

Fig. 14: Radiograph of a case of B-ALL leukemia showing right lumbar rib (yellow arrow)

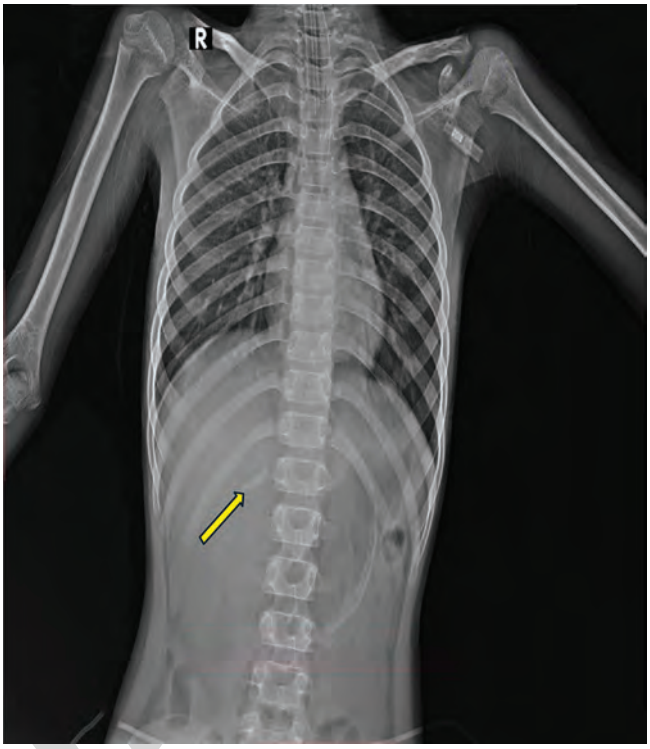

Fig.15: Radiograph of control showing right-sided lumbar rib (yellow arrow)

$p < 0.001$). The association between rib anomalies and childhood cancer was first systematically described by Schumacher et al., who reported a 21.8% prevalence of rib anomalies in pediatric cancer patients compared to 5.5% in controls. Their study particularly highlighted the increased frequency of cervical ribs in children with neuroblastoma, leukemia, and Wilms tumor. Similarly, Loder et al. reported an 18% prevalence of rib anomalies among children with malignancies, with a stronger association seen in neural and lymphoproliferative tumors.

Our prevalence rate of 37.6% is notably higher than these earlier reports, though it is consistent with more recent findings, such as those reported by Zierhut et al., who used advanced imaging techniques to detect rib anomalies and found an increased frequency in children with acute myeloid leukemia (AML), renal tumors, and hepatoblastoma.

Interestingly, unlike Merks et al., who found cervical ribs to be the most frequent and significant anomaly in cancer patients, particularly those with ALL and astrocytoma, our study did not find a statistically significant difference in the distribution of specific rib anomaly types between cancer cases and controls ($p = 0.549$). Rib aplasia emerges as the most commonly observed anomaly in both study groups, somewhat divergent from prior reports that emphasized cervical ribs as the most.

Study Limitations and Future Directions

The present study has several limitations. First, it was a single-center retrospective study, which may limit the generalizability of the findings. Second, the sample size for certain cancer subtypes was relatively small, reducing the power to detect associations with specific rib anomaly patterns. Third, only radiological findings

were assessed, and genetic analyses were not performed to explore underlying molecular mechanisms. Fourth, age and sex distributions between cases and controls were not completely matched, which may have introduced residual confounding. Finally, some radiographs had limited visualization of lower ribs, potentially affecting anomaly classification. Future multicenter prospective studies with larger sample sizes, advanced imaging techniques, and genetic profiling are recommended to better elucidate the developmental and molecular links between rib anomalies and pediatric malignancies.

Conclusion

- The study included an equal number of pediatric cancer patients and non- malignant pediatric controls.
- The most common cancer types among cases were B-ALL and T-ALL, followed by Hodgkin's lymphoma and Wilms tumor. Other cancer types included Burkitt's lymphoma, leukemia, and lymphoma.
- The majority of cancer cases were from younger age-groups, while controls with non-malignant conditions were predominantly from older age-groups.
- Rib anomalies were observed more frequently among cancer cases compared to controls. This difference was statistically significant.
- The most common type of rib anomaly observed was rib aplasia, followed by elongated transverse processes. Other observed anomalies included cervical ribs and bifid ribs.
- Although the overall frequency of rib anomalies was significantly higher in cancer cases, the distribution of specific types of rib anomalies between cases and controls was not statistically different.
- Among cancer types, rib anomalies were more frequent in children with ALL, leukemia, Wilms tumor, T-ALL, and B-ALL.
- There was a statistically significant association between age-groups and the presence of rib anomalies.
- Rib anomalies were significantly more frequent in females compared to males.

Data Availability Statement

The datasets generated and/or analyzed during the current study are available from the corresponding author upon reasonable request, subject to institutional and ethical regulations.

AI Disclosure Statement

The authors used ChatGPT (OpenAI) solely for language editing and grammatical refinement of the manuscript. All scientific content, data analysis, interpretation, and final manuscript approval were performed by the authors, who take full responsibility for the accuracy and integrity of the work.

Acknowledgments

The authors sincerely thank the Department of Anatomy, Department of Pediatrics, and Department of Radiodiagnosis, King George's Medical University, Lucknow, for their support and assistance in conducting this study. The authors also acknowledge the contribution of all healthcare personnel involved in patient care and data management.

References

1. World Health Organization. Cancer in Children. Geneva: World Health Organization; 2021 [cited 2025 Apr 11]. Available from: https://www.who.int/news-room/fact-sheets/detail/cancer-in-children.
2. Arora RS, Eden TOB, Kapoor G. Epidemiology of childhood cancer in India. Indian J Cancer 2009;46(4):264–273. DOI: 10.4103/0019-509X.55546.
3. Pathan SR, Bhende VV, Sharma KB, et al. Addressing the alarming rise in pediatric cancer prevalence in India: A call to action. Health Sci Rep 2025;8(2):e70429. DOI: 10.1002/hsr2.70429.
4. Bashar MA, Begam N. Trend of childhood cancers in India: A review of population based cancer registries data on childhood cancers. Eur J Cancer Prev 2021;31:S7–S8. DOI: 10.1097/01.cej.0000816672.18030.22.
5. Ganguly S, Kinsey S, Bakhshi S. Childhood cancer in India. Cancer Epidemiol 2021;71(Pt B):101679. DOI: 10.1016/j.canep.2020.101679.
6. Singh M, Bhatia P, Sharma P, et al. Assessment of cancer predisposition syndromes in children with leukemia and solid tumors: Germline-genomic profiling and clinical features in a series of cases. Pediatr Hematol Oncol 2024;41(8):620–632. DOI: 10.1080/08880018.2024.2411321.
7. Kratz CP, Jongmans MC, Cavé H, et al. Predisposition to cancer in children and adolescents. Lancet Child Adolesc Health 2021;5(2):142–154. DOI: 10.1016/S2352-4642(20)30275-3.
8. Sait SF, Walsh MF, Karajannis MA. Genetic syndromes predisposing to pediatric brain tumors. Neurooncol Pract 2021;8(4):375–390. DOI: 10.1093/nop/npab012.
9. Bhandari J, Thada PK, Killeen RB, et al. Fanconi Anemia; 2025. In: StatPearls. TreasureIsland (FL): StatPearls Publishing. Available from: https://www.ncbi.nlm.nih.gov/books/NBK559133/.
10. Scollon S, Anglin AK, Thomas M, et al. A comprehensive review of pediatric tumors and associated cancer predisposition syndromes. J Genet Couns 2017;26(3):387–434. DOI: 10.1007/s10897-017-0077-8.
11. Krivit W, Good RA. Simultaneous occurrence of mongolismand leukemia; report of a nationwide survey. AMA J Dis Child 1957;94(3):289–293. DOI: 10.1001/archpedi.1957.04030040075012.
12. Cheng Y, Wang H, Chen Z, et al. Trisomy 21 in patients with acute leukemia. Am J Hematol 2009;84:193–194. DOI: 10.1002/ajh.21339.
13. Gonzalez KD, Noltner KA, Buzin CH, et al. Beyond Li Fraumeni Syndrome: Clinical characteristics of families with p53 germline mutations. J Clin Oncol 2009;27(8):1250–1256. DOI: 10.1200/JCO.2008.16.6959.
14. Marden PM, Smith DW, McDonald MJ. Congenital anomalies in the newborn infant, including minor variations. A study of 4,412 babies by surface examination for anomalies and buccal smear for sex chromatin. J Pediatr 1964;64:357–371. DOI: 10.1016/s0022-3476(64)80188-8.

ORIGINAL RESEARCH

Assessment of Cervical Sagittal Parameters (C2 Slope, T1 Slope, and Cervical Lordosis) in Neck Pain by 1.5 Tesla Magnetic Resonance Imaging

Shrikant Bharti[1], Jolly Agarwal[2], Abhishek K Yadav[3], Abhinav Kumar[4]

Received on: 21 February 2026; *Accepted on:* 16 April 2026; *Published on:* 12 June 2026

Abstract

Aims and background: Globally, the most reported musculoskeletal disorder is neck pain, with an increasing trend due to lifestyle and occupational factors such as sedentary lifestyle behavior and poor posture. Cervical alignment plays a crucial role in maintaining physiological posture and minimizing musculoskeletal strain. Cervical alignment is commonly assessed by using sagittal parameters like cervical lordosis (C2–C7), T1 slope angle, and C2 slope angle (C2). The previous studies have shown correlations between these parameters and spinal balance, with limited evidence of their relationship with neck pain in populations exposed to prolonged static posture. The study aimed to analyze key cervical sagittal alignment parameters, namely the C2 slope angle, T1 slope angle, and cervical lordosis from C2 to C7, in patients complaining of neck pain.

Methodology: The study included a total of 190 patients over 20 years of age complaining of neck pain and underwent cervical MRI on a 1.5-Tesla unit. Exclusions included traumatic neck injuries, osteoporosis, spinal deformities, and previous cervical surgeries. Sagittal cervical parameters were measured using AutoCAD software on MRI scans. Pain was assessed via the Likert pain scale.

Results: The mean age of the study participants was 38.48 ± 12.29 years. Mean sagittal parameters recorded were as follows: C2 slope 13.99° ± 6.85°, T1 slope 17.77° ± 7.17°, and cervical lordosis (C2–C7) 9.49° ± 6.77°. Mean pain score was 6.26 ± 1.14, indicating moderate to severe pain levels. On gender-based analysis, males demonstrated marginally greater cervical lordosis and T1 slope angle than females. Age-group analysis revealed variable trends in sagittal parameters across decades, with no significant reduction in lordosis but persistent pain scores. A statistically significant inverse correlation was observed between the C2 slope and T1 slope ($r = -0.385$, $p < 0.001$), as well as between the C2 slope angle and pain score ($r = -0.208$, $p = 0.004$). In contrast, the T1 slope showed a significant positive relationship with cervical lordosis ($r = 0.329$, $p < 0.001$).

Conclusion: Cervical sagittal parameters show distinct variations in the individuals with neck pain, with the C2 slope identified as an important indicator demonstrating an inverse association with both pain severity and T1 slope. The study supports the clinical utility of measuring sagittal cervical alignment for early risk identification and targeted therapeutic interventions to mitigate neck pain and its associated disability. Further longitudinal investigations are warranted to elucidate causal relationships.

Clinical significance: The study highlights the clinical significance of cervical sagittal parameters in patients with neck pain. C2 slope angle shows a significant negative correlation with pain score, which makes it a simple yet reliable marker of cervical sagittal imbalance. T1 slope and cervical lordosis show a positive association, which supports their role in maintaining cervical alignment. Early identification of these changes can facilitate focused ergonomic correction and prompt clinical management, thereby reducing the risk of progression of neck disability.

Keywords: AutoCAD, C2 slope angle, Cervical lordosis, Cervical sagittal parameter, T1 slope angle.

Journal of Anatomical Sciences (2026): 10.5005/jas-11049-0021

Introduction

The most reported musculoskeletal condition worldwide is neck pain, which creates a substantial health and socioeconomic burden. The Global Burden of Disease Study 2021 reported that approximately 203 million individuals experienced neck pain worldwide in 2020, with projections indicating an increase to about 269 million cases by 2050, largely due to population growth and aging.[1] Occupational factors, such as office work, prolonged computer use, poor posture, and psychosocial stress, are core risk factors responsible for increasing cases of neck pain.[2] Recent advancements in spinal biomechanics have emphasized the importance of cervical sagittal alignment in stabilizing physiological posture alignment and minimizing musculoskeletal strain. Parameters, including cervical lordosis(C2–C7), T1 slope angle (T1S), and C2 slope angle, play a critical role in assessing cervical sagittal balance. T1 slope angle demonstrates a strong association with cervical lordosis, which indicates that individuals with a greater T1 slope angle need greater lordosis to cope with horizontal gaze.[3] The study aimed to analyze key cervical sagittal alignment parameters, namely the C2 slope angle, T1 slope angle, and cervical lordosis from C2 to C7, in patients with neck pain.[4]

[1,2,4]Department of Anatomy, Government Doon Medical College, Dehradun, Uttarakhand, India

[3]Department of Radiology, Government Doon Medical College, Dehradun, Uttarakhand, India

Corresponding Author: Jolly Agarwal, Department of Anatomy, Government Doon Medical College, Dehradun, Uttarakhand, India, Phone: + 91 6398682933, e-mail: drjolly21177@gmail.com

How to cite this article: Bharti S, Agarwal J, Yadav AK, *et al.* Assessment of Cervical Sagittal Parameters (C2 Slope, T1 Slope, and Cervical Lordosis) in Neck Pain by 1.5 Tesla Magnetic Resonance Imaging. J Anat Sciences 2026;34(1):11–17.

Source of support: Nil

Conflict of interest: None

Methodology

This prospective study, conducted over a period of 18 months from February 2025 to October 2026. study was approved under IEC No. GDMC/IEC/2024/6 was carried out jointly with the Department of Anatomy, Orthopedics, and Radiodiagnosis at Government Doon Medical College and Associated Hospitals, Dehradun, Uttarakhand. No clinical trial registry number was required, as this study was not a clinical trial and was based strictly on MRI scans received from the radiology department. The study comprised 190 patients over the age of 20 years presenting with the complaint of neck pain. After giving prior information and taking consent, cervical MRI scans were performed using a 1.5-Tesla MRI machine (uMR580 Full Digital 1.5T MR, United Imaging Healthcare). Patients with traumatic neck pain, spinal surgery, diagnosed cases of osteoporosis, tumor, metastasis, with any spinal deformities, like flat back syndrome, scoliosis, kyphosis, congenital spinal deformity, etc., and pregnant females were excluded from the study.

$$n = \frac{z^2 \times p(1-p)}{E^2}$$

Sample size calculation formula:
Where:

- Prevalence of neck pain, $p = 0.433$
- Z-score for 95% confidence level (standard value), $Z = 1.96$
- Margin of error, $E = 0.07$
- The sample size of the study is 189 (~190).

On the computer, the images obtained from the MRI were opened using MicroDicom Viewer, and the seventh image in the T2-weighted section was exported into JPG format for further measurements in AutoCAD 2024 Software.[5] The exported JPG image was opened in AutoCAD software, where reference lines were drawn along the caudal endplate of the axis (C2), the caudal endplate of the seventh cervical vertebra (C7), and the cranial endplate of the T1 vertebra to calculate the sagittal parameters (Fig. 1).

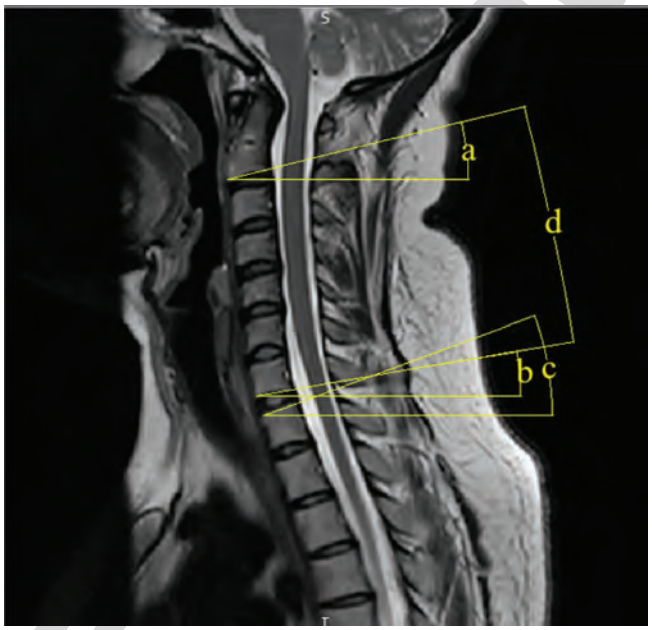

Fig. 1: Radiograph showing several sagittal parameters measured in this study: a: C2 slope angle; b: C7 slope angle; c: T1 slope angle; d: cervical lordosis (C2–C7) angle

The C2 slope angle was determined by drawing a line parallel to the inferior endplate of C2 vertebra and calculating the angle formed with the horizontal plane (Fig. 1 a).

The C2–C7 angle was obtained by drawing lines along the caudal endplate of C2 and C7(Fig. 1 b) and measuring the angle formed between these lines (Figs 1 c and d).

The T1 slope was measured as the angle formed between the upper endplate of the T1 vertebra and the horizontal reference line (Fig. 1 c).

The pain assessment is carried out by the Likert pain scale.[6]

Results

This study evaluated MRI scans of 190 patients aged over 20 years presenting with neck pain, including 95 males and 95 females. Measurements of the C2 slope angle, T1 slope angle, and cervical lordosis (C2–C7) were obtained from the seventh image of the T2-weighted sequence using AutoCAD software (Version 2024). The mean age of the study cohort was 38.48 ± 12.29 years.

The mean C2 slope angle was 13.99 ± 6.85°, whereas the mean T1 slope angle measured 17.77 ± 7.17°. An average cervical lordosis (C2–C7 angle) of 9.49 ± 6.77° was observed. The mean pain score on the Likert scale was 6.26 ± 1.14 (Table 1).

Gender-wise Distribution (Tables 2 and 3)

- Males had a mean age of 37.19 ± 12.18 years, C2 slope angle of 13.42 ± 7.29°, T1 slope angle of 18.04 ± 7.42°, T1 slope angle of 18.04 ± 7.42°, cervical lordosis angle of 10.67 ± 7.44°, and pain score of 6.16 ± 1.08.
- Females had a mean age of 39.78 ± 12.33 years, C2 slope angle of 14.56 ± 6.37°, T1 slope angle of 17.49 ± 6.94°, cervical lordosis of 8.31 ± 5.82°, and pain score of 6.36 ± 1.19.

Correlation Analysis (Overall Population) (Table 4)

A significant negative correlation was found between C2 slope and T1 slope angle ($r = -0.385$, $p \leq 0.001$). C2 slope angle also showed a significant negative correlation with pain score ($r = -0.208$, $p = 0.004$). While T1 slope angle correlated positively with cervical lordosis ($r = 0.329$, $p < 0.001$). Pain score did not show a significant correlation with T1 slope angle ($p = 0.194$) or cervical lordosis ($p = 0.21$) (Table 4 and Fig. 2).

Gender Specific Correlations (Table 5)

- In males, C2 slope angle correlated negatively with T1 slope angle ($r = -0.351$, $p < 0.001$) and pain score ($r = -0.236$, $p = 0.004$). T1 slope angle showed a significant positive correlation with cervical lordosis ($r = 0.403$, $p < 0.001$).

Table 1: Overall mean of age, C2 slope angle, T1 slope angle, cervical lordosis (C2–C7), and Likert pain scale study participants

Parameters	*Mean ± SD*
Age	38.48 ± 12.290
C2 slope angle	13.99 ± 6.851
T1 slope angle	17.77 ± 1.171
Cervical lordosis (C2–C7)	9.49 ± 6.766
Likert pain scale	6.26 ± 1.142

SD, standard deviation

Table 2: Gender distribution of mean age, mean C2 slope angle, T1 slope angle, and Likert pain scale scores

Sex	*No. case*	*Minimum–maximum age (years)*	*Mean age (years)*	*C2 slope angle mean ± SD*	*T1 slope angle mean ± SD*	*Cervical lordosis (C2–C7) angle mean ± SD*	*Likert Pain score mean ± SD*
Male	95	20–62	37.19 ± 12.178	13.42 ± 7.294°	18.04 ± 7.418°	10.67 ± 7.437°	6.16 ± 1.085
Female	95	20–63	39.78 ± 12.329	14.56 ± 6.366°	17.49 ± 6.943°	8.31 ± 5.822°	6.36 ± 1.193

SD, standard deviation

Table 3: Mean C2 slope, T1 slope, and cervical lordosis angle at different age-groups

Age-groups	*Cervical sagittal angle*	*Mean ± SD*
20–29	C2 slope angle	14.67° ± 6.908
	T1 slope angle	18.24° ± 6.270
	Cervical lordosis angle	8.65° ± 6.016
30–39	C2 slope angle	13.45° ± 7.458
	T1 slope angle	18.08° ± 8.247
	Cervical lordosis angle	11.10° ± 7.938
40–49	C2 slope angle	14.26° ± 6.675
	T1 slope angle	16.80° ± 6.751
	Cervical lordosis angle	8.94° ± 5.775
50–59	C2 slope angle	14.45° ± 6.214
	T1 slope angle	16.83° ± 6.793
	Cervical lordosis angle	8.66° ± 6.315
60–69	C2 slope angle	12.47° ± 6.022
	T1 slope angle	19.00° ± 7.280
	Cervical lordosis angle	8.47° ± 6.435

SD, standard deviation

Table 4: Pearson correlation (*r*) and *p* value between C2 slope, T1 slope angle, cervical lordosis (C2–C7) angle, and Likert pain scale in the total study population

Variables	*C2_slope*	*T1_slope*	*Cervical lordosis angle (C2–C7)*	*Likert pain scale*
C2_slope	–	$r = -0.385$, $p \leq 0.001$	$r = -0.114$ $p = 0.117$	$r = -0.208$ $p = 0.004$
T1_slope	$r = -0.385$ $p \leq 0.001$	–	$r = 0.329$ $p \leq 0.001$	$r = 0.095$ $p = 0.194$
Cervical lordosis (C2–C7) angle	$r = -0.114$ $p = 0.117$	$r = 0.329$ $p \leq 0.001$	–	$r = 0.168$ $p = 0.21$
Likert pain scale	$r = -0.208$ $p = 0.004$	$r = 0.095$ $p = 0.194$	$r = 0.168$ $p = 0.21$	–

- In females, C2 slope angle correlated positively with T1 slope angle ($r = 0.424$, $p < 0.001$). No significant association was observed between pain score and sagittal parameters in females.

Age-group Analysis (Table 6)

- In the 20–29 years group, T1 slope correlated positively with cervical lordosis ($r = 0.293$, $p = 0.041$).
- In the 30–39 years group, C2 slope correlated negatively with T1 slope ($r = -0.447$, $p < 0.001$), cervical lordosis ($r = -0.270$, $p = 0.034$), and pain score ($r = -0.284$, $p = 0.026$). T1 slope correlated positively with cervical lordosis ($r = 0.452$, $p < 0.001$).
- In the 40–49 years group, C2 slope showed a negative correlation with T1 slope ($r = 0.341$, $p = 0.045$), whereas cervical lordosis showed a significant positive association with pain score ($r = 0.344$, $p = 0.043$).
- In the 50–59 years group, no significant correlation was observed between slope angles, cervical lordosis, or pain.

Among participants aged 60–69 years, the C2 slope demonstrated a significant inverse correlation with the T1 slope ($r = -0.536$, $p = 0.039$) and a significant positive association with pain scores ($r = 0.522$, $p = 0.046$). Additionally, a strong positive correlation was observed between the T1 slope and cervical lordosis ($r = 0.807$, $p < 0.001$).

Discussion

This study demonstrated an association between cervical sagittal parameters and neck pain. The mean values of C2 slope angle, T1 slope angle, and cervical lordosis (C2–C7) in this study population are consistent with earlier studies, although cervical lordosis

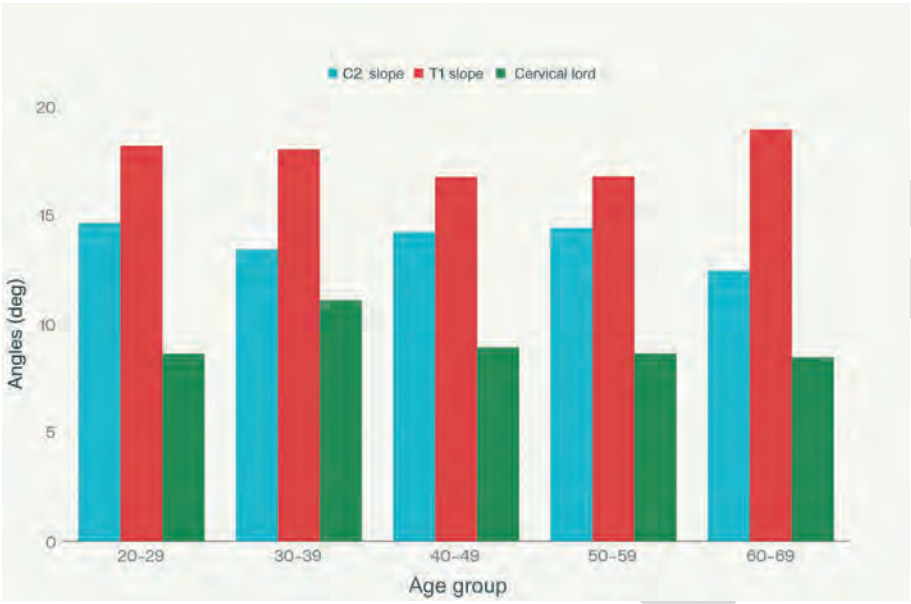

Fig. 2: Bar graph showing C2 slope (°)—mean C2 slope angle across different age-groups (shown in blue bars), T1 slope (°)—mean T1 slope angle across different age-groups (shown in red bars), cervical lordosis (C2–C7) (°)—mean cervical lordosis angle across different age-groups (shown in green bars)

Table 5: Pearson correlation (*r*) and *p* value between C2 slope, T1 slope angle, cervical lordosis (C2–C7) angle, and Likert pain scale in the study population of males and females

Gender	*Variables*	*C2 slope angle*	*T1 slope angle*	*Cervical lordosis angle (C2–C7)*	*Likert pain scale*
Male	C2 slope angle	–	$r = -0.351$ $p \leq 0.001$	$r = -0.082$ $p = 0.432$	$r = -0.236$ $p = 0.021$
	T1 slope angle	$r = -0.351$ $p \leq 0.001$	–	$r = 0.403$ $p \leq 0.001$	$r = 0.113$ $p = 0.276$
	Cervical lordosis angle (C2–C7)	$r = -0.082$ $p = 0.432$	$r = 0.403$ $p \leq 0.001$	–	$r = 0.238$ $p = 0.005$
	Likert pain scale	$r = -0.236$ $p = 0.021$	$r = 0.113$ $p = 0.276$	$r = 0.238$ $p = 0.005$	–
Female	C2 slope angle	–	$r = 0.424$ $p \leq 0.001$	$r = -0.131$ $p = 0.206$	$r = -0.200$ $p = 052$
	T1 slope angle	$r = 0.424$ $p \leq 0.001$	–	$r = 0.228$ $p = 0.27$	$r = 0.085$ $p = 0.413$
	Cervical lordosis angle (C2–C7)	$r = -0.131$ $p = 0.206$	$r = 0.228$ $p = 0.27$	–	$r = 0.81$ $p = 0.438$
	Likert pain scale	$r = -0.200$ $p = 052$	$r = 0.085$ $p = 0.413$	$r = 0.81$ $p = 0.438$	–

was relatively reduced, which is suggestive of early maladaptive changes of postural strain. The significant negative correlation of the C2 slope angle with both T1 slope angle and pain score highlights its value as an important and reliable indicator of cervical sagittal imbalance and related clinical symptoms. T1 slope angle also demonstrates a positive correlation with cervical lordosis and supports its role in maintaining horizontal gaze and overall sagittal harmony.[5,7,8] Gender analysis revealed a strong correlation in the males, whereas females display limited associations, possibly due to different occupational or biomechanical factors. Age-wise analysis revealed that individuals in the 30–39 and 60–69 year age-groups exhibited more marked changes, indicating that both work-related posture and degenerative changes contribute significantly to malalignment of sagittal imbalances and neck pain.[6]

Chai et al. reported that the C2 slope angle was strongly related to disability and sagittal alignment in degenerative cervical kyphosis. They proposed a cutoff value of 26°–30°, indicating severe functional impairment. In this study, the mean C2 slope angle (13.99° ± 6.851) was clinically applicable in symptomatic patients, consistent with prior reports, thereby supporting the utility of the C2 slope angle as a valuable predictor eve in advance pathology.[9]

Jouibari et al. evaluated cervical sagittal parameters comparison in patients with neck pain and healthy patients and found

Table 6: Pearson correlation of C2 slope angle, T1 slope angle, and cervical lordosis (C2–C7) angle in different age-groups

Age-group	*No. of cases*	*Variables*	*C2 slope angle*	*T1 slope angle*	*Cervical lordosis (C2–C7) angle*	*Likert pain*
20–29	49	C2 slope	–	$r = -0.273$ $p = 0.057$	$r = 0.053$ $p = 0.718$	$r = -0.248$ $p = 0.085$
		T1 slope	$r = -0.273$ $p = 0.057$	–	$r = 0.293$ $p = 0.041$	$r = 0.016$ $p = 0.912$
		Cervical lordosis (C2–C7) angle	$r = 0.053$ $p = 0.718$	$r = 0.293$ $p = 0.041$	–	$r = 0.226$ $p = 0.118$
		Likert pain	$r = -0.248$ $p = 0.085$	$r = 0.016$ $p = 0.912$	$r = 0.226$ $p = 0.118$	–
30–39	62	C2 slope	–	$r = -0.447$ $p \leq 0.001$	$r = -0.270$ $p = 0.034$	$r = -0.284$ $p = 0.026$
		T1 slope	$r = -0.447$ $p \leq 0.001$	–	$r = 0.452$ $p \leq 0.001$	$r = 0.184$ $p = 0.152$
		Cervical lordosis (C2–C7) angle	$r = -0.270$ $p = 0.034$	$r = 0.452$ $p \leq 0.001$	–	$r = 0.159$ $p = 0.218$
		Likert pain	$r = -0.284$ $p = 0.026$	$r = 0.184$ $p = 0.152$	$r = 0.159$ $p = 0.218$	–
40–49	35	C2 slope	–	$r = -0.341$ $p = 0.45$	$r = -0.291$ $p = 0.090$	$r = -0.260$ $p = 0.131$
		T1 slope	$r = -0.341$ $p = 0.045$	–	$r = -0.133$ $p = 0.446$	$r = 0.074$ $p = 0.673$
		Cervical lordosis (C2–C7) angle	$r = 0.291$ $p = 0.090$	$r = -0.133$ $p = 0.446$	–	$r = 0.344$ $p = 0.043$
		Likert pain	$r = -0.260$ $p = 0.131$	$r = 0.074$ $p = 0.673$	$r = 0.344$ $p = 0.043$	–
50–59	29	C2 slope	–	$r = -0.365$ $p = 0.051$	$r = -0.171$ $p = 0.376$	$r = -0.204$ $p = 0.289$
		T1 slope	$r = -0.365$ $p = 0.051$	–	$r = 0.244$ $p = 0.202$	$r = 0.034$ $p = 0.861$
		Cervical lordosis (C2–C7) angle	$r = -0.171$ $p = 0.376$	$r = 0.244$ $p = 0.202$	–	$r = -0.140$ $p = 0.467$
		Likert pain	$r = -0.204$ $p = 0.289$	$r = 0.034$ $p = 0.861$	$r = -0.140$ $p = 0.467$	–
60–69	15	C2 slope	–	$r = -0.536$ $p = 0.039$	$r = -0.461$ $p = 0.083$	$r = 0.522$ $p = 0.046$
		T1 slope	$r = -0.536$ $p = 0.039$	–	$r = 0.807$ $p \leq 0.001$	$r = 0.098$ $p = 0.728$
		Cervical lordosis (C2–C7) angle	$r = -0.461$ $p = 0.083$	$r = 0.807$ $p \leq 0.001$	–	$r = 0.266$ $p = 0.337$
		Likert pain	$r = 0.522$ $p = 0.046$	$r = 0.098$ $p = 0.728$	$r = 0.266$ $p = 0.337$	–

significantly lower ($p = 0.02$) T1 slope angle in patients with neck pain, which also correlates with this study result.[10]

Aşkin et al. assessed cervical sagittal angles in Turkish patients with acute and chronic neck pain and reported a mean cervical lordosis of 23.10° ± 8.07. They observed a statistically significant negative correlation between cervical lordosis and disease duration, with higher cervical lordosis values in patients with acute neck pain compared with those with chronic symptoms. This value is much higher than the mean (9.49° ± 6.766) of this study, which may be due to differences in ethnicity.[11]

Park et al. conducted a retrospective study on 3D CT scans on asymptomatic patients and found a mean T1 slope (23° ± 6.5) and a mean cervical lordosis of 12.6° ± 7.8°. They also demonstrated a strong positive correlation between T1 slope and cervical lordosis ($r = 0.83$). In contrast, this study observed a mean T1 slope of 17.8° ± 7.2° and a mean cervical lordosis of 9.5° ± 6.8°, showing a positive but weaker correlation between these parameters ($r = 0.33$) compared with the asymptomatic group.[12]

David et al. conducted a study to see the relation between cervical lordosis and factors such as age, sex, cervical injury, and sedentary lifestyle in 206 individuals. The study revealed a mean cervical lordosis of 8.19 ± 14.00°. In comparison, this study found a mean cervical lordosis of 9.49° ± 6.76. Both studies report reduced cervical lordosis in symptomatic groups.[13]

Protopsaltis et al. also found that the mean value of C2 slope angle is 36.5° ± 19.2 in cervical deformity, whereas this study revealed a relatively lesser mean of 19.8° ± 6.5, which is comparable with less severe malalignment. T1 slope angle also shows a higher value in the author's study, which suggests greater thoracic inclination in advanced pathology. Cervical lordosis (C2–C7) mean value was 8.4° ± 23.1, which is closely aligned with this study. Both studies emphasize the C2 slope angle as the most reliable parameter.[6]

Limitations of the Study

The cross-sectional, single-center design limits causal inference and generalizability. The absence of an asymptomatic control group and reliance on supine MRI may not fully represent functional cervical alignment. Pain assessment was limited to a Likert scale.

Conclusion

This study highlights the significance of cervical sagittal parameters in patients with neck pain. The C2 slope showed a strong negative correlation with T1 slope and pain scores, establishing it as a simple yet valuable marker of sagittal imbalance and clinical symptoms. T1 slope correlated positively with cervical lordosis, confirming its biomechanical role in maintaining alignment. Gender- and age-specific variation further indicated that occupational posture degenerative changes contribute to altered cervical parameters and symptom severity. Early recognition of these associations may aid in identifying at-risk populations and implementing ergonomic or clinical interventions to prevent chronic disability.

Clinical Significance

This study highlights the clinical value of cervical sagittal parameters in patients presenting with neck pain. The significant negative correlation between C2 slope and pain score establishes C2 slope as a simple and reliable indicator of cervical sagittal imbalance that can be easily assessed on routine MRI. The positive association between T1 slope and cervical lordosis confirms their biomechanical role in maintaining cervical alignment and horizontal gaze. Reduced cervical lordosis suggests early postural maladaptation, particularly in occupational neck pain. Early detection of these changes may guide ergonomic correction and timely clinical intervention, helping to prevent chronic neck disability.

Ethical Clearance

Ethical approval for the study was obtained from the Institutional Ethics Committee of Government Doon Medical College and Hospital, Dehradun (Ref No: GDMC/IEC/2024/6, dated 21/08/2024). The committee reviewed and approved the study protocol, including its scientific rationale and ethical considerations. The study was conducted in accordance with institutional guidelines and ICMR/DHR norms, ensuring confidentiality of samples and adherence to the approved protocol.

Data Availability Declaration

The datasets generated and/or analyzed during the current study are available from the corresponding author on reasonable request.

Artificial Intelligence (AI) Disclosure

The authors declare that no AI tools were used in the preparation of this manuscript.

Acknowledgment

The authors would like to express their regards to all teaching and non-teaching staff of the Department of Anatomy, Government Doon Medical College, Dehradun, including my colleagues Dr Shivangi Thakur and Dr Kritika Tyagi. The authors would like to express special thanks to their senior, Dr Anjali Sharan, and Dr Abhinav Kumar for their motivation. They also extend their regards to the employees of the Department of Radiodiagnosis, Government Doon Medical College, who helped them procure soft copies of MRI scans.

Authors' Contributions

Dr Jolly Agarwal and Dr Shrikant Bharti contributed to the conceptualization and design of the study. The intellectual content was developed by Dr Jolly Agarwal, Dr Abhinav Kumar, and Dr Abhishek K Yadav. The investigation was carried out by Dr Shrikant Bharti, Dr Abhinav Kumar, Dr Shivangi Thakur, and Dr Abhishek K Yadav. Manuscript writing was undertaken by Dr Shrikant Bharti, Dr Abhinav Kumar, and Dr Shivangi Thakur. Literature review and writing were performed by Dr Shrikant Bharti and Dr Abhinav Kumar.

Orcid

Shrikant Bharti https://orcid.org/0009-0007-4045-927X

References

1. Wu AM, Cross M, Elliott JM, et al. Global, regional, and national burden of neck pain, 1990–2020, and projections to 2050: A systematic analysis of the Global Burden of Disease Study 2021. Lancet Rheumatol 2024;6(3):e142–e155. DOI: 10.1016/S2665-9913(23)00321-1.
2. Chen X, O'Leary S, Johnston V. Modifiable individual and work-related factors associated with neck pain in 740 office workers: A cross-sectional study. Braz J Phys Ther 2022;22(4):318–327. DOI: 10.1016/j.bjpt.2018.03.003.
3. Weng C, Wang J, Tuchman A, et al. Influence of T1 slope on the cervical sagittal balance in degenerative cervical spine. Spine (Phila Pa 1976) 2016;41(3):185–190. DOI: 10.1097/BRS.0000000000001353.
4. Knott PT, Mardjetko SM, Techy F. The use of the T1 sagittal angle in predicting overall sagittal balance of the spine. Spine J 2010;10(11):994–998. DOI: 10.1016/j.spinee.2010.08.031.
5. Creţan MI, Gafitanu M, Munteanu F. The geometrical parameters of the human intervertebral disc measured using CT and AutoCAD. In: 7th International Multidisciplinary Conference; 2007 May 17–18; Baia Mare, Romania. pp. 140–146.
6. Sullivan GM, Artino AR. Analyzing and interpreting data from Likert-type scales. J Grad Med Educ 2013;5(4):541–542. DOI: 10.4300/JGME-5-4-18.
7. Protopsaltis T, Terran J, Soroceanu A, et al. T1 slope minus cervical lordosis (TS-CL), the cervical answer to PI-LL, defines cervical sagittal deformity in patients undergoing thoracolumbar osteotomy. Int J Spine Surg 2018;12(3):362–370. DOI: 10.14444/5042.
8. Protopsaltis TS, Ramchandran S, Tishelman JC, et al. The importance of C2 slope, a singular marker of cervical deformity, correlates with patient-reported outcomes. Spine (Phila Pa 1976) 2020;45(3):184–192. DOI: 10.1097/BRS.0000000000003214.
9. Chai Z, Yang X, Lu H, et al. Relationship between C2 slope with sagittal parameters and clinical function of degenerative cervical kyphosis. J Orthop Surg Res 2023;18(1):514. DOI: 10.1186/s13018-023-04011-0.
10. Jouibari MF, Le Huec JC, Hameghavandi MHR, et al. Comparison of cervical sagittal parameters among patients with neck pain and

healthy controls: A comparative cross-sectional study. Eur Spine J 2019;28(10):2319–2324. DOI: 10.1007/s00586-019-06117-8.
11. Aşkin A, Bayram KB, Demirdal ÜS, et al. The evaluation of cervical spinal angle in patients with acute and chronic neck pain. Turk J Med Sci 2017;47(3):806–811. DOI: 10.3906/sag-1601-179.
12. Park JH, Cho CB, Song JH, et al. T1 slope and cervical sagittal alignment on cervical CT radiographs of asymptomatic persons. J Korean Neurosurg Soc 2013;53(6):356–359. DOI: 10.3340/jkns.2013.53.6.356.
13. David E, Leonid K, Azaria S, et al. The association between cervical lordosis and age, sex, history of cervical trauma and sedentarity: A CT study. Arch Anat Physiol 2020;5(1):009–015. DOI: 10.17352/aap.000014.

ORIGINAL RESEARCH

Decoding Vascular Patterns of Vasa Recta and Arterial Arcades of Small Intestine: A Morphometric Study with Novel Clinical Applications for Safer Surgeries and Improved Bowel Viability

Garima Sehgal[1], Shweta Nayak[2], Khushboo Yadav[3]

Received on: 02 April 2026; *Accepted on:* 01 May 2026; *Published on:* 12 June 2026

Abstract

Background: Vascular architecture of the small intestine has traditionally been described in terms of arterial arcade (AA) tiers; however, this approach remains largely qualitative and may not fully capture regional vascular variability. A detailed quantitative assessment of AAs and vasa recta (VR) across the jejunum and ileum is essential for better anatomical understanding and improved surgical application.

Aim: To perform a comprehensive morphometric analysis of the AAs and VR of the small intestine and to evaluate segmental variations with potential clinical implications for bowel viability and surgical planning.

Materials and methods: This descriptive cadaveric study was conducted on eight embalmed adult cadavers. The jejunum and ileum with attached mesentery were dissected and divided into four standardized 30 cm segments: S1 (proximal jejunum), S2 (distal jejunum), S3 (proximal ileum), and S4 (distal ileum). The number of AAs, the number of VR, and the length of VR were recorded in each segment. Length measurements were repeated four times per specimen to minimize intra-observer bias, and mean values were used for analysis. Data were expressed as mean ± standard deviation (SD), and comparisons across segments were performed using one-way analysis of variance (ANOVA).

Results: A progressive increase in vascular complexity was observed from the proximal jejunum to the distal ileum. The mean number of AAs increased from 36.50 ± 16.82 in S1 to 70.87 ± 5.28 in S4, whereas the number of VR increased from 21.87 ± 4.02 to 72.25 ± 5.99. In contrast, the mean length of VR decreased from 5.02 ± 0.97 cm in S1 to 2.78 ± 0.51 cm in S4. Variability was greater in proximal segments and decreased distally, indicating a more uniform vascular pattern in the ileum. These differences were statistically significant ($p < 0.05$).

Keywords: Arterial arcades, Ileum, Jejunum, Mesenteric vasculature, Small intestine, Surgical anatomy, Vasa recta.

Journal of Anatomical Sciences (2026): 10.5005/jas-11049-0022

Introduction

The macroscopic anatomy of the small intestinal vasculature has been extensively studied using cadaveric dissection and post-mortem vascular injection techniques, which have provided foundational insights into mesenteric vascular organization.[1–3] These classical approaches have established that the primary arterial supply to the jejunum and ileum is derived from branches of the superior mesenteric artery (SMA), which traverse the mesentery and exhibit a characteristic pattern of bifurcation and anastomosis with adjacent branches arising at different levels.[2,4]

This branching architecture gives rise to arterial arcades (AAs) in the form of looped vascular networks that demonstrate distinct regional variability along the small intestine.[1,2] The jejunum is characterized by fewer (1–2) AAs with long, straight vasa recta (VR), whereas the ileum exhibits a more complex arrangement with three to five arcades and shorter, more numerous VR.[1,2,5] The VR arise from the terminal arcades and course toward the intestinal wall to deliver oxygenated blood to the bowel.[2,4]

Despite these well-documented anatomical patterns, a comprehensive segmental morphometric analysis of AAs and VR along the entire length of the small intestine remains limited. Most previous studies have focused on qualitative descriptions or region-specific observations without detailed loop-by-loop quantification.[3,6]

Additionally, the clinical implications of these vascular variations, particularly in the context of intestinal resection, anastomotic integrity, ischemic vulnerability, and preservation of bowel viability, are not yet fully elucidated.[7–9] Variations in mesenteric vascular architecture may significantly influence susceptibility to ischemia and surgical outcomes, especially in conditions such as acute mesenteric ischemia and bowel necrosis.[7,8]

A precise understanding of these vascular patterns is increasingly relevant in modern surgical practice, including minimally invasive procedures and bowel-preserving strategies, where preservation of adequate perfusion is critical.[9,10]

[1]Department of Anatomy, King George's Medical University, Lucknow, Uttar Pradesh, India

[2]King George's Medical University, Lucknow, Uttar Pradesh, India

[3]Department of Anatomy, Kalyan Singh Government Medical College, Bulandshahr, Uttar Pradesh, India

Corresponding Author: Garima Sehgal, Department of Anatomy, King George's Medical University, Lucknow, Uttar Pradesh, India, Phone: + 91 9044513758, e-mail: garimasehgal@kgmcindia.edu

How to cite this article: Sehgal G, Nayak S, Yadav K, *et al.* Decoding Vascular Patterns of Vasa Recta and Arterial Arcades of Small Intestine: A Morphometric Study with Novel Clinical Applications for Safer Surgeries and Improved Bowel Viability. J Anat Sciences 2026;34(1): 18–21.

Source of support: Nil

Conflict of interest: None

Therefore, this study aims to provide a detailed morphometric evaluation of the vascular architecture of the jejunum and ileum through meticulous loop-by-loop dissection. By dividing the small intestine into standardized segments, this study seeks to generate clinically applicable data that may contribute to safer surgical interventions and improved assessment of bowel viability.

Materials and Methods

This descriptive cadaveric study was conducted in the Department of Anatomy at King George's Medical University (KGMU), Lucknow, Uttar Pradesh, India. A total of eight embalmed adult cadavers (six males and two females; mean age: 73 years) were included in the study.

The entire jejunum and ileum, along with the attached mesentery, were carefully dissected and removed. The mesenteric vasculature was exposed by meticulous dissection of the mesentery, preserving the integrity of AAs and VR.

For standardization, the small intestine was divided into four sequential segments, each measuring 30 cm in length. The jejunal segment was identified starting approximately 3–5 cm distal to the duodenojejunal flexure, whereas the ileal segment extended up to 5–10 cm proximal to the ileocecal junction. Based on proximal-to-distal orientation, the segments were designated as follows:

- S1: Proximal-most segment
- S2 and S3: Intermediate segments
- S4: Distal-most segment

Care was taken throughout the dissection to avoid disruption of vascular continuity.

In each 30 cm segment, the following parameters were recorded:

- Number of AAs: Counted from the primary branch arising from the SMA.
- Number of VR: Counted as straight vessels originating from the terminal arcades within each segment.
- Length of VR: Measured from their point of origin at the AA to their termination at the mesenteric border of the intestinal wall.

All measurements were performed using a digital Vernier caliper with a precision of 0.01 mm to ensure accuracy. Each measurement was repeated four times, and the mean value was considered for final analysis to minimize intra-observer bias.

All observations were documented systematically and subjected to descriptive statistical analysis.

Data were expressed as mean ± standard deviation (SD). One-way analysis of variance (ANOVA) was used to compare morphometric parameters across four intestinal segments (S1–S4). A p-value < 0.05 was considered statistically significant.

Observations and Results

Arterial Arcades (Table 1)

A progressive increase in the number of AAs was observed from the proximal jejunum (S1) to the distal ileum (S4). The mean number of arcades increased steadily, and the range of values also demonstrated a shift toward higher counts distally. There was a clear proximal-to-distal escalation in AA density, with the distal ileum (S4) demonstrating the highest number of arcades (Fig. 1).

Standard deviation was highest in S1 (±16.82), indicating greater variability in the proximal jejunum. A decrease in SD toward distal segments (S3, S4) suggested a more consistent vascular pattern in the ileum.

One-way ANOVA demonstrated a progressive increase in the number of AAs from S1 to S4 ($p < 0.05$). Significant differences were most notable between proximal jejunal (S1) and distal ileal (S4) segments.

Table 1: Segment-wise distribution of AAs (per 30 cm bowel segment, $n = 8$)

Segment	*Region*	*Range*	*Mean ± SD*
S1	Proximal jejunum	24–76	36.50 ± 16.82
S2	Distal jejunum	28–56	42.25 ± 10.04
S3	Proximal ileum	48–64	56.62 ± 5.10
S4	Distal ileum	64–79	70.87 ± 5.28

AAs, arterial arcades; SD, standard deviation

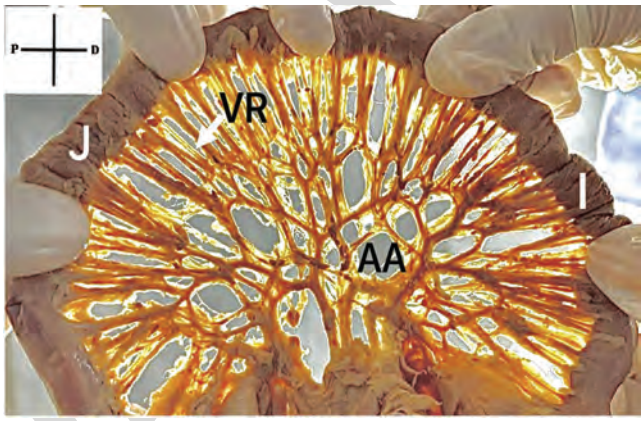

Fig. 1: Showing the S2–S3 junctional segment, jejunal loop (J); 1–2 rows of AA with longer and fewer VR vs ileal loop (I) having 3–4 rows of AA with relatively shorter and numerous VR; proximal (P), distal (D)

Table 2: Segment-wise distribution of VR (per 30 cm bowel segment, $n = 8$)

Segment	*Region*	*Range*	*Mean ± SD*
S1	Proximal jejunum	17–28	21.87 ± 4.02
S2	Distal jejunum	36–49	42.87 ± 5.09
S3	Proximal ileum	49–64	56.50 ± 4.63
S4	Distal ileum	63–80	72.25 ± 5.99

SD, standard deviation; VR, vasa recta

VR Count (Table 2)

The number of VR also showed a marked and consistent increase from jejunum to ileum. A near-linear increase in the number of VR was observed across segments (Fig. 1).

A progressive increase in the number of VR was observed from proximal jejunum (S1) to distal ileum (S4). The mean number sharply increased from 21.87 in S1 to 72.25 in S4, representing more than a threefold increase. The SD remained relatively low across all segments, indicating consistent distribution patterns of VR among specimens. Slightly higher variability is noted in the distal ileum (S4), suggesting minor inter-individual differences in vascular density at the terminal bowel.

Table 3: Segment-wise comparison of length of VR (cm) ($n = 8$)

Segment	*Region*	*Range*	*Mean ± SD*
S1	Proximal jejunum	3.77–6.40	5.02 ± 0.97
S2	Distal jejunum	2.65–5.10	3.82 ± 0.78
S3	Proximal ileum	2.25–4.47	3.28 ± 0.67
S4	Distal ileum	2.15–3.82	2.78 ± 0.51

SD, standard deviation; VR, vasa recta. Range based on mean values per specimen

Length of VR (Table 3)

In contrast to the above parameters, the length of the VR showed a decreasing trend from proximal to distal segments. There was a progressive shortening of VR from the jejunum to ileum, indicating a transition from fewer long vessels proximally to numerous short vessels distally (Fig. 1).

The mean length declined from 5.02 cm in S1 to 2.78 cm in S4, confirming a proximal-to-distal shortening trend. The SD decreased from S1 (±0.97) to S4 (±0.51), indicating greater variability in proximal segments and increasing uniformity in the distal ileal vascular pattern.

Discussion

Various methodologies have been employed in the past to study the vascular anatomy of the small intestine, including cadaveric dissection and *in vivo* imaging, primarily focusing on the number and arrangement of jejunal and ileal branches arising from the SMA.[1,2] However, these approaches have often provided partial insights into the complete vascular architecture. This study sought to address this gap through a meticulous loop-by-loop dissection of the jejunum and ileum, enabling a comprehensive morphometric comparison of mesenteric vascular patterns across standardized segments.

Traditionally, the vascular architecture of the small intestine has been described in terms of the number of AA tiers, with the jejunum exhibiting fewer tiers and the ileum demonstrating multiple layers. While this classification is useful for descriptive anatomy, it remains largely qualitative and does not adequately capture the true vascular density or inter-segmental variability.

In this study, the total number of AAs was quantified within standardized 30 cm segments, providing a more objective and reproducible morphometric parameter. This approach allowed for precise comparison across different regions of the small intestine and enabled statistical analysis of vascular patterns.

Additionally, quantification of arcade number per unit length offers a greater clinical relevance, as it accurately reflects the extent of collateral circulation and potential perfusion capacity of the bowel.

A key finding of this study was the progressive increase in the number of AAs and VR from proximal jejunum to distal ileum, accompanied by a significant reduction in the length of VR. Specifically, the mean number of AAs increased from 36.50 in the proximal jejunum to 70.87 in the distal ileum, whereas the number of VR increased from 21.87 to 72.25 across the same segments. In contrast, the mean length of VR decreased from 5.02 to 2.78 cm. These findings were statistically significant and demonstrate a clear proximal-to-distal vascular gradient.

This pattern is consistent with classical anatomical descriptions, which report that the jejunum is characterized by fewer AAs and longer VR, whereas the ileum exhibits multiple tiers of arcades with shorter and more numerous VR.[1,2,4,5] Previous studies comparing jejunal and ileal vascular patterns have similarly reported a higher density of VR in the ileum.[1,2] Our findings not only corroborate these observations but also extend them by providing segmental quantification and statistical validation.

An important additional observation in this study is the variation in SD across segments, with greater variability noted in the proximal jejunum and relatively lower variability in the distal ileum. This suggests that while the proximal segments exhibit greater anatomical variability, the distal ileum demonstrates a more uniform and predictable vascular pattern. Such consistency in distal vascular architecture may have implications for surgical planning and the reliability of perfusion.

The increased number of AAs in the ileum may be explained by both anatomical and physiological factors. The longer mesentery of the ileum necessitates a more extensive vascular network to ensure adequate perfusion over a greater distance. Furthermore, a tiered arcade system may serve as a mechanical and functional adaptation, providing resilience against mesenteric stretch, torsion, and fluctuations in blood flow. Unlike a single linear arterial pathway, multiple interconnected arcades can distribute hemodynamic stress more effectively and maintain perfusion under varying physiological conditions.

Although earlier studies suggested limited communication between VR within the mesentery, subsequent work has emphasized the importance of the terminal AAs in maintaining collateral circulation, particularly during peristaltic activity.[4,7–9] The presence of multiple arcades in the ileum may therefore provide a protective advantage under conditions, such as hypoxia or hypovolemia, as a dense anastomotic network can sustain tissue perfusion even when individual vessels are compromised.[10]

From a functional perspective, the differences in vascular architecture between the jejunum and ileum may also reflect their differing physiological roles. The jejunum, being the primary site for nutrient absorption, may rely on longer, straighter vessels for efficient perfusion, whereas the ileum, with its comparatively lower absorptive demand, exhibits a more complex but compact vascular network.[1]

From a clinical standpoint, these findings have significant implications. The jejunum is widely used in reconstructive surgery, particularly in jejunal free flap transfer.[11–13] The presence of long, relatively unbranched VR in the jejunum, as confirmed in this study, facilitates microvascular anastomosis by providing consistent and accessible vascular pedicles.

Furthermore, the availability of multiple VR allows for the creation of dual or multiple vascular pedicles. These vessels are capable of perfusing flaps up to 25 cm in length, thereby reducing the risk of ischemia and improving surgical outcomes.[14] Additional advantages include the unbranched course of VR before entering the bowel wall, ease of dissection, and the ability to perform microvascular anastomosis without the need for extensive bowel or vessel resection.[13]

Advanced reconstructive techniques, including double-pedicle jejunal flaps, further enhance flap viability without increasing donor site morbidity, highlighting the clinical relevance of detailed vascular anatomical knowledge.[15]

Although this study did not directly measure vessel diameter, previous reports indicate that jejunal VRs have a larger mean diameter (approximately 0.77 mm) compared with those of the ileum (approximately 0.56 mm). This larger caliber, combined with a simpler AA pattern, enhances surgical handling and contributes to improved perfusion reliability.[13]

Future studies with larger sample sizes and more diverse populations are needed to confirm and expand these findings. Anatomical observations can be combined with imaging techniques to better understand the functional significance.

Further research on blood flow dynamics, vessel diameter, and microcirculation may improve the clinical relevance of these findings. The proposed vascular gradient model can also be explored in relation to intestinal ischemia, anastomotic healing, and surgical outcomes, especially in minimally invasive and bowel-preserving procedures.

Use of three-dimensional reconstruction techniques may further enhance understanding of mesenteric vascular patterns and aid in surgical planning and teaching.

Limitation(s) of the Study

Despite its strengths, this study has certain limitations. First, the sample size was relatively small ($n = 8$), which may limit the generalizability of the findings. Second, the study was conducted on embalmed cadavers, where vascular dimensions and tissue characteristics may differ from those in living individuals due to fixation-related changes. Third, although meticulous measurements were performed, inter-observer variability was not assessed, and only intra-observer bias was minimized through repeated readings. Variations related to age, sex, and underlying comorbidities could not be evaluated due to limited specimen data.

Conclusions

This study provides a comprehensive morphometric evaluation of the vascular architecture of the small intestine, demonstrating a clear proximal-to-distal gradient characterized by increasing AAs and VR density, along with a concomitant decrease in vessel length. This "vascular gradient model" offers a structured understanding of regional vascular variability between the jejunum and ileum.

These findings have direct clinical relevance, particularly in guiding intestinal resections, optimizing anastomotic planning, and enhancing the reliability of jejunal free flap procedures. A precise appreciation of this segmental vascular organization may contribute to safer surgical strategies and improved bowel viability outcomes.

Ethical Approval

This cadaver-based study was conducted on bodies donated through our institutional body donation program with informed consent, in accordance with institutional protocols and applicable ethical and regulatory guidelines and is considered exempt from formal ethics committee review.

Data Availability Declaration

All relevant data generated or analyzed during this study are included in the manuscript.

Artificial Intelligence (AI) Disclosure

No (AI) tools were used for data collection, analysis, interpretation, or generation of scientific content. Artificial intelligence-assisted language tools were used only for grammatical refinement and improvement of manuscript readability.

Acknowledgment

The authors gratefully acknowledge the individuals who donated their bodies for medical education and research, without whom this study would not have been possible. The authors sincerely acknowledge the support of the Department of Anatomy and thank all individuals who contributed directly or indirectly to the completion of this work.

Authors' Contributions

Garima Sehgal: Conceptualization, study supervision, methodology, analysis, Interpretation of results, critical revision of the manuscript, and final approval.

Shweta Nayak: Literature review, data collection, analysis, manuscript drafting and final approval.

Khushboo Yadav: Study supervision, analysis, interpretation of results, manuscript editing, and final approval.

References

1. Standring S, editor. Gray's Anatomy: The Anatomical Basis of Clinical Practice. 41st ed. Elsevier; 2016.
2. Moore KL, Dalley AF, Agur AMR. Clinically Oriented Anatomy. 8th ed. Wolters Kluwer; 2018.
3. Rosenblum JD, Boyle CM, Schwartz LB. The mesenteric circulation: Anatomy and physiology. Surg Clin North Am 1997;77(2):289–306. DOI: 10.1016/s0039-6109(05)70549-1.
4. Michels NA. Blood Supply and Anatomy of the Upper Abdominal Organs with a Descriptive Atlas. Philadelphia: Lippincott; 1955.
5. Skandalakis JE, Colborn GL, Skandalakis LJ, et al. The surgical anatomy of the small intestine. In: Skandalakis JE, editor. Surgical Anatomy and Technique. Springer; 2000.
6. Noer RJ, Derr JW, Johnston CG. The circulation of the small intestine: An evaluation of its revascularizing potential. Ann Surg 1949;130(4):608–621. DOI: 10.1097/00000658-194910000-00004.
7. Acosta S. Mesenteric ischemia. Curr Opin Crit Care 2015;21(2):171–178. DOI: 10.1097/MCC.0000000000000189.
8. Clair DG, Beach JM. Mesenteric ischemia. N Engl J Med 2016;374:959–968. DOI: 10.1056/NEJMra1503884.
9. Bala M, Kashuk J, Moore EE, et al. Acute mesenteric ischemia: Guidelines of the World Society of Emergency Surgery. World J Emerg Surg 2017;12:38. DOI: 10.1186/s13017-017-0150-5.
10. Oldenburg WA, Lau LL, Rodenberg TJ, et al. Acute mesenteric ischemia: A clinical review. Arch Intern Med 2004;164(10):1054–1062. DOI: 10.1001/archinte.164.10.1054.
11. Nakatsuka T, Harii K, Asato H, et al. Analytic review of 2372 free flap transfers for head and neck reconstruction following cancer resection. J Reconstr Microsurg 2003;19(6):363–368. DOI: 10.1055/s-2003-42630.
12. Razdan SN, Albornoz CR, Matros E, et al. Free Jejunal Flap for Pharyngoesophageal Reconstruction in Head and Neck Cancer Patients: An Evaluation of Donor-Site Complications. J Reconstr Microsurg 2015;31(9):643–646. DOI: 10.1055/s-0035-1556872.
13. Urken ML, Buchbinder D, Costantino PD, et al. Oromandibular reconstruction using microvascular composite flaps: Report of 210 cases. Arch Otolaryngol Head Neck Surg 1998;124(1):46–55. DOI: 10.1001/archotol.124.1.46.
14. Chen HC, Tang YB. Microsurgical reconstruction of the esophagus. Semin Surg Oncol 2000;19(3):235–245. DOI: 10.1002/1098-2388(200010/11)19:3<235::aid-ssu5>3.0.co;2-m.
15. Yu P, Chang DW, Miller MJ, et al. Analysis of 49 cases of flap compromise in 1310 free flaps for head and neck reconstruction. Head Neck 2009;31(1):45–51. DOI: 10.1002/hed.20927.

ORIGINAL RESEARCH

To Study Heterogeneity in the Distribution of Microglia and Astrocytes at Different Sites of Brain: Immunohistochemical Analysis by Using CD68 and Glial Fibrillary Acidic Protein, Respectively

Shivangi Thakur[1], Swati Saxena[2], Mamta Gupta[3], Rajesh K Maurya[4], Jolly Agarwal[5], Mahendra K Pant[6]

Received on: 17 March 2026; *Accepted on:* 03 May 2026; *Published on:* 12 June 2026

Abstract

Background: Microglia and astrocytes are regionally specialized glial populations that support homeostasis and participate in neuroinflammation. Regional and sex-associated differences in their distribution may be relevant to the interpretation of neuropathology.

Objective: To evaluate the density and staining intensity of microglia and astrocytes across selected regions of the adult human brain and to compare their distributions by sex.

Methodology: This cross-sectional cadaveric study was conducted at Government Doon Medical College, Dehradun. Brain specimens from 10 cadavers (7 males, 3 females; age range 60–90 years) were sampled from the frontal, parietal, temporal, and occipital cortex and the corpus callosum. Immunohistochemistry (IHC) was performed using CD68 (microglia) and glial fibrillary acidic protein (GFAP) (astrocytes). Cell density was quantified as cells/mm^2 across 15 fields per slide using Olympus cellSens Entry v3.2; results were summarized as mean and standard deviation. Sex-wise comparisons were assessed using the independent-samples *t*-test.

Results: Microglial density was higher in males than in females in most regions, with significant sex-wise differences in the frontal lobe ($p = 0.04$), occipital lobe ($p = 0.02$), and corpus callosum ($p = 0.001$). Astrocyte density was higher in males than in females in most regions except the frontal lobe, with significant differences in the temporal lobe ($p = 0.02$), occipital lobe ($p = 0.04$), and corpus callosum ($p = 0.003$).

Conclusion: Microglia and astrocytes show heterogeneous, region-specific distributions in the adult human brain with differences by sex. These baseline patterns may help contextualize regionally selective vulnerability and glial responses in neuropathological conditions.

Keywords: Astrocytes, CD68, Glial fibrillary acidic protein, Immunohistochemistry, Microglia.

Journal of Anatomical Sciences (2026): 10.5005/jas-11049-0023

Introduction

There are mainly three types of glial cells: Microglia, oligodendrocytes, and astrocytes, which are present in the central nervous system (CNS). Among them, microglia arise from mesenchymal origins, while astrocytes are derived from the neuroepithelium.[1] Pío del Río Hortega, the Spanish neuroscientist, was the first one to introduce the term "microglia" in 1920.[2] Microglia constitute about 0.5–10% of all the glial cells present in the CNS, and they are characterized by their small cell bodies with multiple branching processes.[1,2] According to Lawson et al., the density of microglia varies within the CNS, they ranges from 5% in the cerebral cortex and corpus callosum to about 12% in the substantia nigra, with increased concentrations in gray matter than in white matter.[3]

Microglia are essential in brain development, homeostasis, communication, the regulation of neurogenesis, and in controlling neuroinflammation. They monitor synaptic activity, initiate defense responses against harmful stimuli, and contribute to tissue repair and regeneration by releasing pro-inflammatory factors such as prostaglandins, nitric oxide, cytokines, and chemokines. In conditions like infection, stroke, trauma, or neurodegeneration, microglia undergo significant morphological and functional changes, exerting both protective and harmful effects.[4–7] Aberrant microglial activity contributes to the progression of Alzheimer's disease, where microglia engage with astrocytes to promote neuroinflammation. Markers of both cell types are elevated in Alzheimer's, but the increase in microglial markers is largely due to heightened activation rather than an increase in their overall numbers.[8] Overactive microglia are also implicated in multiple sclerosis, major depressive disorder, and systemic conditions like sepsis, where they play a role in behavioral and immune changes.[9,10]

Astrocytes, on the other hand, are key components of the blood–brain barrier, provide structural support, regulate energy metabolism, and detoxify synaptic spaces by secreting growth

[1,2,4–6]Department of Anatomy, Government Doon Medical College, Dehradun, Uttarakhand, India

[3]Department of Pathology, Government Doon Medical College, Dehradun, Uttarakhand, India

Corresponding Author: Swati Saxena, Department of Anatomy, Government Doon Medical College, Dehradun, Uttarakhand, India, Phone: +91 7880989023, e-mail: 21swatidocsaxena@gmail.com

How to cite this article: Thakur S, Saxena S, Gupta M, *et al*. To Study Heterogeneity in the Distribution of Microglia and Astrocytes at Different Sites of Brain: Immunohistochemical Analysis by Using CD68 and Glial Fibrillary Acidic Protein, Respectively. J Anat Sciences 2026;34(1):22–27.

Source of support: Nil

Conflict of interest: None

factors, cytokines, and extracellular matrix proteins crucial for neuronal repair and regeneration.[11] They account for a significant proportion of brain cells and play an essential role in the regulation of cerebral blood flow and the maintenance of glucose homeostasis. Playing the role of the brain's principle source of energy, astrocytes are associated with neurodegenerative diseases namely Alzheimer's disease and amyotrophic lateral sclerosis (ALS). Evidence indicates that in the early stages of these conditions, astrocytic atrophy disrupts synaptic connections, impairs neurotransmitter balance, and contributes to neuronal death.[10]

Immunohistochemistry (IHC) is a diagnostic method which is based on antigen–antibody interactions, which allows the detection of specific protein expression within cells by using targeted antibodies.[2] It is especially valuable in pathology because it preserves tissue and cellular architecture, enabling not only identification of antigens but also correlation with particular cell types and histological patterns. Immunohistochemistry is widely applied in surgical and anatomic pathology for cell classification and diagnostic purposes, relying on antibodies directed against cellular antigens to determine cell types.[12,13]

For the identification of microglia, which are specialized macrophages of the brain, CD68 serves as a well-recognized marker for microglia, while glial fibrillary acidic protein (GFAP) is recognized as the primary intermediate filament protein in astrocytes and is accepted as a specific astrocytic marker in the CNS.[8,10]

Aim

The present study aims to examine and evaluate the regional density of microglia and astrocytes in the adult human cadaveric brain.

Objectives

- To evaluate the density score of microglia and astrocytes in different regions of the brain.
  - Gray matter of the frontal lobe.
  - Gray matter of the parietal lobe.
  - Gray matter of the occipital lobe.
  - Gray matter of the temporal lobe.
  - Corpus callosum.
- To assess gender-wise differences in the distribution of microglia and astrocytes in different regions of the brain.
- To observe the intensity of staining of microglia and astrocytes at the above-mentioned sites.

Methodology

Type of Study

Retrospective Study

The present study was conducted from February 2025 to April 2026 jointly in the Department of Anatomy and the Department of Pathology at Government Doon Medical College, Dehradun (Uttarakhand). Prior approval from ethical committee was taken with reference number GDMC/IEC/2024/5. No Clinical Trial Registry number was required as this study is not a clinical trial and it is done on the cadavers present in the department. The study included brain specimens from 10 cadavers out of which 7 specimens were from male cadavers and 3 specimens were from female cadavers with age ranges from 60 to 90 years (mean age is 80.8). The brain samples were retrieved from donated body received in the department of anatomy. The ethical clearance was obtained prior from the Ethics Committee, Government Doon Medical College, Dehradun.

Inclusion Criteria

Samples will be procured from cadavers present in the Anatomy Department of GDMC, Dehradun.

Exclusion Criteria

The area of brain showing evidence of abrasion, infection, and laceration were excluded from the study.

Tissue Processing and Staining

The brain specimens were taken from five sites, viz., all four cortical areas and the corpus callosum, measuring about 1 × 1 cm. The tissues were processed, and slides were made using Poly L-Lysine precoated glass slides on which IHC was performed, CD-68 was used for microglia, and GFAP was used for astrocytes. With the help of Olympus CellSens Entry version 3.2 software, the density of microglia and astrocytes was measured by counting the number of microglia and astrocytes present per field on a total of 15 fields per slide. The mean was calculated to reduce the chances of error.

Statistical Analysis

The data were entered and tabulated in a Microsoft Excel sheet and are subjected to statistical analysis. The results were expressed as mean and standard deviation.

Results

The quantitative analysis of microglial cells and astrocytes was performed on all four cortical areas (the frontal cerebral cortex, parietal cerebral cortex, occipital cerebral cortex, and temporal cerebral cortex) and the corpus callosum. Visual assessment of the scoring of immunohistochemical staining is subjective in nature. The number of microglia per mm^2 was found to be higher in males as compared to females at all sites except the corpus callosum. The maximum number of microglia was found in the temporal lobe of males (32.14 ± 15.94) and the minimum in the parietal lobe of males (17.42 ± 8.71). In females, the maximum number was found in the corpus callosum (45 ± 11.51), and the minimum was in the parietal lobe (12 ± 8.04) and the temporal lobe (12 ± 6.68) (Table 1; Figs 1 and 2).

Table 1: Number of microglia at different sites of brain

S. No.	*Areas of brain*	*Gender*	*Mean No./mm²*	*Standard deviation*	*t-test*	*p-value*
1.	Frontal lobe	Males	28.14	±10.11	2.33	**0.04**
		Females	12.66	± 2.49		
2.	Parietal lobe	Males	17.42	± 8.71	0.82	0.43
		Females	12	± 8.04		
3.	Temporal lobe	Males	32.14	± 15.94	1.94	1.08
		Females	12	± 6.68		
4.	Occipital lobe	Males	23.14	± 11.24	3.24	**0.02**
		Females	17	± 5.71		
5.	Corpus callosum	Males	20	± 3.70	–4.61	**0.001**
		Females	45	± 11.51		

Bold values indicate statistically significant *p*-values ($p < 0.05$)

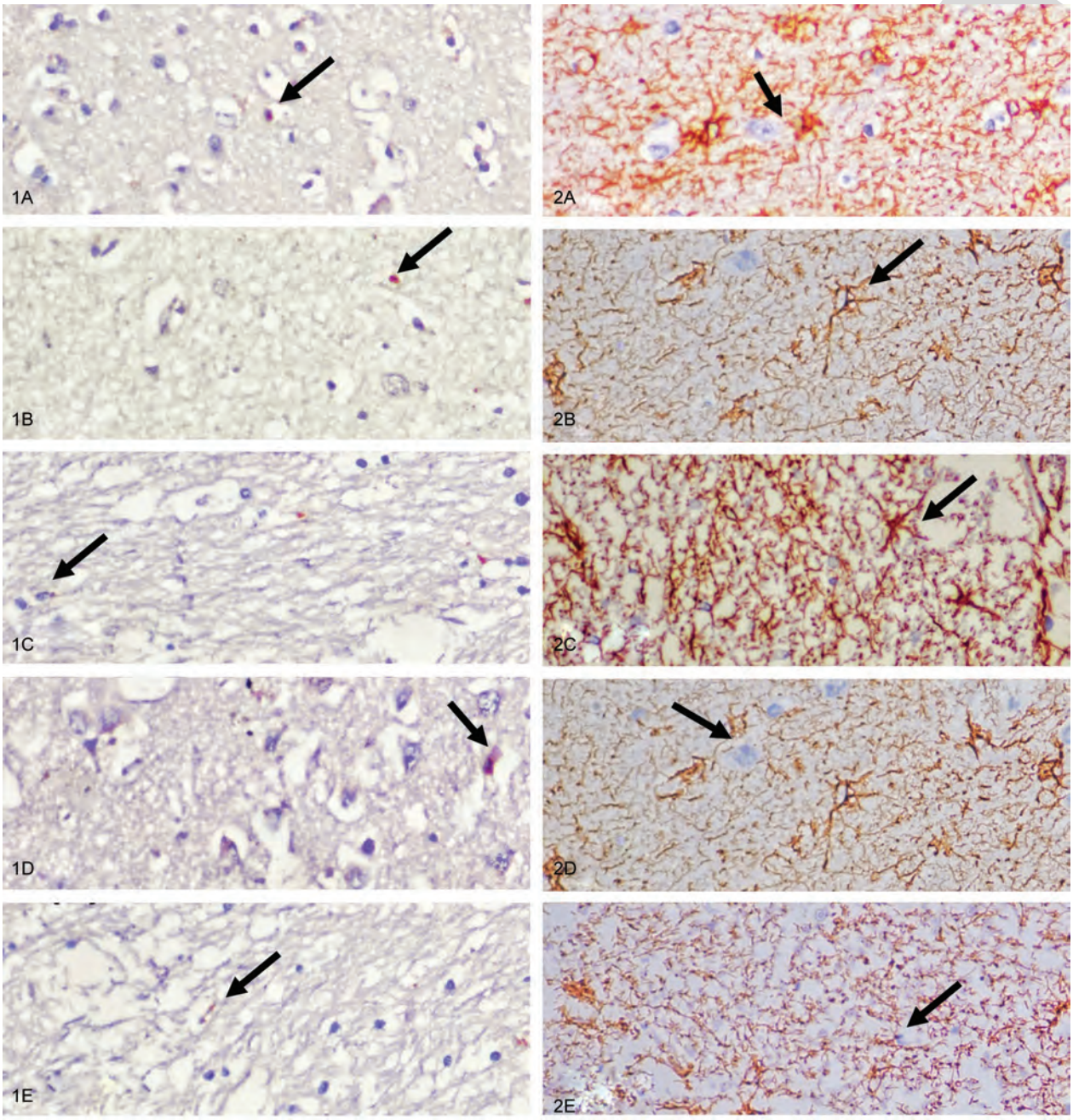

Fig. 1: Distribution of microglia (1) and astrocytes (2) at different sites of brain. (A) Distribution of microglia at frontal lobe; (B) Parietal lobe; (C) Temporal lobe; (D) Occipital lobe; and (E) Corpus callosum

The number of astrocytes per mm^2 was found to be higher in males as compared to females at all sites except the frontal lobe. The maximum number of astrocytes was found in the temporal lobe (77.33 ± 7.71) of females and the minimum in the corpus callosum (33.33 ± 14.52). In males, they were maximum in the corpus callosum (64.57 ± 26.86) and minimum in the frontal lobe (32.71 ± 11.41) (Table 2; Figs 1, 3, and 4).

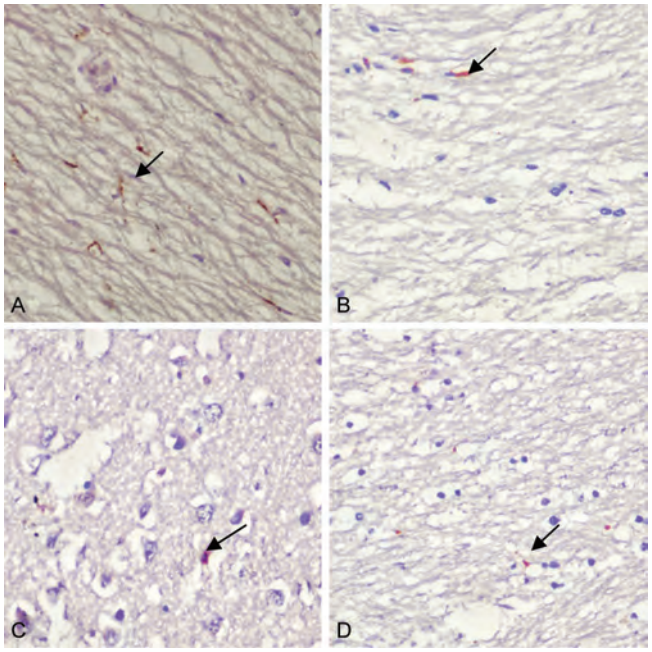

Figs 2A to D: Distribution of microglia. (A) Temporal lobe of males; (B) Temporal lobe of female; (C) Corpus callosum of males; and (D) Corpus callosum of female

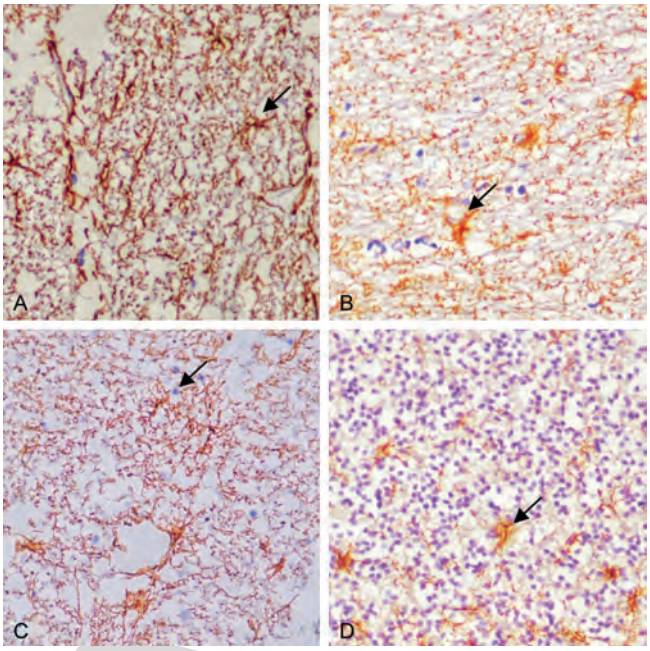

Figs 3A to D: Distribution of astrocytes. (A) Temporal lobe of males, (B) temporal lobe of female; (C) Corpus callosum of males; and (D) Corpus callosum of female

Table 2: Number of astrocytes at different sites of brain

S. No.	*Areas of brain*	*Gender*	*Mean No./mm²*	*Standard deviation*	*t-test*	*p-value*
1.	Frontal lobe	Males	32.71	± 11.41	−0.67	0.25
		Females	39	± 13.49		
2.	Parietal lobe	Males	55	± 27.54	−0.95	0.85
		Females	55.66	± 26.38		
3.	Temporal lobe	Males	58	± 23.59	0.86	**0.02**
		Females	77.33	± 7.71		
4.	Occipital lobe	Males	56.57	± 28.71	−1.97	**0.04**
		Females	39.66	± 15.17		
5.	Corpus callosum	Males	64.57	± 26.86	1.69	**0.003**
		Females	33.33	± 14.52		

Bold values indicate statistically significant *p*-values ($p < 0.05$)

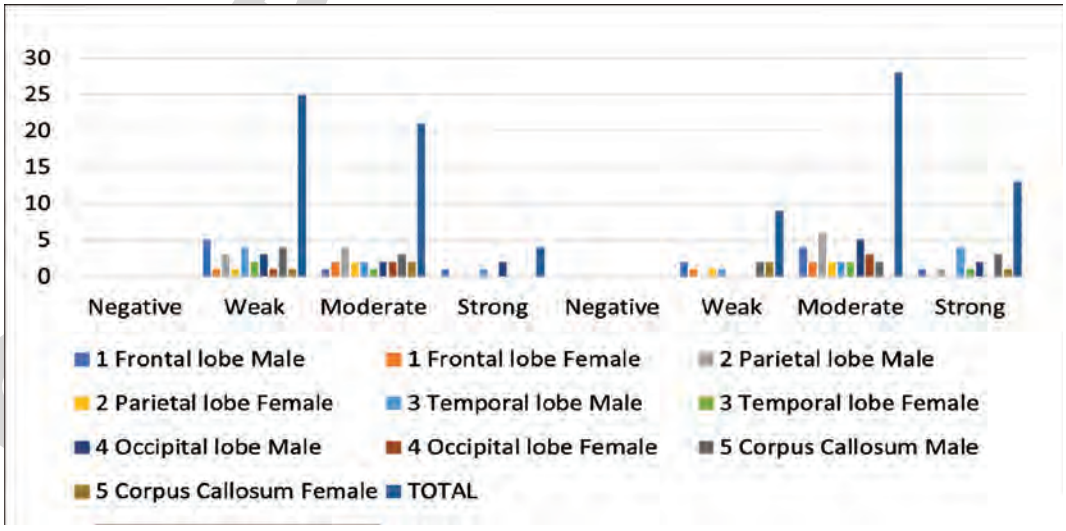

Fig. 4: Distribution of scores of the intensity of grading in microglia and astrocytes at different sites of brain (Grade 0 = Negative, Grade I = Weak, Grade II = Moderate, Grade III = Strong)

Discussion

Quantitative analysis of microglia and astrocytes at different sites of the brain is of relevance important for the diagnosis of neuropathological diseases and age-related changes. Hansen et al. conducted a study to evaluate the immunohistochemical quantification of fibrous astrocytes in the aging cerebral cortex of humans in 25 patients aged 24 to 100 years and found that astrocytes showed wide variability, with lower counts in young individuals and higher counts in older individuals. They also found a higher mean density of astrocytes in the >70 age-group, indicating a late-life acceleration of fibrous gliosis.[14]

Savchenko et al. conducted a study to see the microglia and astrocytes distribution in the normal adult rat brain using LC1, which exhibits strong specificity for IHC microglia staining. They found a higher density in the frontal lobe (123 ± 10 cells/mm^2) and the lowest density in the occipital lobe (98 ± 8 cells/mm^2), while the astrocytes counts were 2–3 times more than microglia, highest number being found in the hypothalamus and hippocampus (>260 cells/ram^2) and the lowest number being found in the cerebral cortex, midbrain, medulla oblongata, and cerebellum (<200 cells/ram^2).[15]

Mittelbronn et al. examined the regional distribution of microglia in 20 disease-free adult human brains and reported that the lowest CD68 expression was found in all gray matter areas of the cerebellum (0.3%), frontal (4.7%), parietal (3.6%), and occipital (2.9%) lobe sections and in white matter areas highest expression of CD68 was found in the pons (upper pons, 9.2%, and lower pons, 9.8%) and the medulla oblongata (11%).[16]

Kongsui et al. studied the morphology of microglia and their distribution density within the healthy prefrontal cortex of adult rats and reported that the microglia present within the cortex are heterogenous with respect to size. In the absence of injury and inflammation, the distribution of microglia within the prefrontal cortex is relatively homogenous. At Bregma + 2.5, the single-cell count (cells) was 257.90 (7.28) and the density was 9.55 (0.27).[17]

Olude et al. examined the morphology, heterogeneity, and density of astrocytes in the developing African giant rat and reported that astrocyte density ranged from 1 to 8 cells/mm^2 in the cortex to 7–17 cells/mm^2 in the dentate gyrus. The astrocyte count was highest in both juvenile and adult dentate gyri, while the minimum number was found in the brain stem and subcortex.[18]

Alrafiah and Alshali conducted a study to evaluate the prolonged formalin fixation effect on the staining characteristics of 20 human brain tissues by using the CD68 marker, and they reported that histological and immunohistochemical techniques produced reliable staining results even in human brain tissue fixed in formalin for a long duration. The study observed positive microglial cells in the frontal and temporal grey matter.[19,20]

The data of the present study are nearly similar to the study of Savchenko et al. The count of microglia was found to be higher in the temporal lobe in males (32.14 ± 15.94) and in the corpus callosum (45 ± 11.51) in females. The temporal lobe serves a crucial role in the processing of memory, the perception of auditory stimuli, language comprehension, and emotional regulation. Because of these complex, high synaptic activities and metabolic demands, microglia numbers are higher in the temporal lobe. The temporal lobe also performs a vital role in synaptic pruning. The temporal lobe is more susceptible to ageing and neurodegenerative disease. A high density of astrocytes was found in all four cortical areas in males and the temporal lobe (77.33 ± 17.71) and parietal lobe (55.66 ± 26.38) in females. The difference in distribution of microglia and astrocytes in the brain of males and females is due to genetic, hormonal, environmental and developmental factors. These gender-based differences not only impact their distribution but also their functions and how they respond to stress and injury.[21–24] It can be assumed that the varying astrocyte and microglia densities across different regions of the brain are influenced by the specialized functions of these cells in those areas, the types of neurons present, the neurotransmitters released, and the unique functional characteristics of each brain region. The variations observed between our findings and those of other researchers are likely due to differences in the markers used, the fixation methods applied, differences in ethnicity and age, underlying neuropathological conditions, if any present and the approaches adopted for data analysis.

Limitations of the Study

This study was conducted on a limited number of cadaveric brains, and all the sample which are procured are from elderly cadavers. Only selected cortical areas and the corpus callosum were studied. Although multiple fields were analyzed to reduce error, manual counting, and visual grading of staining intensity may still involve observer bias.

Conclusion

The present study was performed to evaluate the density score of microglia and astrocytes in different brain regions, which will help in understanding the pathogenesis of various neuropathological diseases like Alzheimer's disease, because their dissimilar density at different regions of the brain depends on the functioning of these cells and the types of transmitters secreted by them. As per our study, the temporal lobe in males and the corpus callosum in females are rich in microglia, and to prevent memory disorder related to stress, they can become pharmacologically relevant cells. Astrocytes are influenced by sex hormones and the regional functional demands of the brain. Higher astrocyte density in the corpus callosum of males may support increased white matter connectivity and axonal metabolism, whereas enrichment in the temporal lobe of females reflects greater synaptic activity related to cognitive and emotional processing. These differences arise from sex-specific neurodevelopmental and hormonal influences. This study improves our understanding of sex-specific differences in brain cellular organization. It may help in the early diagnosis, prevention and development of gender-specific treatment strategies for neurological and neuropsychiatric disorders, thereby improving overall public health outcomes. It can be assumed that the heterogeneous densities of astrocytes and microglia across different adult brain regions are influenced by the specific functions of these cells in those areas, the types of neurons present, the neurotransmitters released, and the unique functional characteristics of each brain region.

Data Availabilitiy Statement

All data supporting the findings of this study are contained within the manuscript. Specific datasets can be made available in part upon reasonable request to the corresponding author.

Artificial Intelligence (AI) Disclosure

The authors affirm that no AI tools or technologies were used in the design, conduct, analysis, or reporting of this study.

Acknowledgments

The author would like to thank all the teaching and non-teaching staff of the Department of Anatomy, GDMC, Dehradun, including her fellow colleagues, Dr Shrikant Bharti and Dr Kritika. She would like to give special thanks to her seniors, Dr Anjali Sharan and Dr Abhinav Kumar, for their constant support and motivation. She would also like to extend her regards to her family members, friends, and Dr Sonam Maheshwari (Statstician).

Authors' Contributions

The study involved contributions from four investigators across different domains. The concept of the study was developed by Dr Shivangi Thakur, Dr Swati Saxena, Dr Mamta Gupta, Dr Rajesh K Maurya, and Dr Mahendra K Pant. The study design was formulated by Dr Swati Saxena and Dr Mahendra K Pant. The definition of intellectual content was carried out by Dr Mamta Gupta, Dr Swati Saxena, and Dr Mahendra K Pant. Sample collection, along with tissue processing and staining, was performed by Dr Shivangi Thakur. The manuscript was written by Dr Shivangi Thakur. Data analysis was conducted by Dr Shivangi Thakur, Dr Swati Saxena, and Dr Mamta Gupta.

Orcid

Swati Saxena https://orcid.org/0000-0002-4615-1352
Jolly Agarwal https://orcid.org/0000-0002-0379-1296

References

1. Perry VH, Hume DA, Gordon S. Immunohistochemical localization of macrophages and microglia in the adult and developing mouse brain. Neuroscience 1985;15(2):313–326. DOI: 10.1016/0306-4522(85)90215-5.
2. Stankov A, Belakaposka-Srpanova V, Bitoljanu N, et al. Visualisation of microglia with the use of immunohistochemical double staining method for CD-68 and Iba-1 of cerebral tissue samples in cases of brain contusions. Pril (Makedon Akad Nauk Umet Odd Med Nauki) 2015;36(2):141–145. DOI: 10.1515/prilozi-2015-0062.
3. Lawson LJ, Perry VH, Dri P, et al. Heterogeneity in the distribution and morphology of microglia in the normal adult mouse brain. Neuroscience 1990;39(1):151–170. DOI: 10.1016/0306-4522(90)90229-w.
4. Askew K, Li K, Olmos-Alonso A, et al. Coupled proliferation and apoptosis maintain the rapid turnover of microglia in the adult brain. Cell Rep 2017;18(2):391–405. DOI: 10.1016/j.celrep.2016.12.041.
5. Chen L, Yang P, Kijlstra A. Distribution, markers, and functions of retinal microglia. Ocular immunology and inflammation 2002;10(1): 27–39. DOI: 10.1076/ocii.10.1.27.10328.
6. Lenz KM, Nugent BM, Haliyur R, et al. Microglia are essential to masculinization of brain and behavior. J Neurosci 2013;33(7):2761–2772. DOI: 10.1523/JNEUROSCI.1268-12.2013.
7. Ochocka N, Kaminska B. Microglia diversity in healthy and diseased brain: Insights from single-cell omics. Int J Mol Sci 2021;22(6):3027. DOI: 10.3390/ijms22063027.
8. Hopperton KE, Mohammad D, Trépanier MO, et al. Markers of microglia in post-mortem brain samples from patients with Alzheimer's disease: A systematic review. Mol Psychiatry 2018;23(2):177–198. DOI: 10.1038/mp.2017.246.
9. Lemstra AW, Groen in't Woud JCM, Hoozemans JJM, et al. Microglia activation in sepsis: A case-control study. J Neuroinflammation 2007;4:4. DOI: 10.1186/1742-2094-4-4.
10. Wiese S, Karus M, Faissner A. Astrocytes as a source for extracellular matrix molecules and cytokines. Front Pharmacol 2012;3:120. DOI: 10.3389/fphar.2012.00120.
11. Sidoryk-Wegrzynowicz M, Wegrzynowicz M, Lee E, et al. Role of astrocytes in brain function and disease. Toxicol Pathol 2011;39(1):115–123. DOI: 10.1177/0192623310385254.
12. Magaki S, Hojat SA, Wei B, et al. An introduction to the performance of immunohistochemistry. Methods Mol Biol 2019:1897:289–298. DOI: 10.1007/978-1-4939-8935-5_25.
13. Cizkova K, Foltynkova T, Gachechiladze M, et al. Comparative analysis of immunohistochemical staining intensity determined by light microscopy, ImageJ and QuPath in placental Hofbauer cells. Acta Histochem Cytochem 2021;54(1):21–29. DOI: 10.1267/ahc.20-00032.
14. Hansen LA, Armstrong DM, Terry RD. An immunohistochemical quantification of fibrous astrocytes in the aging human cerebral cortex. Neurobiology Aging 1987;8(1):1–6. DOI: 10.1016/0197-4580(87)90051-0.
15. Savchenko VL, Nikonenko IR, Skibo GG, et al. Distribution of microglia and astrocytes in different regions of the normal adult rat brain. Neurophysiology 1997;29(6):343–351. DOI: 10.1007/BF02463354.
16. Mittelbronn M, Dietz K, Schluesener H, et al. Local distribution of microglia in the normal adult human central nervous system differs by up to one order of magnitude. Acta Neuropathologica 2001;101(3)249–255. DOI: 10.1007/s004010000284.
17. Kongsui R, Beynon SB, Johnson SJ, et al. Quantitative assessment of microglial morphology and density reveals remarkable consistency in the distribution and morphology of cells within the healthy prefrontal cortex of the rat. J Neuroinflammation 2014;11(1):182. DOI: 10.1186/s12974-014-0182-7.
18. Olude MA, Mustapha OA, Aderounmu OA, et al. Astrocyte morphology, heterogeneity, and density in the developing African giant rat (Cricetomysgambianus). Front Neuroanat 2015;9:67. DOI: 10.3389/fnana.2015.00067.
19. Alrafiah A, Alshali R. The effect of prolonged formalin fixation on the staining characteristics of archival human brain tissue. Folia Morphol (Warsz) 2019;78(2):230–236. DOI: 10.5603/FM.a2018.0099.
20. Boos GS, Failing K, Colodel EM, et al. Glial fibrillary acidic protein and ionized calcium-binding adapter molecule 1 immunostaining score for the central nervous system of horses with non-suppurative encephalitis and encephalopathies. Front Vet Sci 2021;8:660022. DOI: 10.3389/fvets.2021.660022.
21. Garcia-Segura LM, Duenas M, Busiguina S, et al. Gonadal hormone regulation of neuronal-glial interactions in the developing neuroendocrine hypothalamus. J steroid Biochem Mol Biol 1995;53(1–6):293–298. DOI: 10.1016/0960-0760(95)00066-9.
22. Bordt EA, Ceasrine AM, Bilbo SD. Microglia and sexual differentiation of the developing brain: A focus on ontogeny and intrinsic factors. Glia 2020;68(6):1085–1099. DOI: 10.1002/glia.23753.
23. Bortolanza M, Gobbo D, Fang L, et al. Sex-specific properties of astrocytes: From development to evolutionary insights. Neurochem Res 2025;50(4):267. DOI: 10.1007/s11064-025-04512-w.
24. Berkiks I, García-Segura LM, Nassiri A, et al. The sex differences of the behavior response to early life immune stimulation: Microglia and astrocytes involvement. Physiol Behav 2019;199:386–394. DOI: 10.1016/j.physbeh.2018.11.037.

ORIGINAL RESEARCH

Use of Cadaveric Tissue as an Alternative to Normal Tissue/ Surgical Specimen—A Histological Endeavor

Anurag[1], Shilpa Gupta[2], Shubha Srivastava[3]

Received on: 9 April 2026; *Accepted on:* 14 May 2026; *Published on:* 12 June 2026

Abstract

Aim and background: Cadaver dissection during anatomy teaching is an important part of medical training and a valuable introduction to pathology. Therefore, an alternative to normal tissue or surgical specimens could be cadaveric tissue procured from preserved cadavers.

Materials and methods: The study was conducted at the Department of Anatomy, National Capital Region Institute of Medical Sciences (NCRIMS), Meerut. The cadaver was freshly embalmed by perfusing standard embalming fluid. The tissue samples, liver, muscle, spleen, kidney, small intestine, appendix, esophagus, artery, and trachea, for research were obtained from the freshly embalmed cadavers. The tissues were processed, and hematoxylin & eosin (H&E) slides were prepared. A total of 180 slides were examined under a binocular light microscope by all the researchers and compared (as per the comparing criteria) with a histological slide of the same tissue available in the Department of Anatomy, NCRIMS, Meerut.

Results: After examining the 180 slides by all investigators, the slides were classified as good, satisfactory, and poor and in reference to the mentioned criteria. Among the total slides prepared, the percentages of good, satisfactory, and poor slides were 75.6, 16.1, and 8.3, respectively. After the statistical analysis, the result obtained was found to be significant ($p < 0.0001$).

Conclusion: The use of histological tissue from cadavers for educational purposes is reliable and provides an ample source of material for the preparation of histological slides.

Keywords: Cadaveric tissue, Hematoxylin & eosin stained, Histology slides.

Journal of Anatomical Sciences (2026): 10.5005/jas-11049-0024

Introduction

Histology is an integral part of medical education and is included in the basic sciences of the medical curriculum, thereby providing adequate learning that mainly emphasizes the structural organization of tissues.[1] Histology of normal tissues is a necessity for the diagnosis of various pathological conditions, and here lies the barrier of the availability of normal human tissues and various ethical issues faced in the process of procuring normal human tissues. Thus, the histological slides available for teaching and research are prepared either from animal tissues or from the tissues obtained during surgical procedures.[2]

Dissection during anatomy teaching is an important part of medical training and can be a valuable introduction to pathology. Despite modern technology and emerging teaching and learning methods, the cadavers continue to remain the mainstay of the anatomy curriculum.[3,4]

Therefore, an alternative to normal tissue or surgical specimens could be the cadaveric tissue procured from preserved cadavers, which has been obtained after following a standard protocol, which exempts it from ethical issues.[2]

Optimal preservation of cadavers is one of the most important considerations for the study of the structural organization of tissues. The traditional method of embalming, a technique of preserving cadavers, uses a solution mainly consisting of formaldehyde. The desired properties required for histological slides obtained from cadavers are the long-term structural preservation of organs and tissues, minimal shrinkage or distortion, and no alteration to the microscopic structure.[5]

Even when formalin causes shrinkage of a tissue, it does not alter its microscopic structure. Ferdinand Blum states that formaldehyde is effective in restoring the color and shape of tissues without affecting the microscopic structure of the tissue.[6,7]

Various studies also show that embalming solutions for cadavers containing low formaldehyde can also be used reliably for histopathologic investigation.[8]

Therefore, the present study was conducted to determine the histological details of various tissues obtained from cadavers. We aim to find out whether cadaveric tissue could replace normal tissue for histology slides, which may help clinicians and histopathologists with a practically unlimited source of normal histological tissue for comparison with pathological specimens.

Materials and Methods

The present study is a comparative study conducted in the Department of Anatomy, National Capital Region Institute of Medical Sciences (NCRIMS), Meerut, from January 2021 to

[1–3]Department of Anatomy, National Capital Region Institute of Medical Sciences, Meerut, Uttar Pradesh, India

Corresponding Author: Shilpa Gupta, Department of Anatomy, National Capital Region Institute of Medical Sciences, Meerut, Uttar Pradesh, India, Phone: +91 8909646311, e-mail: shilpagupta16ana@gmail.com

How to cite this article: Anurag, Gupta S, Srivastava S. Use of Cadaveric Tissue as an Alternative to Normal Tissue/Surgical Specimen—A Histological Endeavor. J Anat Sciences 2026;34(1):28–34.

Source of support: Nil

Conflict of interest: None

February 2025. Our material included cadaveric tissue procured from the cadavers available in the Department of Anatomy during the research period. The cadavers were freshly embalmed by perfusing a standard embalming fluid.[9] It was assumed that the donated bodies received as cadavers were free from any systemic disease. The tissue samples for research were obtained from freshly embalmed cadavers and included: (1) Liver, (2) muscle, (3) spleen, (4) kidney, (5) small intestine, (6) appendix, (7) esophagus, (8) artery, and (9) trachea.

The procured tissue was then fixed in 10% formalin, which contains approximately 4% w/v of formaldehyde.

Increasing concentrations of alcohol were used for dehydration to remove free water, followed by the use of the clearing agent xylene to remove the alcohol before infiltration.

After clearing, the tissue sections were impregnated with paraffin wax, and embedding was performed to create tissue blocks to facilitate sectioning. The samples were sectioned using a rotary microtome, and the sections were then placed on glass slides for staining. Before staining, the paraffin was dissolved with xylene, and the slides were rehydrated through a graded alcohol of decreasing concentration. The tissue was then stained with hematoxylin and counterstained with eosin, before being mounted and covered with a coverslip. Twenty slides of each tissue were prepared, with a total of 180 slides.[10]

A total of 180 slides were examined under a binocular light microscope by all of the researchers, and a detailed histological description of each tissue was obtained. Each tissue was then compared with a histological slide of the same tissue available in the Department of Anatomy, NCRIMS, Meerut.

Comparing Criteria[11]

1. Arrangement of various cellular elements in relation to one another.
2. Sharpness of the cellular outline.
3. Cell size.
4. Intracellular details.
5. Size and position of the nuclei.
6. Staining properties of the nuclei.
7. Connective tissue state and staining analysis.

Each slide was categorized as good, satisfactory, or poor based on the above criteria. A slide was categorized as "good" if it fulfilled all criteria without any cellular definition limitations at 10× and 40× magnification; as "satisfactory" when the slide was mostly adequate but there was some limitation in one of the criteria, and as "poor" when the slide had a significant limitation in two or more of the criteria.[2]

Results

Our study, on cadaveric tissue slides, shows characteristics such as intact surface epithelium and underlying stromal tissue. The nuclei, cell membranes, and the cytoplasmic details were clear and well preserved. There was no evidence of necrosis. About 75.6% of the slides were found to be of good standard when compared with the aforementioned criteria.[11] The statistical analysis was done using the Chi-square test. There was a statistically significant difference in the proportions across the samples ($p < 0.0001$).

Table 1 shows the number of good, satisfactory, and poor slides of each cadaveric tissue used in the research.

The given pie chart shows the proportion of good, satisfactory, and poor slides out of the total 180 slides (Fig. 1).

Table 1: The number of good, satisfactory and poor slides of each cadaveric tissue

Cadaveric tissue	*Number of good slides*	*Number of satisfactory slides*	*Number of poor slides*
Liver	17	1	2
Kidney	20	0	0
Spleen	16	1	3
Trachea	18	0	2
Muscle	15	4	1
Appendix	2	16	2
Esophagus	15	3	2
Small intestine	16	1	3
Artery	17	3	0
Percentage of slides	75.6	16.1	8.3

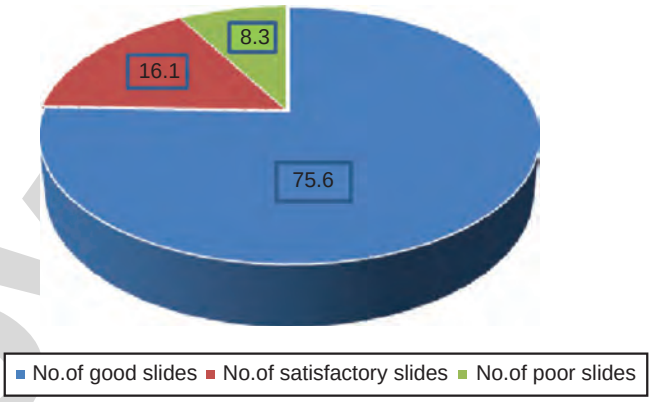

Fig. 1: Pie chart showing the proportion of good, satisfactory, and poor slides out of the total 180 slides

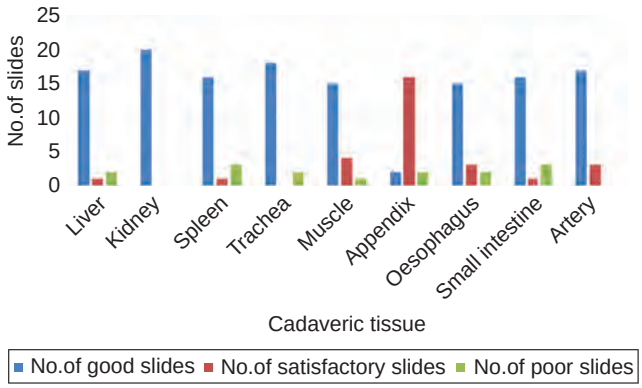

Fig. 2: Bar diagram depicting the comparison of good, satisfactory, and poor slides of individual cadaveric tissue

The given bar diagram depicts the comparison of good, satisfactory, and poor slides of individual cadaveric tissue (Figs 2 to 13).

Discussion

The preparation of slides from cadaveric tissue is considered as an alternative method, as it helps in integrating gross and microscopic anatomy teaching.[12] The cadavers, when properly embalmed,

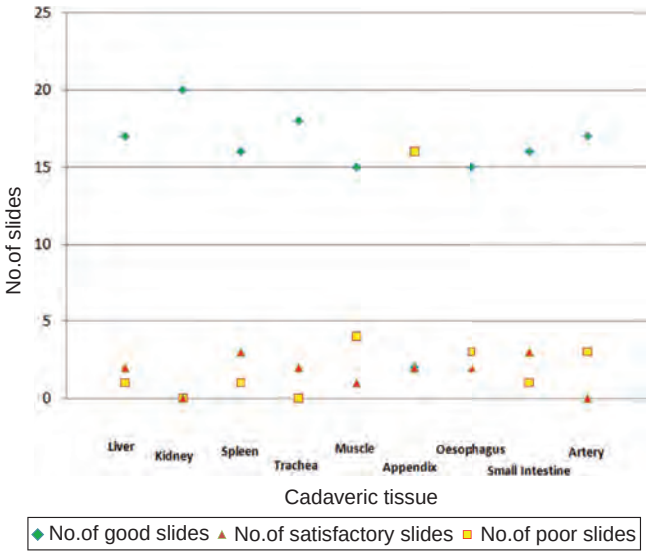

Fig. 3: Scatter diagram for criteria-based quality slides

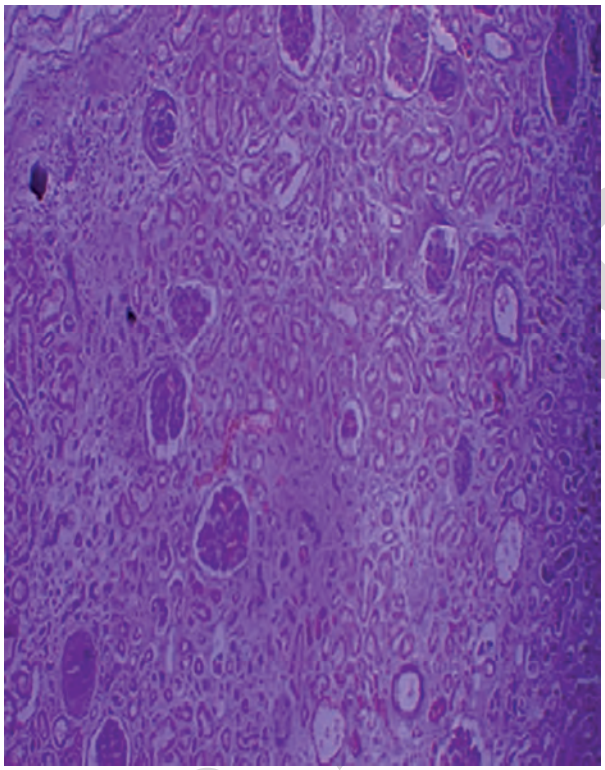

Fig. 4: The photographic image showing T.S. of H&E-stained cadaveric kidney (10×)

their tissues well processed and stained during histology slide preparation, preserve the essential histological features which can be used in undergraduate teaching.

In the present study, the tissue samples were taken grom freshly embalmed cadavers, which contributed to the good quality of the prepared slides.

Our study strictly followed the mentioned criteria 11 to obtain results that fall under the "good" and "satisfactory" slides.

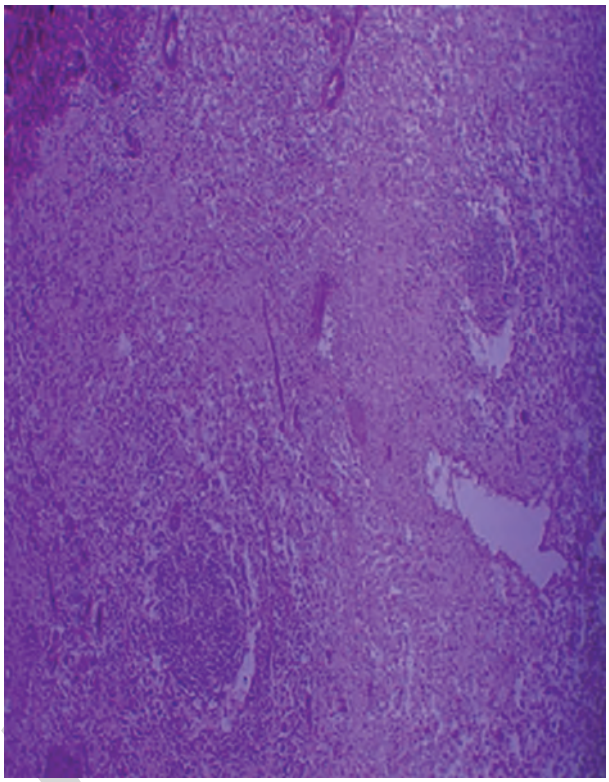

Fig. 5: The photographic image showing T.S. of H&E-stained cadaveric spleen (10×)

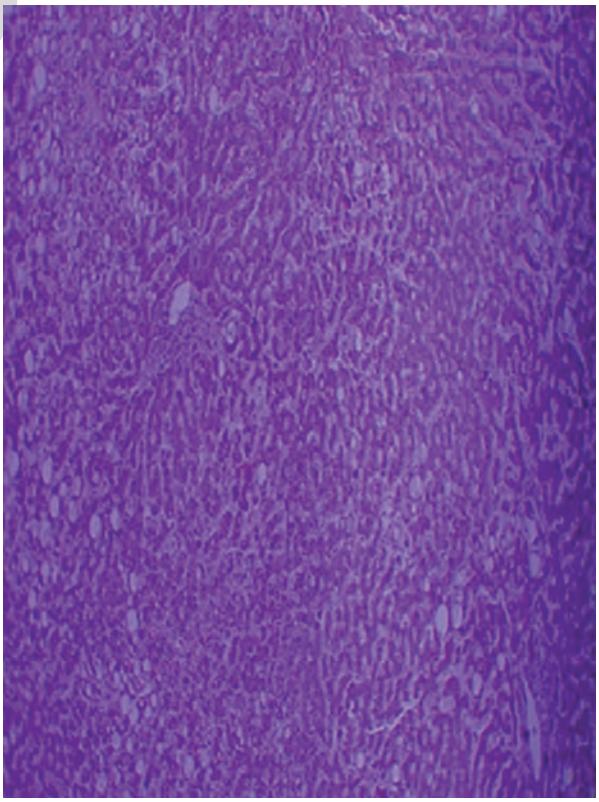

Fig. 6: The photographic image showing T.S. of H&E-stained cadaveric liver (10×)

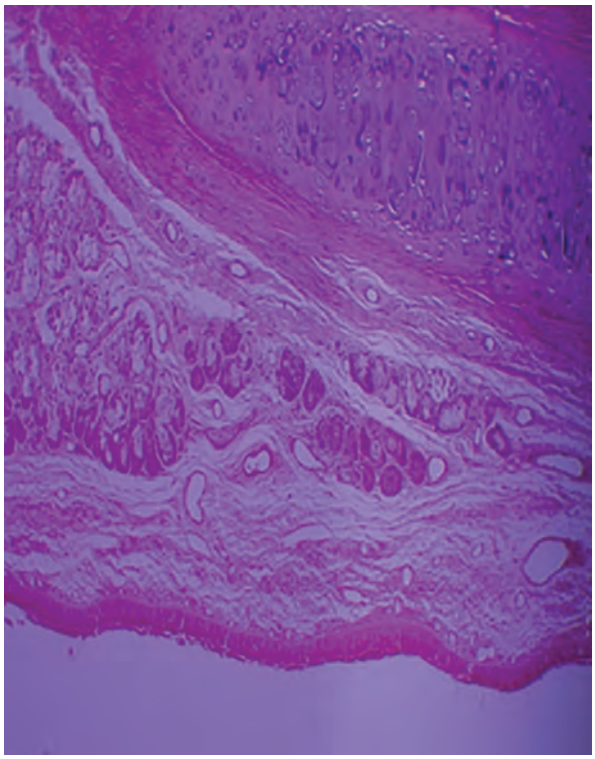

Fig. 7: The photographic image showing T.S. of H&E-stained cadaveric trachea (10×)

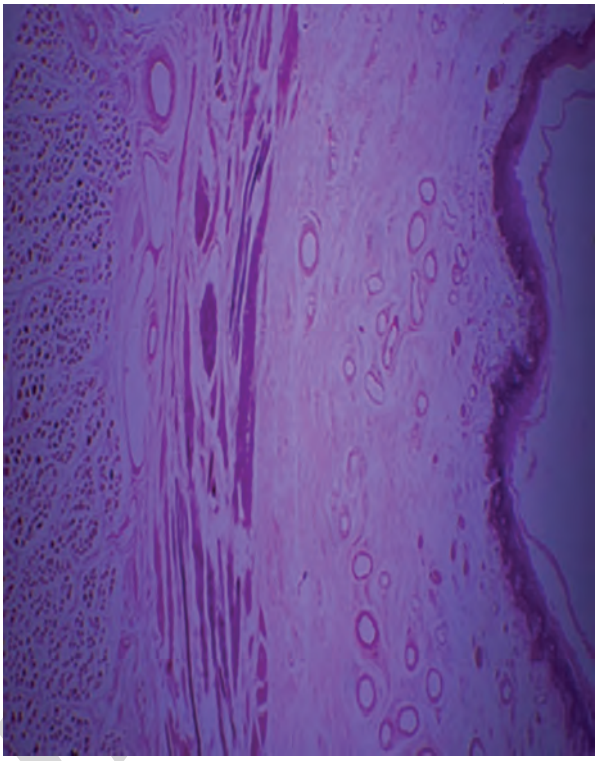

Fig. 9: The photographic image showing T.S. of H&E-stained cadaveric esophagus (10×)

Fig. 8: The photographic image showing T.S. of H&E-stained cadaveric artery (10×)

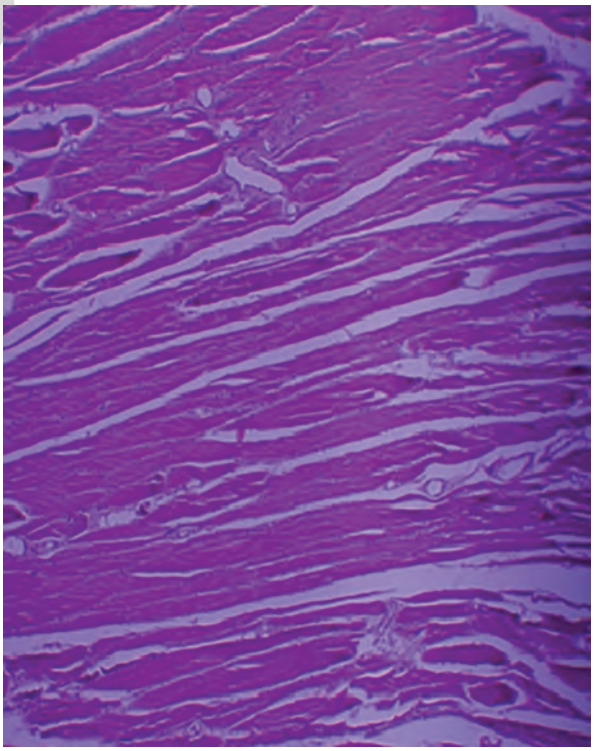

Fig. 10: The photographic image showing L.S. of H&E-stained cadaveric skeletal muscle (10×)

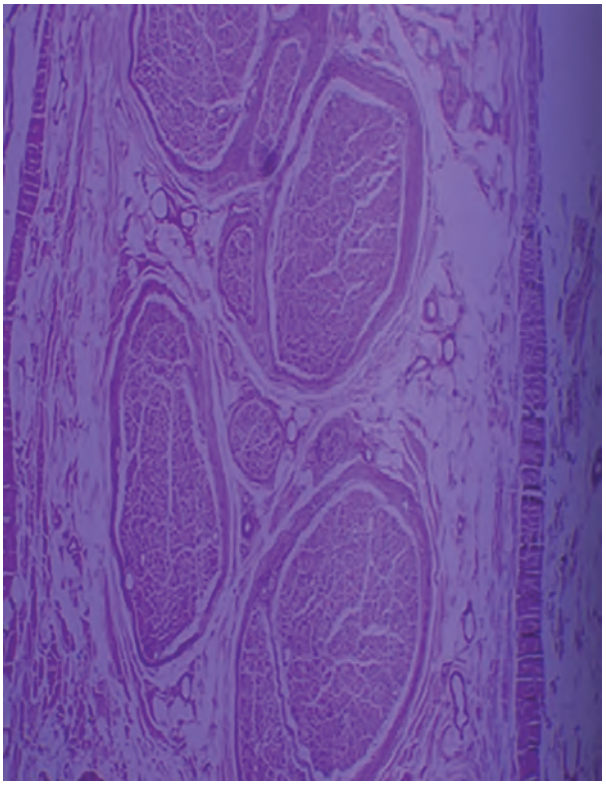

Fig. 11: The photographic image showing T.S. of H&E-stained cadaveric skeletal muscle (10×)

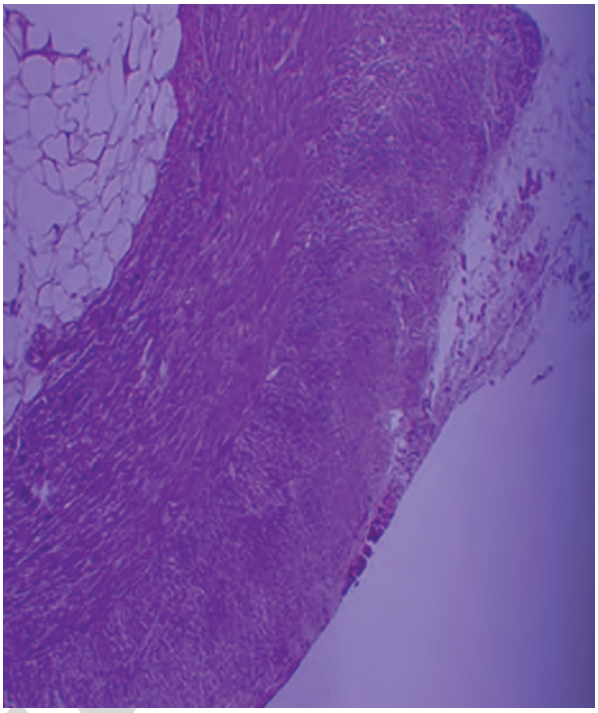

Fig. 13: The photographic image showing T.S. of H&E-stained cadaveric appendix (10×)

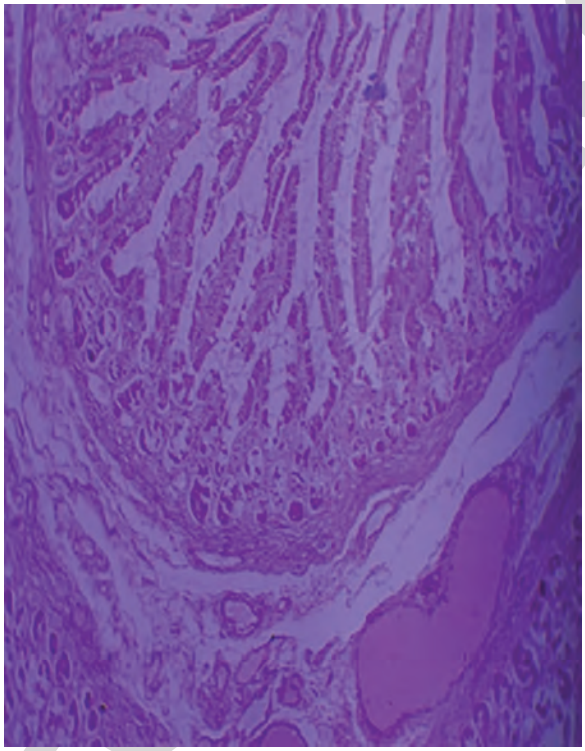

Fig. 12: The photographic image showing T.S. of H&E-stained cadaveric small intestine (jejunum) (10×)

The disparity for good, satisfactory, and poor slides may be due to the delay from the time of death till the initiation of the embalming process.

Nicholson et al. show that tissue from embalmed cadavers for teaching can be used for routine histology. They obtained tissues from the heart, liver, kidney, skeletal muscle, and skin from cadavers embalmed with four different formalin-containing fluids. The characteristic morphology was well observed in skin and skeletal muscle sections, and in tissues embalmed with fluids that did not contain phenol.[13]

Shukrian et al. analyzed testicular and ovarian tissue samples from cadavers and compared them with human biopsy samples obtained from surgical procedures. It was concluded that the visibility of epithelial structures, stromal organization, blood vessels with blood cells, and even pathological features like ovarian cysts highlights its potential as a realistic and clinically relevant alternative to animal tissue.[14]

Gupta and Gauba reported that all the histological slides from cadaveric tissue, including skin, muscle, cartilage, artery, spleen, brain, trachea, liver, and small intestine, showed excellent tissue organization. The nuclei, cell membrane, and cytoplasmic details are clear and well preserved. They concluded that a human cadaver could be an ideal source of tissue for teaching and research.[2]

Wood et al. studied 17 cadavers for pathology and histopathology and showed that cadaver-derived material is of good quality and can be used in histopathology teaching.[15]

Kalyankar et al. show the histology of longitudinal and horizontal sections of skeletal muscle tissue obtained from cadavers and compared them with slides of the same tissues obtained from a guinea pig. She concluded that cadaveric tissues are suitable for

histology teaching slides and for research activities. Similarly, Kim et al. in 2013 studied the fiber type composition of the supraspinatus muscle from cadaveric tissue, supported by a similar study on rotator cuff muscle and the teres major muscle by Lovering and Russ in 2008.[16–18]

Rae et al. collected tissue samples from hearts, livers, lungs, and kidneys. The lung group had the lowest percentage of "good" ratings (24.2%) and the highest percentage of "poor" ratings (23.1%). The heart group had the minimum "poor" ratings (0.0%), and the heart tissue slides had the highest percentage of "good" ratings (58.5%). These results indicate that heart tissue is more reliable than lung, kidney, or liver tissue when utilizing tissue from the cadavers for research or educational purposes.[19]

Abuhaimed et al. obtained 112 tissue samples of thyroid, skeletal muscle, bone, skin, heart, and both lungs. Of all the slides, 34.2 and 60.3% were of good and satisfactory quality, respectively, whereas the remaining 5.5% were of poor quality. Thick skin (84.6%) and bone (81.8%) tissues had the highest % of "good" results. The thyroid (20%) and lung (13.6%) tissues had the highest percentage of "poor" quality slides. [20]

In a study by Swapna et al., tissue samples were obtained from four organs, i.e., kidney, spleen, liver, and lung. Cellular morphology appeared well preserved in these organs and can be considered fairly reliable for forensic investigations.[21]

Viveki PR et al. conducted a study on 96 histology slides prepared from cadaveric tissues such as skin, elastic cartilage, the muscular artery, skeletal muscle, and the peripheral nerve. It was concluded that almost all the tissues taken from cadavers were either of good or satisfactory quality, with thick skin and elastic cartilage being the best rated.[11]

The present study is in agreement with the above discussion studies, with a few deviations depending on the tissues selected and the limitations of the process.

Limitations of Study

The time interval between death and the embalming of the body was uncertain. Although the cadavers were embalmed within 1 hour of receiving the body.

Conclusion

The present study emphasizes that the percentage of good and satisfactory slides obtained from cadaveric tissues can be an asset for teaching purposes and research. This study found that most slides prepared from cadaveric tissues were of good and satisfactory quality. However, further study and research are required to authenticate the use of cadaveric tissues in the preparation of histological slides.

Ethical Approval

Approval was obtained from the IEC under the registeration number ECR/1396/INST/UP/2020.

Clinical Significance

Not applicable.

Data Availability Declaration

We had taken the tissue from a cadaver received in the Department of Anatomy, NCRIMS, Meerut, through standard protocol.

AI Disclosure

No AI tools used.

Acknowledgments

The author would like to thank the donor and relatives, the statistician, Department of Pathology, Technical Staff.

Authors' Contributions

The study involved contributions from three investigators. The concept for the study design was done by Dr Anurag, Dr Shilpa Gupta, and Dr Shubha Srivastava. Sample collection, along with tissue processing and staining, was performed by Dr Anurag. The manuscript was written by Dr Shilpa Gupta, Dr Shubha Srivastava, and Dr Anurag. Data analysis by Dr Shilpa Gupta, Dr Shubha Srivastava, and Dr Anurag.

Orcid

Anurag https://orcid.org/0000-0003-2881-5378

References

1. Hussein IH, Raad M, Safa R, et al. Once upon a microscopic slide: The story of histology. J Cytol Histol 2015;6(6):377. DOI: 10.4172/2157-7099.1000377.
2. Gupta T, Gauba K. Cadaveric tissue histology: A viable alternative. Journal of Clinical and Diagnostic Research (JCDR) 2011;5(8):1505–1509. Available from: https://jcdr.net/articles/PDF/1743/3%20-%202667.pdf.
3. Ghosh SK. Cadaveric dissection as an educational tool for anatomical sciences in the 21st century. Anat Sci Educ 2016;10(3):286–299. DOI: 10.1002/ase.1649.
4. Geldenhuys EM, Burger EH, Helden PDV, et al. Optimizing the use of cadavers by integrating pathology during anatomical dissection. Anat Sci Educ 2016;9(6):575–582. DOI: 10.1002/ase.1617.
5. Kaliappan A, Rohini, Gupta T, et al. Innovative cadaver preservation techniques: A systematic review. Medica (Bucur) 2023;18(1):127–135. DOI: 10.26574/maedica.2023.18.1.127.
6. Musiał A, Gryglewski W, Kielczewski S, et al. Formalin use in anatomical and histological science in the 19th and 20th centuries. Folia Medi Cracov 2016;56(3):31–40. PMID: 28275269.
7. Coleman R, Kogan I. An improved low-formaldehyde embalming fluid to preserve cadavers for anatomy teaching. J Anat 1998;192:443–446. DOI: 10.1046/j.1469-7580.1998.19230443.x.
8. Nlebedum U, Ikpegbu E, Nnadozie O, et al. Effect of embalming fluid on histological appearance of organs from embalmed West African dwarf goat cadavers. Histologic 2013;1–15. Available from: https://www.researchgate.net/publication/237837412_Effect_of_Embalming_Fluid_on_Histological_Appearance_of_Organs_From_Embalmed_West_African_Dwarf_Goat_Cadavers.
9. Ajmani ML. Embalming principles and legal aspects. 2nd edition. JAYPEE 2019:85–86. DOI: 10.5005/jp/books/18242.
10. Kim S, Christopher L, John DB. Bancroft's Theory and Practice of Histological Techniques, 8th ed. Elsevier; 2019. pp. 12–150.
11. Viveki PR, Kumar MP, Viveki RG. Histology slides from cadaveric tissue: An alternative? Al Ameen J Med Sci 2024;17(3):199–205. ISSN: 0974-1143.
12. Judy A, Provoklimek. A novel method preparing histology slides to integrate the teaching of gross and microscopic anatomy. J Vet Med Educ 2002;29(3):137–141. DOI: 10.3138/jvme.29.3.137.
13. Nicholson HD, Samalia L, Gould M, et al. A comparison of different embalming fluids on the quality of histological preservation in human cadavers. Eur J Morphol 2005;42(4–5):178–184. DOI: 10.1080/09243860500473306.

14. Shukrian L, Rerrie S, Chapple B, et al. Evaluation of human cadaver tissue for undergraduate medical histology education. Scholars Crossing of Liberty University 2025.
15. Wood A, Whiten S, McVee J, et al. Histopathology from the dissecting room: Are cadavers a suitable source of educationally useful histopathology specimens? An Int J Experi Clini Anatomy 2015;9(1):26–33. DOI: 10.2399/ana.14.048.
16. Kalyankar A, Sukre S, Dope SK, et al. Microscopic study of skeletal muscle in embalmed cadavers. Int J Anat Res 2016;4(3):2547–2551. DOI: 10.16965/ijar.2016.270.
17. Kim SY, Lunn DD, Dyck RJ, et al. Fiber type composition of the architecturally distinct regions of human supraspinatus muscle: A cadaveric study. Histol Histopathol 2013;28(8):1021–1028. DOI: 10.14670/HH-28.1021.
18. Lovering RM, Russ DW. Fiber type composition of cadaveric human rotator cuff muscles. J Orthop Sports Phys Ther 2008;38(11): 674–680. DOI: 10.2519/jospt.2008.2878.
19. Rae G, Newman WP, McGoey R et al. The histopathologic reliability of tissue taken from cadavers within the gross anatomy laboratory. Anat Sci Educ 2018;11(2):207–214. DOI: 10.1002/ase.1743.
20. Abuhaimed AK, Almulhim AM, Alarfaj FA, et al. Histologic reliability of tissues from embalmed cadavers: Can they be useful in medical education? Saudi J Med Med Sci 2020;8(3):208–212. DOI: 10.4103/sjmms.sjmms_383_19.
21. Swapna R, A Jojo, Tintu TS, et al. Effect of embalming fluid on the histological appearance of organs—a cadaveric study. Ind J Forensic Med Toxicology 2020;14(4):373–378.

CASE REPORT

Additional Muscular Extension of Coracobrachialis Muscle: A Case Report

Fatima Begum[1], Vinay Sharma[2]

Received on: 16 February 2026; *Accepted on:* 23 March 2026; *Published on:* 12 June 2026

Abstract

Introduction: The coracobrachialis muscle (CBM), a muscle of the ventral group of muscles in the arms, is known for its variations in terms of origin and insertion, and sometimes it causes the clinical complications associated with these variations.

Case report: An additional muscular slip was noted during the dissection of the right axilla and upper arm of a male cadaver. This slip formed a bridge over the median nerve and other neurovascular structures of the arm, and it finally inserted into the medial intermuscular septum and the medial border of the humerus.

Conclusion: Variations of the CBM in its origin and insertion may be of clinical importance, it can reduce movements, can compress important neurovascular structures, or can be surprising for an operating surgeon. Therefore, knowledge of such variations is clinically relevant.

Keywords: Coracobrachialis, Coracobrachialis brevis, Variations of coracobrachialis, Ventral group of muscles of arm, Woods muscle.

Journal of Anatomical Sciences (2026): 10.5005/jas-11049-0019

Background

The coracobrachialis muscle (CBM) is the smallest muscle of the anterior or ventral group of muscles in the arm in comparison to the brachialis and biceps brachii muscles. However, similar to other muscles of the compartments, variations of the coracobrachialis are a concern of researchers both numerically and clinically. The CBM is classically described as taking its origin from the apex of the coracoid process of the scapula, where it is blended with the medial side of the short head of the biceps brachii. The tendon is continued into a muscular belly, which is inserted into the medial border and anteromedial surface of the shaft of the humerus. Its variations in terms of origin and insertion have been noted by many researchers, that may originate from two or more than two heads or insertion in two-slip convention and additional insertion into the distal part of the shaft of the humerus, the medial epicondyle of the humerus, or in the form of a fibrous band to the medial intramuscular septum of the arm.[1,2]

Some variations associated with the CBM may have clinical significance, as these additional slips can be used as muscle grafts, or they may compress the neurovascular bundle of the brachium and present like entrapment neuropathy. Thus, reporting such variations are clinically relevant to surgeons, neurologists, and anatomists.

Study Design

This variation of the coracobrachialis was found during the routine dissection of the right axilla and arm of a male cadaver during an undergraduate teaching session in the Department of Anatomy at the Muzaffarnagar Medical College, Muzaffarnagar. The dissection step was completed according to Cunningham's Manual of Practical Anatomy.

Observations

During the routine dissection of the right axilla and arm of an embalmed cadaver for undergraduate teaching in the dissection hall, in flexor compartment of the arm, a muscular slip was observed which was connected the medial edge of the terminal part of the CBM and was directed medially and inferiorly in order to reach the medial border of the humerus bone and inserted into the medial intermuscular septum. During its course, it crossed over the nerves present in the brachium. This muscular slip bridged over the branches of the brachial plexuses nerves, especially over the median nerve (as shown in Fig. 1). A "Y"-shaped port between this slip and the medial border of the biceps brachii was noted. The median nerve entered into the apex of this "Y"-shaped port and proceeded further.

Discussion

Just like variations of other muscles of the ventral compartment of the arm, variations of the CBM are clinically significant. The concept of the two parts CBM was introduced by Wood in 1867 by stating that the musculocutaneous nerve passes between two parts of the CBM, i.e., the coracobrachialis longus (CBL) and the coracobrachialis brevis (CBB).[3]

An almost similar thought, that the musculocutaneous nerve is trapped between these two heads of the coracobrachialis while

[1]Department of Anatomy, Government Doon Medical College, Dehradun, Uttrakhand, India

[2]Department of Anatomy, Muzaffarnagar Medical College, Muzaffarnagar, Uttar Pradesh, India

Corresponding Author: Vinay Sharma, Department of Anatomy, Muzaffarnagar Medical College, Muzaffarnagar, Uttar Pradesh, India, Phone: +91 9837154651, e-mail: vinay_sharma1979@yahoo.com

How to cite this article: Begum F, Sharma V. Additional Muscular Extension of Coracobrachialis Muscle: A Case Report. J Anat Sciences 2026;34(1):35–36.

Source of support: Nil

Conflict of interest: None

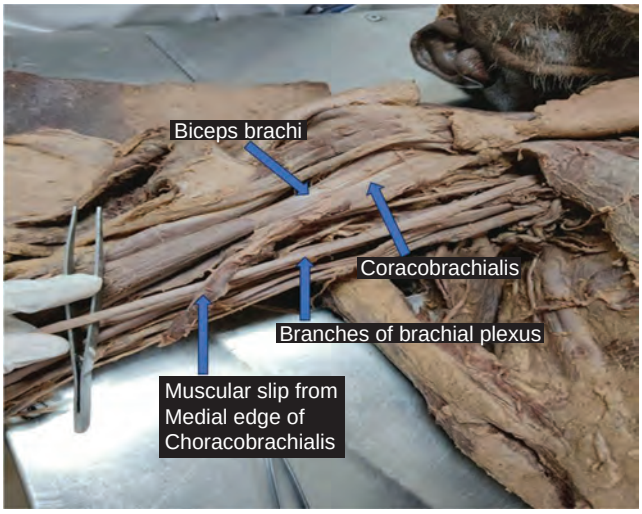

Fig. 1: Shows muscular slip overbridging structures present in brachium

the third head has disappeared, was presented by El-Naggar and Saggaf.[4]

In lower phylums, the CBM is identified in three different parts: (a) The CBB whose inserted into humerus bone above the tendon of the latissmus dorsi; (b) the coracobrachialis medius inserts on the humerus below the tendon of the latissmus dorsi; and (c) the CBL (Wood's muscle), which runs inferiorly on the humerus and makes a muscular bridge over the median nerve and the brachial artery.[5]

The present finding is almost similar to the CBL part, or Wood's muscle that bridges over the neurovascular bundle of the arm. This type of muscle variant was described by Georgiev et al.[6]

While this type of variation of the CBM is one of the most common variations that may extend up to the medial epicondyle of the humerus, but this specific extension of coracobrachialis or muscular slip can cause high-level entrapment neuropathy of the median nerve and may restrict the abduction movements of the arm.[1,7]

In the present case, it was not possible to separate the superficial fibers possibly running in the form of a muscular slip, but such kind of variant may be associated with two or more heads.[8,9] Therefore, not only the insertion but also the origin of such an accessory muscular slip is a notable variation.

Conclusion

The coracobrachailis is a muscle of the ventral group of the arm that may have lost its heads and parts during evolution, but sometimes parts of this muscle appear in the form of variations in humans, as reported by many authors and classified by a few of them.

When such a variant appears in a human being, it mostly does not affect the movements of the upper limb but sometimes these may restrict movements and some time may cause the compression of neurovascular structures.

At times, such a variant can surprise surgeons during surgical procedures on the axilla and the upper part of the arm.

On the other hand, these variants may be helpful in muscle grafts and surgeries like Laterjet's procedure.

Limitation

Case report so study to be conducted on appropriate sample size.

Clinical Significance

Mentioned in introduction and conclusion.

Ethical Approval

The institutional ethical committe approves the research study under the reference ID: MMC/IEC/2025/318.

Data Availability Declaration

Not applicable.

Acknowledgment

The authors would like to express his sincere gratitude to CS Ramesh Babu, his mentor, for his valuable guidance and continuous support. And also extend his heartfelt thanks to Dr Jolly Agarwal, Head of the Department, Doon Medical College, for the encouragement and support throughout this work.

Author's Contribution

Dr Fatima Begum - Data collection and pictures.
Dr Vinay Sharma - Composition and uploading the article.

Orcid

Vinay Sharma https://orcid.org/0009-0008-5590-9808

References

1. Kumar N, Shetty SD, Sn S, et al. Presence of accessory coracobrachialis and its clinical importance—A case report. Int J Anat Var 2012;5:27–28.
2. Paraskevas G, Koutsouflianiotis K, Iliou K, et al. Accessory coracobrachialis muscle with two bellies and abnormal insertion-case report. Acta Med Acad 2016;45(2):155. DOI: 10.5644/ama2006-124.173.
3. Wood J. On human muscular variations and their relation to comparative anatomy. J Anat Physiol 1867;1:44–59. PMID: 17230706.
4. El-Naggar MM, Al-Saggaf S. Variant of the coracobrachialis muscle with a tunnel for the median nerve and brachial artery. Clin Anat 2004;17:139–143. DOI: 10.1002/ca.10213.
5. Vrzgula M, Mihalik J, Vicen M, et al. Anatomical study of the ventral upper arm muscles with a case report of the accessory coracobrachialis muscle. Medicina 2023;59:1445. DOI: 10.3390/medicina59081445.
6. Georgiev GP, Landzhov B, Tubbs RS. A novel type of coracobrachialis muscle variation and a proposed new classification. Cureus 2017;9:e1466. DOI: 10.7759/cureus.1466.
7. Warner JJ, Paletta GA, Warren RF. Accessory head of the biceps brachii. Case report demonstrating clinical relevance. Clin Orthop Relat Res 1992;280:179–181. PMID: 1611739.
8. Szewczyk B, Polguj M, Paulsen F, et al. A proposal for a new classification of coracobrachialis muscle morphology. Surg Radiol Anat 2021;43(5):679–688. DOI: 10.1007/s00276-021-02700-1.
9. Olewnik Ł, Zielinska N, Karauda P, et al. The cooccurrence of a four-headed coracobrachialis muscle, split coracoid process and tunnel for the median and musculocutaneous nerves: The potential clinical relevance of a very rare variation. Surg Radiol Anat 2021;43:661–669. DOI: 10.1007/s00276-020-02580-x.

BRIEF RESEARCH COMMUNICATION

Situs Inversus Totalis: A Pictorial Review

CS Ramesh Babu[1], Vinay Sharma[2], Bindu Agrawal[3], Arjun Kumar[4], OP Gupta[5]

Received on: 21 February 2026; *Accepted on:* 23 March 2026; *Published on:* 12 June 2026

Abstract

Introduction: Situs inversus totalis is a complex congenital anomaly of laterality defect affecting thoracoabdominal organs and major vascular structures, which is a mirror image of the normal asymmetric arrangement of these structures. Normal asymmetric arrangement is referred to as "situs solitus."

Materials and methods: We retrospectively reviewed multidetector computed tomography (MDCT) scans of 1,030 patients who underwent abdominopelvic scanning for various suspected pathologies. We present here the radiological features of incidentally detected cases of situs inversus totalis in four females and three males.

Observations and discussion: Though a mirror-image arrangement of thoracoabdominal organs is expected, not all cases exhibit all the classical features of situs inversus, and some cases show variable presentation. Dextrocardia, right aortic arch, descending aorta (DA) on the right side, bilobed lung on the right, trilobed lung on the left, both venae cavae on the left, stomach and spleen on the right side, and liver and gallbladder on the left side were observed in all seven cases. Mirror-image pattern of three-branched arch was observed in three cases, and in the remaining four cases, the arch had only two branches. The cecum was seen in the left iliac fossa only in four cases. None of the subjects exhibited any sign of congenital heart disease.

Conclusion: Our study has indicated that all the classical features of situs inversus totalis may not be present in all cases. Some minor variations are observed in some cases.

Keywords: Dextrocardia, Laterality defect, Left inferior vena cava, Left superior vena cava, Right aortic arch, Situs solitus.

Journal of Anatomical Sciences (2026): 10.5005/jas-11049-0018

Introduction

Humans, like most other vertebrates, exhibit external left-right symmetry, but internally, the unpaired thoracoabdominal organs and great vessels, such as the venae cavae and aorta, show distinct left-right asymmetry. Such asymmetry is seen in paired lungs also. The normal asymmetric position of thoracoabdominal organs is designated as "situs solitus." The mirror-image reversal of positioning is named as "Situs inversus totalis" (situs inversus viscerum), and "Situs ambiguus" denotes any other indeterminate abnormality of left-right development.[1–3] It has been estimated that situs inversus occurs with an incidence of 1 in 6,500 to 1 in 25,000 births.[1,4] It is more frequent in males (1.5:1), but others suggest that there is no gender predilection.[1] Some prefer to subdivide situs inversus into complete and incomplete varieties. In complete situs inversus, all thoracic and abdominal viscera are reversed, and some prefer to name it as situs inversus with dextrocardia. In the partial or incomplete type, called situs inversus incompletus or situs inversus partialis, only some abdominal organs show reversal of position, and the apex of the heart points to the left (levocardia).[5] Hence, this subtype is also called situs inversus with levocardia, and its incidence is estimated at 1 in 2,00,000.[6]

Situs ambiguus, also referred to as heterotaxy, is an indeterminate arrangement of some thoracoabdominal organs and vasculature across the left-right axis that does not resemble situs inversus totalis. Situs ambiguus is comparatively rare and frequently associated with congenital heart disease in about 50–90% cases.[7,8] In contrast, only 3–5% cases of situs inversus are associated with congenital heart disease.[7] Therefore, many cases of situs inversus remain silent without exhibiting any symptoms and are detected only incidentally. We present here the radiological features of situs inversus totalis incidentally noted in seven patients who underwent contrast-enhanced CT angiography for various other reasons. Computed tomography provides finer anatomical details, which are essential for understanding all the features of situs inversus.

[1]Muzaffarnagar Medical College, Muzaffarnagar, Uttar Pradesh, India
[2]Department of Anatomy, Muzaffarnagar Medical College, Muzaffarnagar, Uttar Pradesh, India
[3]Department of Radiology, Muzaffarnagar Medical College, Muzaffarnagar, Uttar Pradesh, India
[4]Department of Anatomy, Ajay Sangaal Institute of Medical Sciences & Research, Shamli, Uttar Pradesh, India
[5]Department of Radiology, Dr. O.P. Gupta Imaging Center, Meerut, Uttar Pradesh, India

Corresponding Author: Vinay Sharma, Department of Anatomy, Muzaffarnagar Medical College, Muzaffarnagar, Uttar Pradesh, India, Phone: + 91 9837154651, e-mail: vinay_sharma1979@yahoo.com

How to cite this article: Babu CSR, Sharma V, Agrawal B, *et al.* Situs Inversus Totalis: A Pictorial Review. J Anat Sciences 2026;34(1):37–43.

Source of support: Nil

Conflict of interest: None

Materials and Methods

This study is a retrospective analysis of multidetector computed tomography (MDCT) scans from 1,030 patients (537 males, 493 females). The scans were retrieved from the archives of a single imaging center. The patients underwent contrast-enhanced CT scanning for suspected abdominal pathologies, and the imaging center routinely obtains written informed consent from all the patients before scanning. The scanning was performed by a

64-channel MDCT scanner (GE Optima-60) and 85–100 mL of non-ionic contrast (Omnipaque 300 mg I/mL) medium intravenously at the rate of 5 mL/sec. Scans obtained from the diaphragm to the upper part of the thigh were analyzed in a separate work station (AW Volume Share 4.5) with multiplanar reformatting and volume rendered (VR) and maximum intensity projection (MIP) images obtained. Incidentally, in seven patients, mirror-image positional changes of several abdominal organs and vasculature were noted, and these subjects further underwent thoracic imaging to complete the investigation.

Observations

We incidentally detected seven cases of situs inversus totalis (four females, three males), who underwent contrast-enhanced MDCT for various reasons. The estimated frequency of the condition is 0.67%. One female patient was 4 years old, and the rest were adults with an age range of 22–60 years. None of the subjects was reported to have any associated congenital heart disease. All cases exhibited dextrocardia with the cardiac apex pointing to the right and a right-sided aortic arch (RAA) (Fig. 1). Mirror-image branching pattern of three branches, namely the left brachiocephalic trunk (LBCT), right common carotid artery (RCCA), and right subclavian artery (RSCA), was noted in three cases (Fig. 2A). In four cases, only two branches were observed, namely the bovine trunk (common trunk of left brachiocephalic artery and RCCA) and RSCA (Fig. 2B). Superior vena cava is left-sided in all cases, with the right brachiocephalic vein (RBCV) crossing supra-aortic branches from right to left side (Fig. 3). Trilobed left lung and bilobed right lung were present in all cases (Figs 4B and C). Descending aorta (DA) was seen to the right of the vertebral column in all cases (Fig. 4A).

In all seven cases, the stomach and spleen were located on the right side, and the liver with the gallbladder was located on the left side. The cecum and appendix were located in the left iliac fossa in four cases, suggestive of intestinal malrotation (Figs 5 and 6).

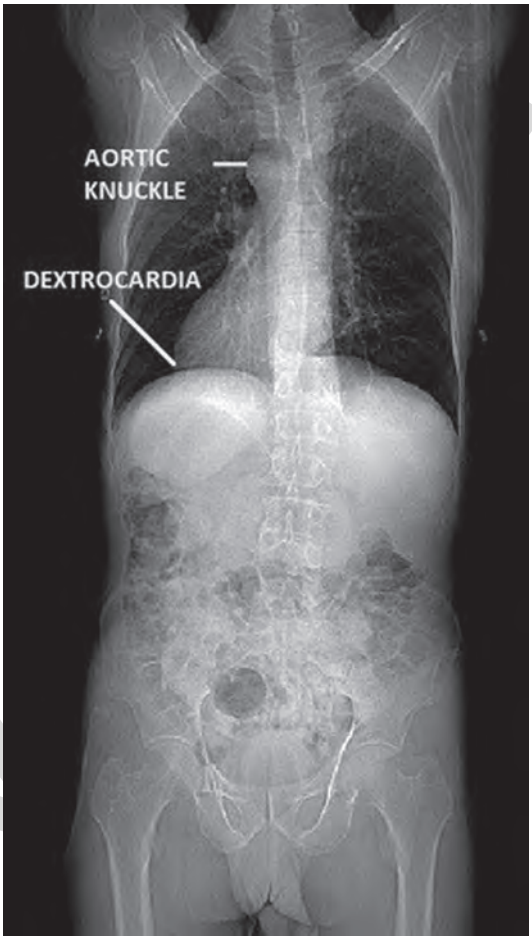

Fig. 1: CT-Scout X-ray showing dextrocardia with cardiac apex pointing to the right. Also note the presence of an aortic knuckle along the right margin of the cardiac shadow

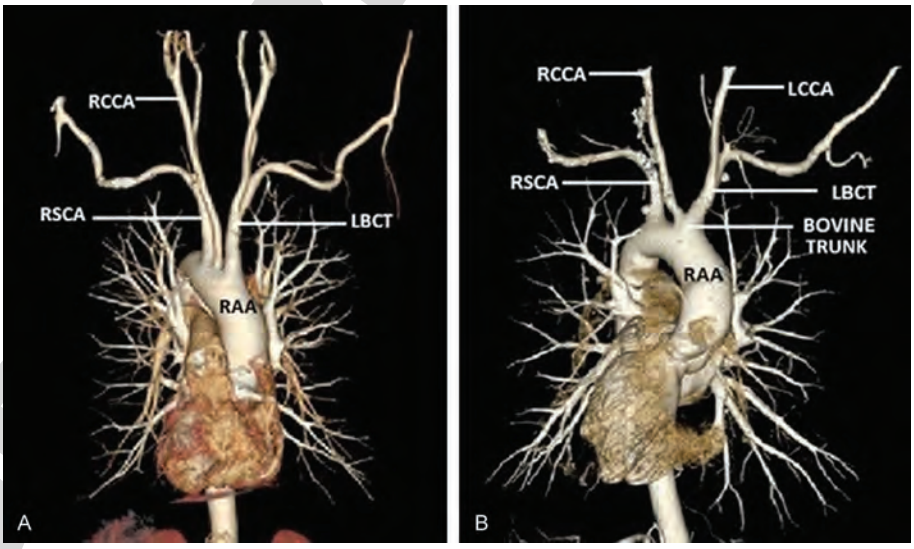

Figs 2A and B: (A) Volume-rendered 3D image of RAA with mirror-image branching pattern of LBCT as the first branch, RCCA, and RSCA as the last branch; (B) Volume-rendered 3D image showing the RAA with two branches: Bovine trunk—common trunk of LBCT and the RCCA as the first branch, and RSCA as the last branch. The cardiac apex is pointing to the right (dextrocardia)

LBCT, left brachiocephalic trunk; LCCA, left common carotid artery; RAA, right-sided aortic arch; RCCA, right common carotid artery; RSCA, right subclavian artery

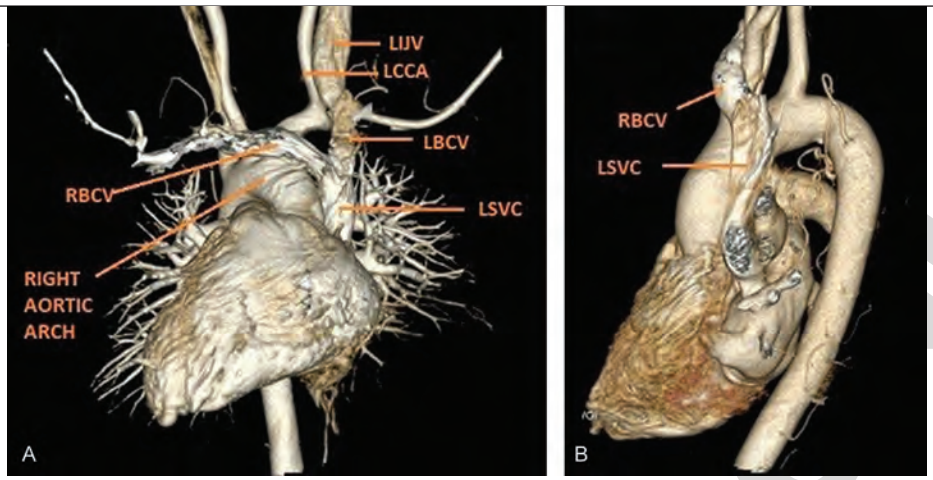

Figs 3A and B: Volume rendered 3D images showing right aortic arch and LSVC. (A) The RBCV is long and crosses in front of supra-aortic branches from right to left to join a short left LBCV to form the LSVC; (B) Left superior vena cava can be seen passing posteriorly to drain into the morphological right atrium, which is present to the left of the midline. The cardiac apex is directed to the right (dextrocardia)

LBCV, left brachiocephalic vein; LCCA, left common carotid artery; LIJV, left internal jugular vein; LSVC, left superior vena cava; RBCV, right brachiocephalic vein

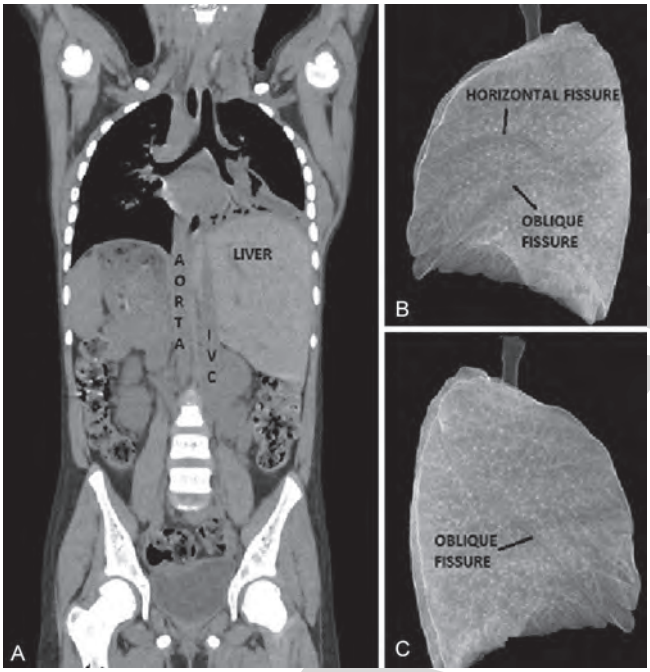

Figs 4A to C: (A) Coronal section; (B and C) VR images. A trilobed lung and eparterial bronchus is seen on the left side (A and B). A bilobed lung with hyparterial bronchus is seen on the right side (A and C), presenting a mirror-image pattern. Note the presence of DA on the right and IVC on the left

IVC, inferior vena cava

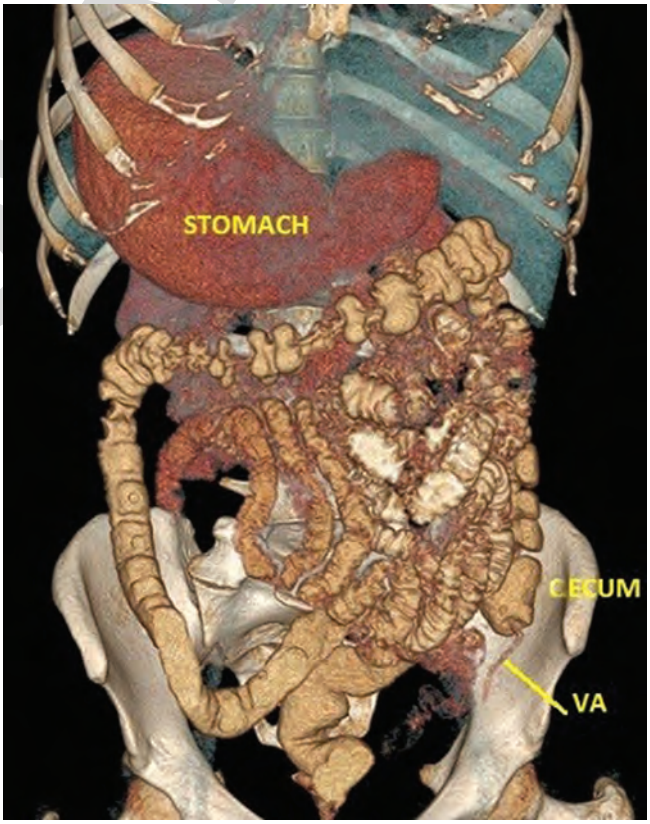

Fig. 5: Volume rendered 3D image after oral contrast showing stomach and intestines. Note the position of the stomach on the right side and the cecum occupying the left iliac fossa. Note the position of the ascending colon on the left and the descending colon on the right

VA, vermiform appendix

Superior mesenteric artery (SMA) and superior mesenteric vein (SMV) rotation sign is clearly seen in two cases only (Fig. 7). Upper poles of the kidneys were observed at the same level in three cases, and in the remaining four cases, the upper pole of the left kidney (LK) was at a lower level because of the presence of the liver on the left side. Preaortic right renal vein (RRV) crossing the aorta to join the left-sided inferior vena cava (IVC) was noted in two cases (Figs 8 to 11), and in the rest, the RRV was observed passing behind the abdominal aorta (AA). In one case, an interrupted IVC with azygos continuation was seen. The enlarged azygos vein was seen on the left side and joined the left superior vena cava (LSVC) (Figs 9 to 11). The portal vein also has a reversed course to the left to reach

the porta hepatis, and in one case, it showed trifurcation at the porta hepatis (Fig. 12). The characteristic features of thoracoabdominal organs and vasculature observed are summarized in Table 1.

Discussion

Mirror-image positioning of viscera, along with blood supply, known as situs inversus totalis, involving thorax as well as abdominal organs and great vessels, is a global positioning defect. This condition occurs due to failure to establish normal left-right asymmetry in the early embryonic period, resulting in a wide spectrum of laterality defects. Humans with situs inversus totalis may be free from any clinical symptoms throughout their life, and this condition is usually detected incidentally during radiological investigations, surgical procedures, or on autopsy. In suspected cases, employing advanced cross-sectional radiological imaging will provide the crucial roadmap and definitive plan for the successful implementation of surgical and interventional procedures.[9]

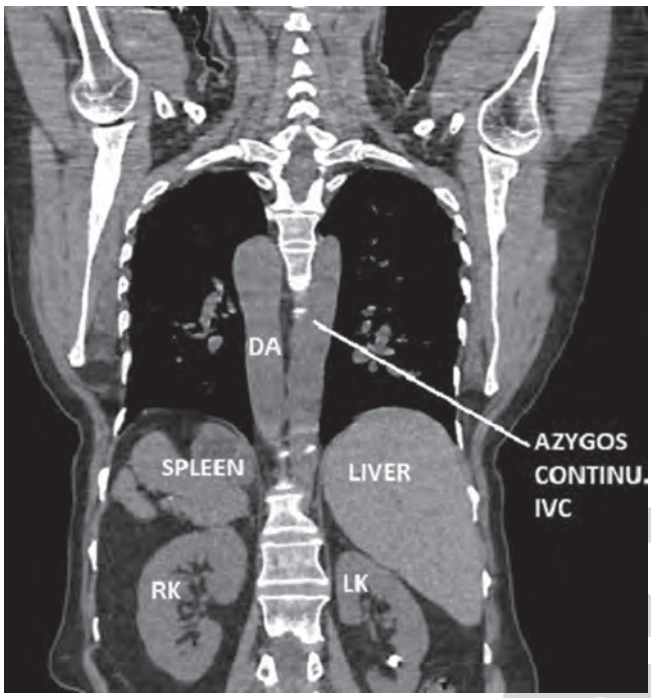

Fig. 6: Coronal section showing the presence of an interrupted IVC with azygos continuation. DA is located on the right side of the vertebral column. The right kidney (RK) is present at a higher level than the LK. The liver is on the left side and the spleen on the right side

DA, descending aorta; IVC, inferior vena cava; LK, left kidney; RK, right kidney

Laterality determination is established very early in the embryonic period with the determination of three embryonic axes: Craniocaudal, dorsoventral, and right-left axes. Conserved pathways of asymmetric gene expression result in a cascade of lateralized signaling, which is then elaborated into morphological asymmetry.[9–13]

Approximately 80 genes are considered determining factors for the determination of normal left-right asymmetric positions of various organs. Some of them include *LEFTY1*, *LEFTY2*, *FGF8*, *ZIC3*, *NODAL*, and *NKX2.5*.[11–13] The "master gene" that determines the left side is the transcription factor named *PITX2*. Expression of regulatory factor *MAD3* and maintenance of its high concentration on the left side of the primitive streak is regulated by serotonin, a neurotransmitter. *MAD3* impacts negatively on the expression of *NODAL* on the left side of the primitive streak. The crucial role of 5HT in laterality determination came to light from epidemiological studies, which showed that usage of selective serotonin reuptake inhibitors (SSRIs), such as Prozac and Paxil, resulted in the presence of a variety of laterality defects.[12]

The most crucial developmental step occurring during the early embryonic period for asymmetrical organs of the digestive system, heart, and lungs is the left-to-right patterning. Asymmetry of the thoracoabdominal viscera is determined in the post-gastrulation phase and early somatic period by the regulated expression of various factors of the *NODAL-PITX2* pathway by the primitive node/posterior end of notochord, which act as "Left-Right Organizer."[14–16] Proper morphogenesis and positioning of asymmetrical internal organs are accurately controlled by sequential delivery and expression of genetic signals at appropriate time periods. It appears that the signaling system for the determination of the laterality of different organs may be separate and distinct. Failure of fine-tuned coordination of such signaling systems might result in situs

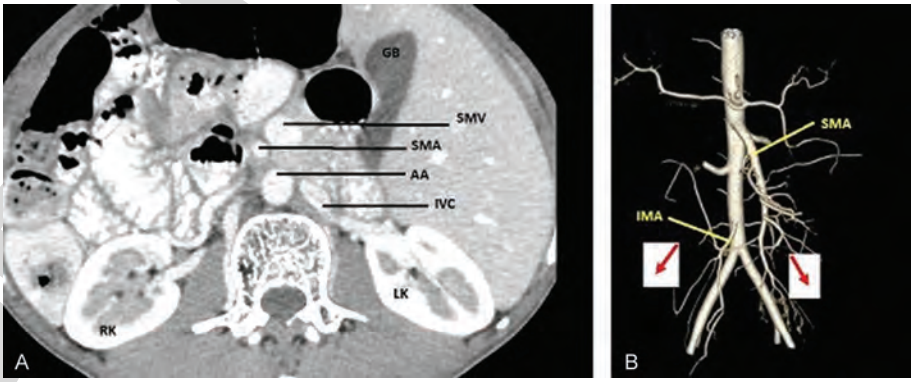

Figs 7A and B: (A) Axial scan showing the presence of the SMV to the left of the SMA. This SMA–SMV rotation sign suggests intestinal malrotation. The AA is situated to the right of the IVC; (B) Volume rendered image showing the reversed direction of the SMA toward the left side and the inferior mesenteric artery (IMA) toward the right

AA, abdominal aorta; GB, gallbladder; IMA, inferior mesenteric artery; IVC, inferior vena cava; LK, left kidney; SMA, superior mesenteric artery; SMV, superior mesenteric vein

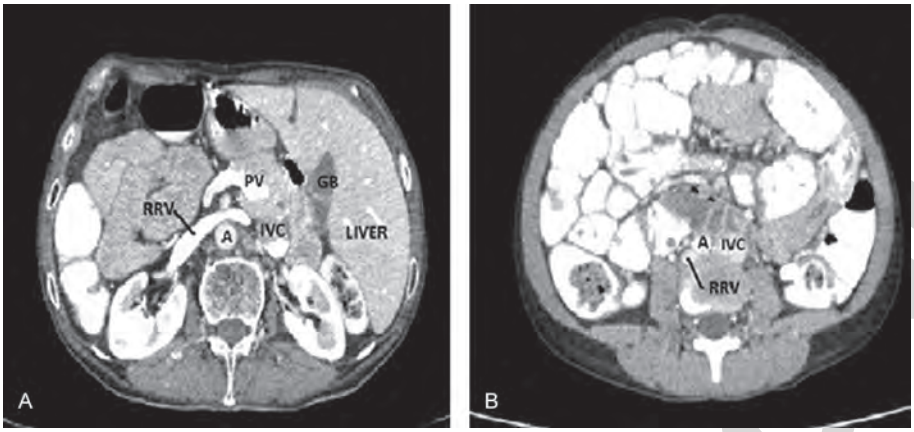

Figs 8A and B: (A) Axial section showing preaortic RRV, which crosses anterior to the right-sided AA (A) to join the left-sided IVC; (B) Axial section showing the RRV passing posterior to AA (A) (retroaortic RRV)

GB, gallbladder; PV, portal vein; IVC, inferior vena cava on the left side

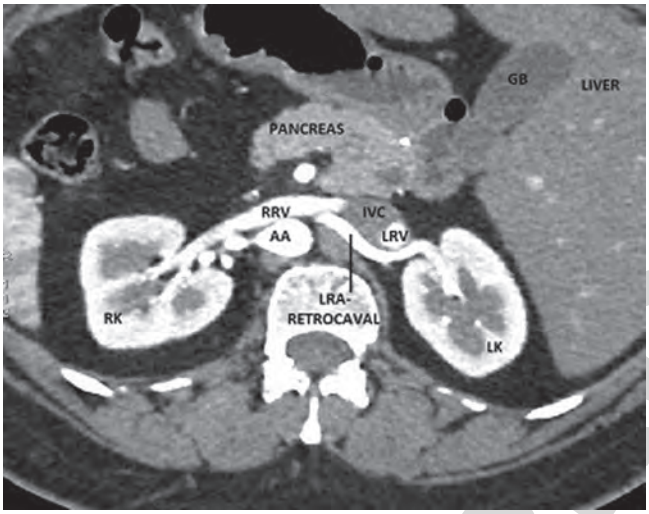

Fig. 9: Axial scan showing preaortic course of RRV crossing AA anteriorly before it drains into left IVC. The left renal artery (LRA) has a retrocaval course to reach the hilum

LK, left kidney; RK, right kidney

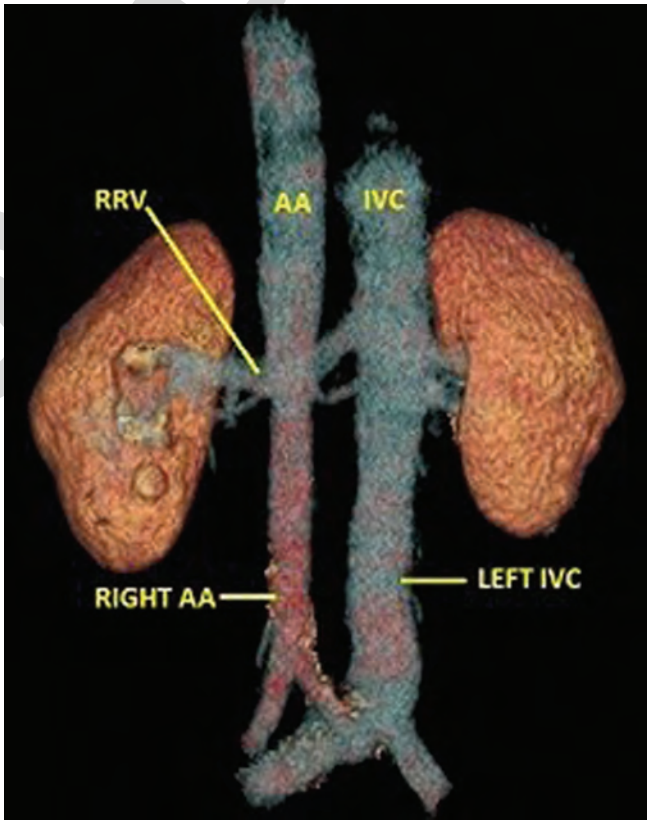

Fig. 10: Volume rendered image showing right AA and left IVC and RRV in preaortic position

AA, abdominal aorta; IVC, inferior vena cava; RRV, right renal vein

anomalies of abdominal organs with a normally positioned heart (situs inversus with levocardia).

All reported cases of situs inversus do not exhibit features of reversal of the position of all thoracoabdominal organs and great vessels. Many cases exhibit variable presentation. Published literature suggests that situs inversus is associated with comorbidities of the digestive system and vascular anomalies.[13,17,18] Presence of an interrupted left IVC continuing as azygos vein was also reported.[19]

Limitation

Retrospective study.

Conclusion

Situs inversus totalis, presenting as reversal of position of thoracoabdominal organs and great vessels, remains asymptomatic in many cases and is incidentally diagnosed when the patient is subjected to clinical and radiological evaluation for health conditions not related to this condition.

Clinical Significance

It may be associated with comorbidities such as duodenal atresia, biliary atresia, and acute appendicitis, which lead to the detection of the condition due to these associated symptoms. Rarely, the defect involves only some abdominal organs with a normally positioned

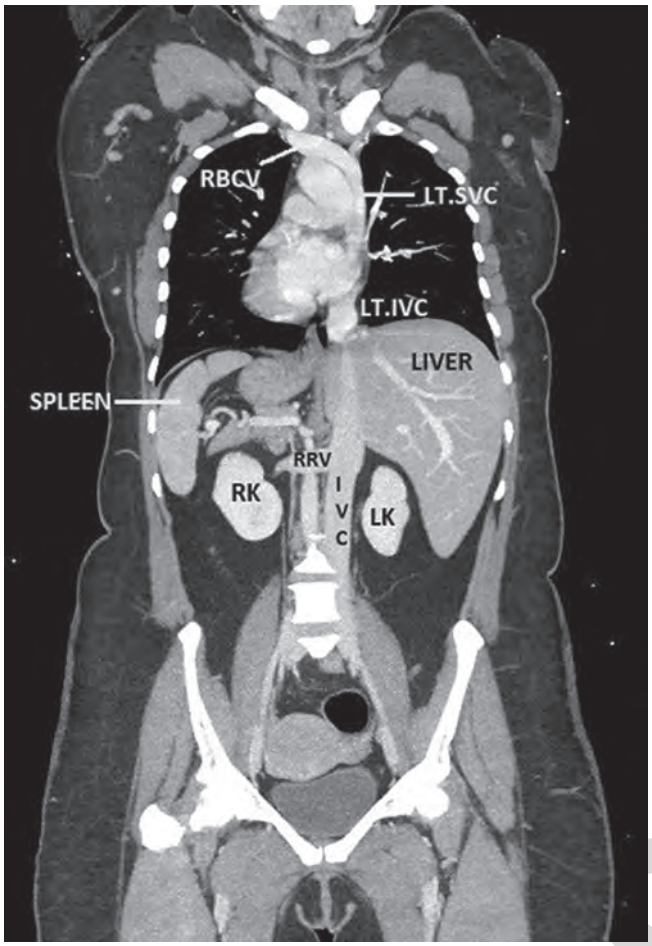

Fig. 11: Coronal section showing left IVC receiving RRV, which crosses the aorta anteriorly. The left IVC passing retrohepatically joins the morphological right atrium, which is also receiving the LSVC. The spleen is present on the right and the liver on the left. The RBCV crosses to the left anterior to the supra-aortic branches

IVC, inferior vena cava; LK, left kidney ; RBCV, right brachiocephalic vein; RK, right kidney; RRV, right renal vein

heart (levocardia); this is known as situs inversus abdominis (situs inversus partialis or incompletus). Surgeons and radiologists should be aware of such diversity of presentation to avoid any possible danger to the patient during surgical or radiological interventional procedures.

Disclaimer

- The manuscript is not a clinical trial, so not necessary to register.
- The manuscript is a pictorial review of cases incidentally detected while retrospectively analyzing abdominal CT scans.

Ethical Committee Certificate

IEC approval for the retrospective analysis of abdominal CT for studying the abdominal aorta and its branches is attached. (Ref No. MMC/IEC/2024/178 dated 18.11.2024).

Data Availability

The complete data is available within the manuscript and additional can be provided on request to the corresponding author.

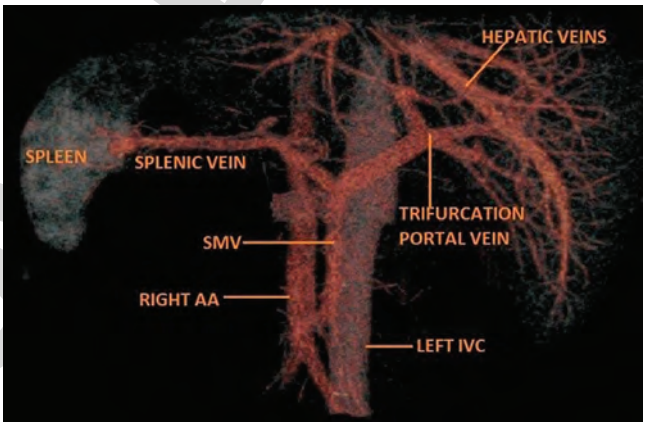

Fig. 12: A composite VR image showing formation of the portal vein, its oblique course to the left, and its trifurcation into three branches at the porta hepatis

AA, abdominal aorta; IVC, inferior vena cava; SMV, superior mesenteric vein

Table 1: Observed anatomical features of situs inversus totalis

Region	*Name of the organ*	*Features*
Thorax	Heart	Dextrocardia: Apex directed to the right. Cardiac chambers are inversely positioned; for example, the morphological right atrium is on the left side.
	Lungs	On the right side, a bilobed lung with a hyparterial bronchus; on the left side, a trilobed lung with an eparterial bronchus.
	SVC	Positioned on the left (LSVC); normal formation by union of two brachiocephalic veins on the left side. The RBCV crosses anterior to the supra-aortic branches.
	Arch of the aorta	Right arch with three mirror-image branches (three cases) or two branches with bovine trunk (four cases).
	DA	To the right of the vertebral column.
Abdomen	Stomach	Right-sided in the right hypochondrium.
	Spleen	Single, in the right hypochondrium.
	Liver	Left-sided with a large left lobe in the left hypochondrium.
	Gallbladder	Left-sided.
	Small intestine	Duodenal loop on the left side; small bowel loops are centrally placed.
	Pancreas	Head on the left side and tail extends to the right.

(Contd...)

Table 1: *(Contd...)*

Region	*Name of the organ*	*Features*
	Cecum, appendix	In the left iliac fossa or near midline (in four cases only).
	Kidneys	The upper pole of the LK at a lower level than that of the RK. RRV preaortic and LRA retrocaval (in two cases only).
	IVC	Left-sided, normal formation. Azygos continuation seen in one case.
	AA	To the right of the vertebral column.

AA, abdominal aorta; DA, descending aorta; IVC, inferior vena cava; LK, left kidney; LRA, left renal artery; LSVC, left superior vena cava; RBCV, right brachiocephalic vein; RK, right kidney; RRV, right renal vein

Artificial Intelligence (AI) Disclosure

No AI tool is used.

Authors' Contribution

Concept and design – CSRB, VS, BA, AK, and OPG.
Collection and interpretation of images – CSRB, BA, AK, and OPG
Manuscript writing and references – CSRB, VS, and BA

Acknowledgments

Sri Nikhil Sharma, Arjun Baliyan, Medical Education Department, Muzaffarnagar Medical College, for technical support.

Orcid

CS Ramesh Babu https://orcid.org/0000-0002-6505-2296
Vinay Sharma https://orcid.org/0009-0008-5590-9808

References

1. Eitler K, Bibok A, Telkes G. Situs inversus totalis: A clinical review. Int J Gen Med 2022;15:2437–2449. DOI: 10.2147/IJGM.S295444.
2. Jacobs JP, Anderson RH, Weinberg PM, et al. The nomenclature, definition and classification of cardiac structures in the setting of heterotaxy. Cardiol Young 2007;17(Suppl S4):1–28. DOI: 10.1017/S1047951107001138.
3. Kim SJ. Heterotaxy syndrome. Korean Circ J 2011;41:227–232. DOI: 10.4070/kcj.2011.41.5.227.
4. Cassey B. Two rights make a wrong: Human left-right malformations. Hum Mol Genet 1998;7(10):1565–1571. DOI: 10.1093/hmg/7.10.1565.
5. Merklin RJ, Varano NR. Situs inversus and cardiac defects. A study of 111 cases of reversed asymmetry. J Thorac Cardiovasc Surg 1963;45:334–342. PMID: 13935010.
6. Kanani J, Sheikh MI. Situs inversus partialis (levocardia): An incidental discovery of an extremely rare during the autopsy of a female with suicidal poisoning. Surg Exp Pathol 2024;7:10. DOI: 10.1186/s42047-024-00154-4.
7. Ramavathu KVM. Imaging findings in a case of situs inversus totalis. BJR Case Rep 2021;7:20200202. DOI: 10.1259/bjrcr.20200202.
8. Winer-Muram HT, Tonkin ILD. The spectrum of heterotaxic syndromes. Radiol Clin North Am 1989;27(6):1147–1170. PMID: 2685879.
9. Huang L, Mitchell BJ, Andronikou S, et al. Heterotaxy syndrome: This is the left, right? S Afr J Radiol 2015;19(2):5. DOI: 10.4102/sajr.v19i2.902.
10. Soofi M, Alpert MA, Barbadora J, et al. Human laterality disorders: Pathogenesis, clinical manifestations, diagnosis and management. Am J Med Sci 2021;362(3):233–242. DOI: 10.1016/j.amjms.2021.05.020.
11. Levin M. Left-right asymmetry in embryonic development: A comprehensive review. Mech Dev 2005;122:3–25. DOI: 10.1016/j.mod.2004.08.006.
12. Sadler TW. In Langman's Medical Embryology. 13th ed. Wolters Kluwer, New Delhi, 2016. pp. 59–66.
13. Osarenkhoe JO. Situs inversus: A review of 191 published cases. Open J Intern Med 2022;12:85–94. DOI: 10.4236/ojim.2022.122010.
14. Grimes DT, Burdine RD. Left-right patterning: Breaking symmetry to asymmetric morphogenesis. Trends Genet 2017;33(9):616–628. DOI: 10.1016/j.tig.2017.06.004.
15. Forrest K, Barricella AC, Pohar SA, et al. Understanding laterality disorders and the left-right organizer: Insights from zebra fish. Front Cell Dev Biol 2022;10:1035513. DOI: 10.3389/fcell.2022.1035513.
16. Lin AE, Krikov S, Reihle-Colarusso T, et al. Laterality defects in the National Birth Defects Prevention Study (1998–2007): Birth prevalence and descriptive epidemiology. Am J Med Genet A 2014;0(10):2581–2591. DOI: 10.1002/ajmg.a.36695.
17. Bahlmann O, Schomerus C, Gebremedhin E. A complete situs inversus viscerum with hepatic, intestinal and renal vascular anomalies: One case report and review of literature. Eur J Anat 2019;23(61):459–463.
18. González-Castillo A, Rojas S, Ortega M, et al. Variations in vascular anatomy and unilateral adrenal agenesis in a female cadaver with situs inversus totalis. Surg Radiol Anat 2018;40:1169–1172. DOI: 10.1007/s00276-018-2060-y.
19. Loukas M, Strike DRG, Tubbs RS, et al. An interrupted inferior vena cava in a situs inversus: A case report and review of literature. Folia Morphol 2009;68:184–187. PMID: 19722164.